

NGU



Norges geologiske
undersøkelse

Nr. 322

Bulletin 35



Universitetsforlaget 1975

Trondheim · Oslo · Bergen · Tromsø

STORTINGS-
18 SEP 1976
BIBLIOTEK.



NGU
Norges geologiske
undersøkelse

Geological Survey of Norway

Norges geologiske undersøkelse (Geological Survey of Norway), Leiv Eirikssons vei 39, Trondheim. Telephone: national (075) 15860, international + 47 75 15860. Postal address: Box 3006, N-7001 Trondheim, Norway.

Administrative Director: Dr. philos. *Knut S. Heier*

Geological division: Director Dr. philos. *Peter Padget*

Geophysical division: Director *Inge Aalstad*

Chemical division: Director *Aslak Kvalheim*

The publications of *Norges geologiske undersøkelse* are issued as consecutively numbered volumes, and are subdivided into two series, Bulletin and Skrifter.

Bulletins comprise scientific contributions to the earth sciences of regional Norwegian, general, or specialist interest.

Skrifter comprise papers and reports of specialist or public interest of regional, technical, economic, environmental, and other aspects of applied earth sciences, issued in Norwegian, and with an Abstract in English.

EDITOR

Statsgeolog Dr. *David Roberts*, Norges geologiske undersøkelse, P.O.Box 3006, N-7001 Trondheim, Norway.

PUBLISHER

Universitetsforlaget, P.O.Box 307, Blindern, Oslo 3, Norway. American Office: P.O.Box 142, Boston, Massachusetts 02113, U.S.A.

EARLIER PUBLICATIONS AND MAPS

A list of NGU publications and maps, 'Fortegnelse over publikasjoner og kart utgitt av Norges geologiske undersøkelse', is revised at irregular intervals. The last issue appeared in 1971 and copies can be obtained from the Publisher.

The most recent maps available from NGU are listed inside the back cover.

MANUSCRIPTS

Instructions to contributors to the NGU Series can be found in NGU Nr. 273, pp. 1-5. Offprints of these instructions can be obtained from the editor. Contributors are urged to prepare their manuscripts in accordance with these instructions.

Intrusive Rocks of the Northern Iveland-Evje Area, Aust-Agder

SVEND PEDERSEN

Pedersen, S. 1975: Intrusive rocks of the northern Iveland-Evje area, Aust-Agder. *Norges geol. Unders.* 322, 1-11.

In the northern Iveland-Evje area extensive magmatic activity occurred during the so-called Sveconorwegian igneous period. Two intrusive episodes can be distinguished though apparently they occurred close in time. The oldest intrusions are represented by amphibolites which were emplaced under plutonic conditions and thus were able to deform the gneissic host rock (globulitic type of intrusion). At the close of this first episode basic dykes were intruded. During the second episode monzonite and granite were intruded, followed by monzonitic conical sheets and radiating dykes. Aplitic dykes and pegmatites brought the igneous activity to a close.

S. Pedersen, Institute of General Geology, Østervoldgade 5, DK-1350 Copenhagen K, Denmark

Introduction

The Iveland-Evje area is dominated by an elongated body of amphibolite measuring 35 km in a north-south direction and 10-15 km east-west. The massif was mapped and described by Barth (1947) as the Iveland-Evje amphibolite. Well known from the area are the many pegmatites containing rare minerals (for descriptions see Andersen 1926, 1931; Barth 1928, 1931, 1947; Bjørlykke 1934, 1937) and the nickel mineralisation (Vogt 1893, 1923; Bjørlykke 1947).

This paper presents the results of a re-mapping of the northern part of the Iveland-Evje area and deals with the magmatic rocks found there.

The re-mapping was carried out by the author in 1967 and 1968 with two more short stays in 1970 and 1973. During the first field season the author was a member of the team working on the 'Telemark Project' (1962-1967) organised by the Mineralogisk-Geologisk Museum, Oslo. The mapping was carried out at scale 1 : 25 000 and is more detailed than the earlier mapping by Barth (1947).

In the area mapped (Plate 1) there are two main rock units: the regional amphibolite facies gneisses and the younger magmatic rocks. The gneisses will not be treated in any detail in this paper. Their outcrop pattern only partly reflects the regional gneiss structure, since it is influenced by the shape of the main body of magmatic rocks. The latter comprises the *Hørvingsvatn Complex* (Pedersen 1973) and the *Flåt Complex*. Only a part of the Flåt Complex has been mapped as yet. The complexes are examples of intrusions emplaced under plutonic conditions in deep crustal environments.



Description of the intrusive rocks

THE HØVRINGSVATN COMPLEX

The Høvringsvatn Complex is situated around the lake Høvringsvatn north-east of Evje (Plate 1). The outcrop of the complex is elliptical in shape with a NNE-SSW orientation of the longest axis. The complex includes amphibolite, monzonite, granite, aplite and pegmatite. It is surrounded by gneisses to the west, north and east.

Barth (1947) described the amphibolite from the locality Bertesknapen (Bertesknappen amphibolite) as a schistose amphibolitic rock, but the present author's observations indicate that in general the amphibolitic rocks only rarely possess a marked schistose structure (in the sense of Turner & Weiss 1963).

The modal compositions of the rocks described below are given in the Appendix (p. 9).

Amphibolite: Amphibolite is the oldest unit of the Høvringsvatn Complex. It crops out mainly in a large area in the marginal part of the Høvringsvatn Complex and in a smaller isolated area in the centre of the complex (Plate 1). In addition it occurs as layers and lenses enclosed in the younger rocks. The contact with the gneiss is not exposed, but structural investigations indicate that the outer border of the amphibolitic body trends parallel to the strike of the foliation in the surrounding gneiss. The structures in the amphibolite also indicate that it wedges out to the north.

The amphibolite has a varying appearance. Normally it is a fine- to medium-grained dark rock, sometimes alternating with irregular light bands. In the western part a more pronounced banding is seen, while to the east the rock has an almost homogeneous appearance. Here, however, it is possible in places to find some coarse-grained bands consisting almost entirely of hornblende. There is only rarely any sign of a preferred mineral orientation.

In the western part the amphibolite occasionally contains both hypersthene and diopside (sample no. 4883, see Appendix). The hypersthene grains are replaced to a certain degree by hornblende. Exsolution lamellae of diopside are seen in the hypersthene.

Basic dykes: Generally it is only possible to follow these dykes in the Høvringsvatn Complex over short distances (Fig. 1). This is due partly to poor exposures and partly to the irregular intrusive form of the dykes. The dykes never exceed one metre in width and are often no more than 20-30 cm wide.

The dykes are of amphibolitic composition, and pyroxenes have never been observed (see Appendix). Two types can be distinguished:

a) Dark dykes made up entirely of fine-grained amphibolite; these may carry plagioclase mesocrysts. Biotite is also present and shows a preferred orientation parallel to the contacts. Small patches of ultramafic rock have been observed in the central parts of one of these dykes.

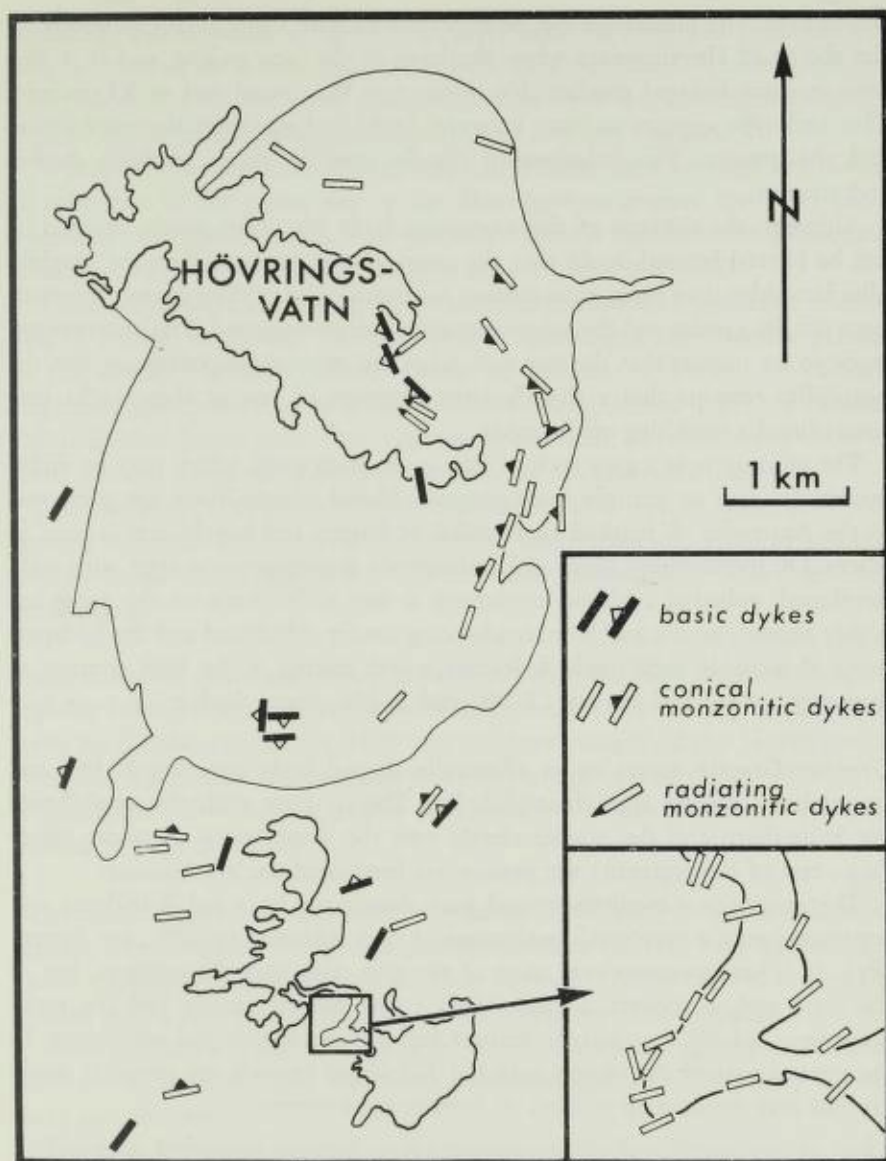


Fig. 1. Basic and monzonitic dykes within the Høvringsvatn Complex.

b) Complex dykes with a fine-grained border zone and a coarse-grained central part. The contact between the central part and the border zone is very well defined. The central part is dominated by aggregates of amphiboles which are orientated perpendicular to the contacts. Nearer to the border zone plagioclase-rich material with scattered amphibole aggregates is present. The rock-type making up the fine-grained border zone is the same as the amphibolite of dyke type *a*.

Monzonite: The monzonite can be observed in nearly continuous outcrops on the shores of Høvringsvatn when the level of the lake is low, and it is also seen in some isolated patches, for instance at Gautestad and at Kleppslund. This rock-type appears to form a central body that underlies the amphibolite and the granite. This relationship can be seen in many roadside ditches and streams.

Although the contacts of the monzonite body are often poorly exposed, it can be proved beyond doubt that the monzonite is younger than the amphibolite but older than some cross-cutting monzonitic dykes. The contact relations between the granite and the monzonite are more complicated. The observations made so far suggest that the two rock-types are penecontemporaneous, but the possibility remains that a slightly later intrusion of one of these rocks may have caused a remelting of the other.

The monzonite is a grey rock of fine to medium grain which may be either weakly foliated or entirely homogeneous. Modal compositions are presented in the Appendix. A marked aggregation of biotite and hornblende is seen in places. On the southern shore of Høvringsvatn a homogeneous type with well-developed, euhedral feldspar mesocrysts is met with. Some of the rocks are highly altered, biotite and hornblende being totally chloritised and the feldspars being thoroughly sericitised. A feature worth noting is the high content of accessory sphene and apatite (2–5% and 1–3%, respectively).

Granite: Granite occurs as an elliptically shaped body covering 15 km² and containing a central area of amphibolite. The contacts with the amphibolite are knife-sharp and the granite clearly cuts the amphibolite. In some places (e.g., east of Rasevetvatn) the granite has brecciated the amphibolite.

The granite is a medium-grained rock dominated by a red K-feldspar and containing only a very small percentage of dark minerals (< 2%, see Appendix). It is homogeneous over most of the area, also near the contacts, but in the west and south-west it grades into a fine-grained variety and the rocks sometimes exhibit a cataclastic texture and a characteristic red coloration. In the central part of the pluton euhedral K-feldspar crystals are present; single crystals may measure up to 2 cm × 3 cm in cross-section.

Monzonitic dykes: Structurally it is possible to distinguish between two types of minor monzonitic intrusions; conical sheets and radiating dykes. The terms conical sheets and radiating dykes are used to distinguish these intrusions from typically subvolcanic cone sheets and radial dykes, although the intrusion mechanism was probably the same.

The conical sheets form semicircular outcrops and their dips point towards a centre just south of Høvringsvatn (Fig. 1). In spite of many interruptions it is possible to follow them from Gautestad to west of Vikstøl. The radiating dykes have been observed in the outcrops on the shores of Høvringsvatn (Fig. 1). Outside the Høvringsvatn Complex monzonitic dykes are seen at Flåt cutting the Mykleås amphibolite and the marginal granite of the Flåt

Complex, and in several roadside exposures between Evje and Byglandsfjord they are seen to cut biotite gneiss, but here their structural attitude is not yet understood. The widths of the dykes vary from some few centimetres to more than 20 m; individual dykes are only rarely of constant thickness.

Where the monzonitic dykes intrude amphibolite their contacts are almost straight, but in the gneiss and in the Høvringsvatn granite they may show extremely irregular contacts. This obviously reflects the different rheological conditions of the host rocks at the time of monzonite intrusion.

The monzonitic dykes are light grey and fine-grained with a distinct orientation of biotite, amphibole and also sphene, apatite and ore minerals parallel to the contact. In some of the dykes an incipient formation of biotite-amphibole aggregates may be observed. Some of the thicker dykes are banded. The individual bands show little contrast in the field, the differences being in grain size and the proportions and orientations of component minerals.

The monzonitic dykes are often associated with aplitic material which appears as border aplites, cross connections, sheet veins and more or less discordant veins. Often the aplites are intensely pygmatically folded or even boudinaged.

Aplites: Aplitic dykes are present throughout both the Høvringsvatn Complex and the Flåt Complex as decimetre-thick discordant veins. They cut all rock-types except the pegmatites. Near the southern margin of the Høvringsvatn Complex, where they are most common, they are of coarser grain.

The aplites often have a weakly developed preferred orientation of biotite parallel to their contacts.

Pegmatites: Pegmatites are most commonly developed in the amphibolite terrain. Here some of the famous giant pegmatites carrying rare minerals are found, especially east and south of Høvringsvatn (Andersen 1931). In the granite only a few centimetre-thick quartz veins have been observed.

Other pegmatite bodies and veins occur in the surrounding gneiss. None of these are as large as those inside the complexes and apparently they do not carry rare minerals.

The most important minerals in the pegmatites are K-feldspar, quartz, and a little plagioclase. In some pegmatites albite (often cleavelandite) is observed. Biotite and in some cases green muscovite are common.

THE FLÅT COMPLEX

The area of intrusive rocks occurring south-west of the Høvringsvatn Complex is provisionally called the Flåt Complex. The Flåt Complex includes two rock units, the marginal granite and the Mykleås amphibolite. *The marginal granite* is a grey, nearly homogeneous rock dominated by K-feldspar megacrysts which may define a lineation. *The Mykleås amphibolite* (named by Barth 1947) is a fine- to medium-grained, dark grey or black amphibolite easily distinguished from the Høvringsvatn amphibolite on account of its porphyritic texture.

Noteworthy for both the marginal granite and the Mykleås amphibolite is the large amount of sphene (2–7%) and apatite (1–10%). The contact between the marginal granite and the Mykleås amphibolite is not exposed.

The Flåt Complex apparently forms a separate intrusion. Mapping of the complex has not yet been completed, however, and all that can be said at present about the age relations between the two complexes is that the Flåt Complex is older than the monzonitic dykes of the Høvringsvatn Complex since both the marginal granite and the Mykleås amphibolite are cut by these dykes. The Flåt Complex is therefore left out of the following discussion of the structural evolution.

The structural evolution

A structural analysis has revealed no clear evidence of a regional deformation having affected the intrusive complexes. The Høvringsvatn Complex, which is elongated in the NNE–SSW direction, is clearly discordant in relation to the regional structures in the gneisses in which folds with WNW–ESE axis dominate the pattern. On outcrop scale, however, the gneiss foliation is seen to be concordant with the border of the complex, and near the contact the fold axes change attitude so that they become oriented parallel to the contact (Fig. 2). This local concordance could be the result of a forceful intrusion of the complex into *plastic* surroundings.

The Høvringsvatn amphibolite was the first rock to be emplaced and this amphibolitic intrusion can be compared to the metabasic bodies in the Moss area, Østfold, described as globuliths by Berthelsen (1970). Berthelsen (1970, p. 73) defined a globulith as: 'an intrusive body or a group of closely associated bodies of globular or botryoidal shape and with almost concordant contacts resulting from the effect of the intrusion/s on its/their immediate surroundings'. He imagined that their intrusion took place 'in a regionally pre-heated rock complex under plutonic conditions with pressures and temperatures (and P_{H_2O}) not much below those required to start regional anatexis'.

The intrusion of basic dykes terminated the episode of basic intrusive activity. In the Høvringsvatn Complex this basic intrusive episode was followed by an episode during which intermediate and acid rocks were emplaced. As mentioned earlier these rocks — the Høvringsvatn monzonite and the Høvringsvatn granite — show very complicated contact relations and it has not yet been possible to establish their chronological order.

The amphibolitic body in the centre of the Høvringsvatn granite conceivably forms a huge xenolith which sank into the granite from the roof. The more or less 'chaotic' structures characteristic of the amphibolitic member make it difficult if not impossible to prove this by structural analysis, but the fact that the body considered to be a xenolith is heavily veined by granitic apophyses concurs with this interpretation.

The closing stage of the younger intrusive episode was marked by the intrusion of monzonitic conical sheets and radiating dykes inside the Høvrings-

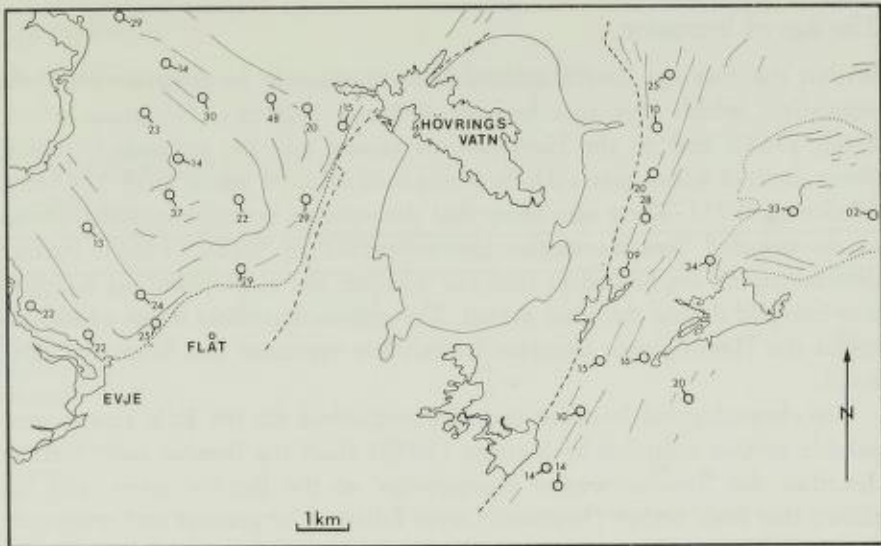


Fig. 2. Constructed fold axes in the gneisses showing their changing attitude towards the margin of the intrusive complexes.

vatn Complex and other monzonitic dykes in the gneiss and in the Flåt Complex. The monzonitic dykes are cut by aplitic dykes. In places, however, both the monzonite and the aplitic veins can be seen to be influenced by shearing and flattening. This deformation could well have been caused by the stresses set up during the emplacement of the conical sheets. The intimate association of aplite and monzonite in many of these dykes suggests a close time relationship between the intrusion of these two rock-types. Possibly the pegmatites were also intruded just after the monzonite.

Two intrusive episodes, an older basic and a younger intermediate/acid phase, can thus be distinguished in the Høvringsvatn Complex. Both episodes ended with a period of dyke emplacement. The whole of this intrusive development apparently took place under plutonic conditions. The lack of fine-grained contact zones in the Høvringsvatn monzonite and the Høvringsvatn granite indicates that these intrusions were emplaced into host rocks already having quite elevated temperatures. The dyke generations provide evidence of tensional conditions in the crust, but as dykes of both generations show irregular to scalloped contacts, they need not be taken as evidence of uplift of the complex at the termination of each of the intrusive episodes. In consequence these episodes are considered to have followed one after the other almost without interruption and they are believed to have been emplaced at a deep level in cratonic crust (Berthelsen 1972).

The Høvringsvatn Complex is therefore classified as a discordant anorogenic intrusion. Its age, therefore, can be considered a *real* minimum age for the surrounding basement rocks.

The age of intrusion

Within the area age determinations have been made on minerals from the pegmatites, which gave ages between 900 and 1000 m.y. (Neumann 1960; Broch 1964), and on the Høvringsvatn granite and the monzonitic conical sheets, both of which gave a Rb/Sr whole rock isochron age of 1038 ± 43 m.y. (Pedersen 1973). These ages show that the younger intrusive episode belongs to the so-called 'Sveconorwegian igneous period' of Welin (1966). Further determinations are needed to find out whether the amphibolite, as believed, was intruded during the same period. The gneissic basement rocks which surround the Høvringsvatn Complex conceivably represent pre-Sveconorwegian rocks.

The chronology of intrusive episodes established for the Evje area is comparable to that compiled by Starmer (1972) from the Bamble area. Starmer describes the 'Sveconorwegian regeneration' of the Bamble series, and has shown that basic bodies (hyperites) were followed by granites and granitoids, the intrusive period terminating with pegmatites.

Acknowledgements. - I wish to thank Professor A. Berthelsen, Curator J. A. Dons and Professor H. Neumann for their help during the mapping and geological interpretation, and M. Schierling, who drew the map and the figures. T. C. R. Pulvertaft kindly improved the English.

REFERENCES

- Andersen, O. 1926: Feldspat I. *Norges geol. Unders.* 128a.
 Andersen, O. 1931: Feldspat II. *Norges geol. Unders.* 128b.
 Barth, T. F. W. 1928: Zur Genesis der Pegmatite im Urgebirge. *N. Jahrb. f. Min. etc., B. Bd. 58*, abt. A, 385-432.
 Barth, T. F. W. 1931: Feldspat III. *Norges geol. Unders.* 128b.
 Barth, T. F. W. 1947: The nickeliferous Iveland-Evje amphibolite and its relation. *Norges geol. Unders.* 168a.
 Berthelsen, A. 1970: Globulith. A new type of intrusive structure, exemplified by metabasic bodies in the Moss area, SE Norway. *Norges geol. Unders.* 266, 70-85.
 Berthelsen, A. 1972: Analysen orogener und kratonischer Strukturen aus der Tiefenzone. *Geol. Rundschau*, 61, 1, 34-44.
 Bjorlykke, H. 1934: The mineral paragenesis of the granite pegmatites of Iveland, Setesdal, Southern Norway. *Norsk geol. Tidsskr.* 14, 211-309.
 Bjorlykke, H. 1937: The granite pegmatites of Southern Norway. *J. Min. Soc. Am.* 22, no. 4, 241-255.
 Bjorlykke, H. 1947: Flåt Nickel Mine. *Norges geol. Unders.* 168b.
 Broch, O. A. 1964: Age determination of Norwegian minerals up to March, 1964. *Norges geol. Unders.* 228, 84-112.
 Neumann, H. 1960: Apparent ages of Norwegian minerals and rocks. *Norsk geol. Tidsskr.* 40, 173-191.
 Pedersen, S. 1973: Age determination from the Iveland-Evje area, Aust-Agder. *Norges geol. Unders.* 300, 33-39.
 Starmer, I. C. 1972: The Sveconorwegian regeneration and earlier orogenic events in the Bamble series, South Norway. *Norges geol. Unders.* 277, 37-52.
 Turner, F. J. & Weiss, L. E. 1963: *Structural Analysis of Metamorphic Tectonites*. McGraw-Hill Book Company, Inc., New York.
 Vogt, J. H. L. 1893: Bildung von Erzlagertstätten durch Differentiationsprozesse in basischen Eruptivmagma. *Z. Prakt. Geol.*, 4-11, 125-143 and 257-269.
 Vogt, J. H. L. 1923: Nickel in igneous rocks. *Econ. Geol.* 18, 4, 307-353.
 Welin, E. 1966: The absolute time scale and the classification of Precambrian rocks in Sweden. *Geol. Fören. Stockholm Förh.* 88, 29-33.

Appendix

Modal compositions of the rocks described in the text

HØVRINGSVATN COMPLEX

Amphibolite

	4710	4729	4883	4884	1048	1049	1112
Quartz		4	2	16	1	x	
Plagioclase	67	45	37	21	60	58	40
Hornblende	32	48	38	13	20	40	60
Hypersthene			8				
Diopside			9				
Accessories	x	x	1	x	4	x	
Ore minerals	x	3	5		1	2	x
Chlorite					14		
Biotite		x	1	50			

x: < 1%

Basic dykes

	1173	058	4867
Plagioclase	17	21	19
Hornblende	60	77	75
Biotite	17		4
Sphene	4		
Ore minerals		2	2
Epidote	x		
Chlorite	1		

x: < 1%

Monzonite and granite

	1050	1162	054	4862	4863	4864	1098
Quartz	9	10	11	32	22	16	3
Plagioclase	31	29	17	24	32	18	27
K-feldspar	28	29	37	41	43	63	46
Amphibole	13	14	14	x	x		10
Biotite			15	1	2	2	8
Sphene	3	2	3	1	1	1	3
Apatite	1	1	1	x	x	x	2
Zircon		x			x		
Ore minerals			x	1	x	x	1
Carbonate		1		x			
Fluorite			x		x		
Chlorite	15	13					
Epidote			1	x	x	x	

x: < 1%

Specimens 1050, 1162 and 054 - Høvringsvatn monzonite

Specimens 4862, 4863 and 4864 - Høvringsvatn granite

Specimen 1098 - monzonitic cone sheet

FLAT COMPLEX

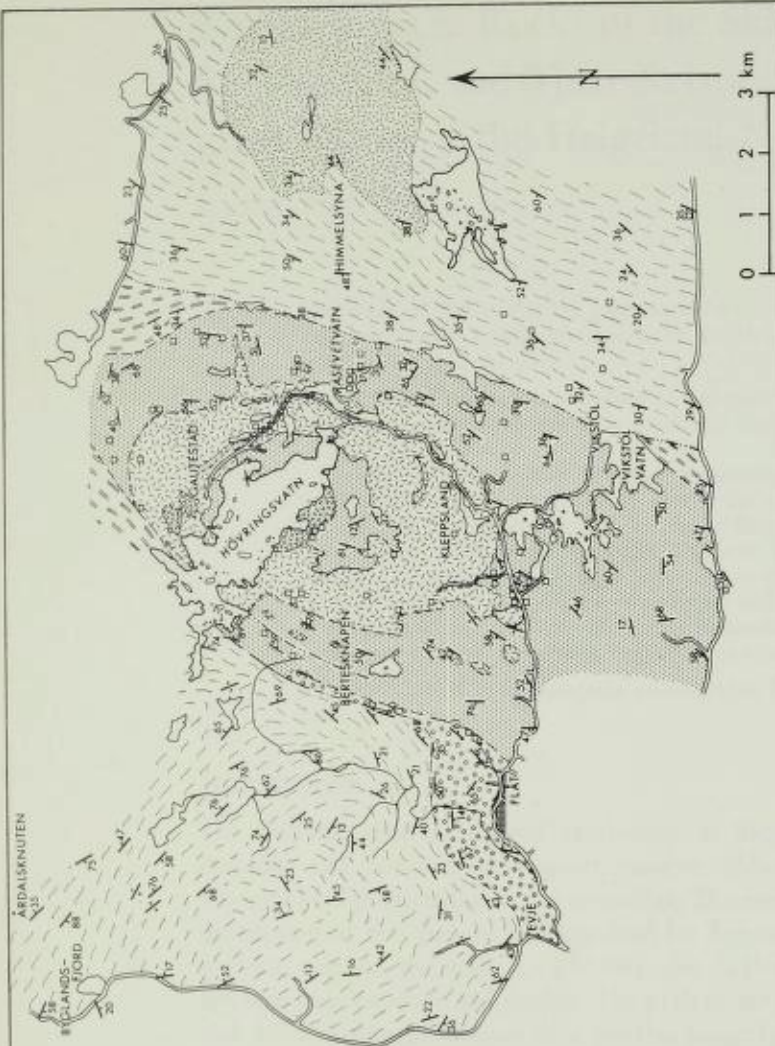
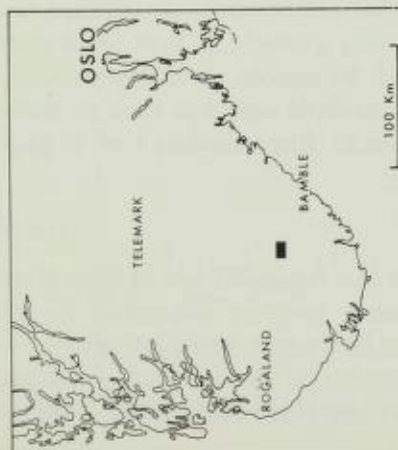
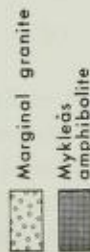
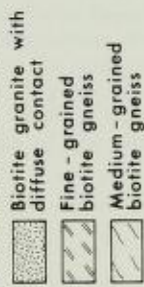
	4875	4877	4818a	4872
Quartz	4	10	9	12
Plagioclase	71	46	50	40
K-feldspar				36
Amphibole	3	18	11	1
Biotite	13	4	13	7
Sphene	5	x	5	2
Apatite	2	5	4	1
Ore minerals	1	8	3	1
Chlorite	x	8	5	x
Epidote	x	x	x	x

x: < 1%

Specimens 4875, 4877 and 4818a - Mykleås amphibolite

Specimen 4872 - marginal granite (only a rough estimate based on 1301 points)

GEOLOGICAL MAP
OF THE
NORTHERN IVELAND - EVJE AREA,
AUST-AGDER

**LEGEND****FLÅT COMPLEX****HÖVRINGSVATN COMPLEX****BASEMENT ROCKS****Boundary established**

— inferred

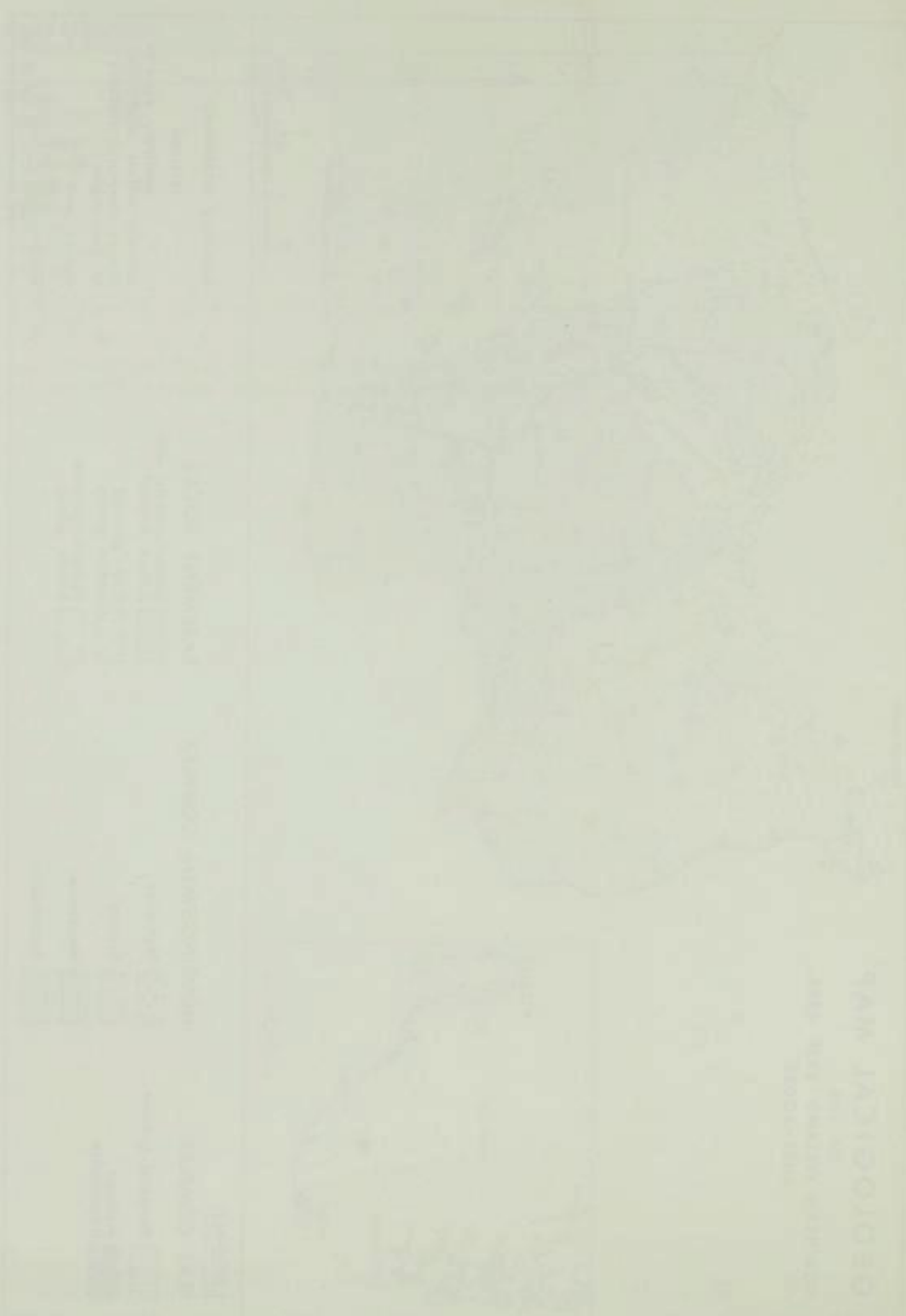
--- arbitrary, used to indicate diffuse boundaries

— Planar structural element of any origin

— Master joint

— Roads

S. P. 75



The Low-grade Rocks of the Skålvær Area, S. Helgeland, and Their Relationship to High-grade Rocks of the Helgeland Nappe Complex

MAGNE GUSTAVSON

Gustavson, M. 1975: The low-grade rocks of the Skålvær area, S. Helgeland, and their relationship to high-grade rocks of the Helgeland Nappe Complex. *Norges geol. Unders.* 322, 13–33.

The geological setting and petrology of low-grade rocks of the Helgeland Nappe Complex are discussed and it is concluded that the low-grade rocks are part of the nappe complex.

Correlations with similar low-grade sequences in (1) the Leka area on the coast some 90 km to the south, (2) part of the western Trondheim Region, and (3) the Köli part of the Seve-Köli Nappe Complex of Västerbotten, Sweden, are suggested. These correlations enable a better evaluation of the stratigraphical positions of parts of the high-grade sequences in Southern Helgeland than has hitherto been possible. Another conclusion which can be drawn is that there is no great difference between the eugeosynclinal deposits of the Nordland facies type and the Trondheim Region facies type.

M. Gustavson, Norges geologiske undersøkelse, P.O. Box 3006, N-7001 Trondheim, Norway

Introduction

The Skålvær area is situated south-west of Sandnessjøen at about 66°N latitude, and consists of a great number of small islands and skerries topographically belonging to the strandflat. The area is included in the general description of this part of S. Helgeland by Rekstad (1917). On the accompanying map on the scale 1 : 250 000, the Skålvær islands were given the symbols of mica schist and marble. The present writer visited the area in 1972 and 1973 during the course of a general mapping programme in Helgeland carried out by the Geological Survey of Norway (NGU) under the writer's leadership. It was immediately obvious that the metamorphic facies of the rocks was distinctly lower than in adjoining areas and thus called for special attention. The present paper is an account of the rock-types, their relations to the rocks of adjoining areas and some implications of these relations for the age and stratigraphy of the Caledonian rocks of southern Helgeland.

Geological setting

The main structural units of the Helgeland region are shown in Fig. 1. The easternmost parts of Norwegian territory consist of relatively low-grade (greenschist facies) rocks belonging to the Köli part of the Seve-Köli Nappe Complex (Kulling 1955; Zachrisson 1973); these rocks have been described by Strand (1953, 1955, 1958, 1960, 1963) and Foslie & Strand (1956). The

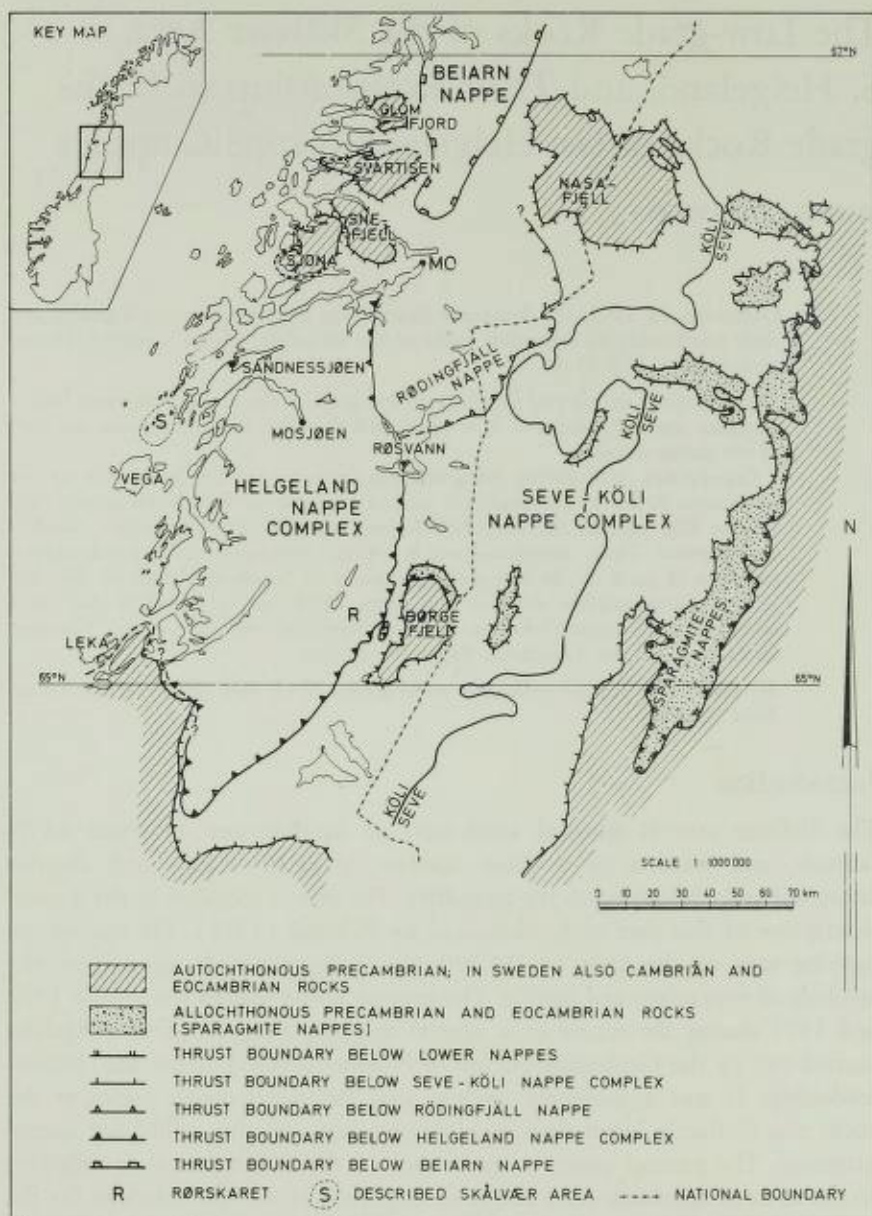


Fig. 1. Map showing the main litho-tectonic units of southern Helgeland and adjoining areas in Sweden.

Köli sequence is overlain to the west by the Rödingfjäll Nappe (Kulling 1955) and above this by the Helgeland Nappe Complex (Ramberg 1967; Gustavson 1973). In the southern part, the Helgeland Nappe Complex is in direct contact with the low-grade Köli rocks. Both the Helgeland and the Rödingfjäll Nappes are mainly in the almandine-amphibolite facies and are composed of approximately the same rock-types (mica schists and gneisses, calcareous mica

schists, marbles, amphibolites, serpentinites and granitoid intrusive rocks). Descriptions of parts of the high-grade areas have been given by Ramberg (1967), Gustavson & Grønhaug (1960), Nissen (1965, 1974), Kollung (1967), Myrland (1972) and Gustavson (1973). The rocks of the Helgeland Nappe Complex extend to the coast and are also present in areas adjoining the Skålvær islands. An account of the rocks occurring immediately east of the Skålvær area has recently been presented by Nissen (1974).

In the northern area, medium- to high-grade rocks are also present in the Beiarn Nappe (Rutland & Nicholson 1965). The exact relations between the Beiarn Nappe and the Rödöfjäll and Helgeland Nappes are still not clear.

Precambrian basement is present east and south of the Caledonian nappes and also crops out in a number of tectonic windows within the nappe areas. In western areas of central and northern Nordland the crystalline basement has been Caledonised, whereas to the east the basement rocks are comparatively unaffected by the Caledonian deformation (Rutland & Nicholson 1965; Gustavson 1966, 1972; Nicholson & Rutland 1969). It is, therefore, likely that Caledonised Precambrian basement is present below the Caledonian nappes in the coastal area of southern Helgeland. Further discussion of this and other structural aspects within the region will be reserved for a separate paper.

Apart from the areas to the east of the Helgeland Nappe Complex, low-grade rocks have also been described from the Leka district to the south-west (Birkeland 1958; Prestvik 1972, 1974). The rocks there include mafic and ultramafic intrusives, metavolcanics and metasediments. Up to now, other occurrences of equally low-grade rocks have not been described from the coastal districts of this part of North Norway. However, during fieldwork in 1972 the present writer mapped metagreywackes and conglomerates of relatively low grade on the islands between Leka and Vega (Gustavson 1975).

Petrology

The main rock-types of the Skålvær area (Plate I) are dark phyllite and mica schist, conglomerate, dark dolomitic limestone or marble, greenstone and some light, fine-grained quartzo-feldspathic rocks which probably represent metamorphosed quartz-keratophyre. Structurally, the layering is steeply inclined to the east with a N-S strike in the central area. Way-up criteria have not been found. However, an interpretation of the probable relationship between the various rock-types is shown on the cross section in Plate I. This interpretation implies that the rocks can be arranged in the following tectono-stratigraphic sequence, from top to bottom:

- Quartz keratophyre.
- Dark phyllite and mica schist.
- Dolomite conglomerate and metagreywacke.
- Dark, dolomitic crystalline limestone and calcite marble.
- Greenstone.

That this rock succession is also probably the correct age sequence is sup-



Fig. 2. Greenstone with pillow structure, Grundværsnavaren.

ported by the fact that dolomitic boulders are predominant in the conglomerate, although frequently of a paler type of dolomite than the adjoining dolomitic limestone.

Some details of the main rock-types are presented below.

GREENSTONE

Greenstone occurs on several small islands along a north-south line east of Skålvær (Plate I). The southernmost point where greenstones have been observed is on Grundværsnavaren, just west of Grundvær, and the northernmost locality on islands east of Ørnøyene (north of Skålvær, where the strike swings north-west). The effusive origin of the greenstones in this belt is fairly obvious, whereas greenstone-like rocks to the west of this, for instance on Bersøy and islands west of Lisøy, are probably metagabbros (p. 23).

The greenstones have a massive or schistose appearance. Where present, the schistosity is vertical-dipping and orientated N-S, parallel with the general strike of the layering. Massive greenstones frequently show pillow- or pillow-like structures (Figs. 2, 3). Definite pillows show sharp boundaries, are rather closely packed and measure up to 0.5 m in diameter (Fig. 2); more dubious smaller structures may represent either broken pillows or fragmented lava flow material, and these show diffuse boundaries (Fig. 3). The groundmass in the latter type of greenstone is unstratified and massive in structure.

The pillows generally have a homogeneous appearance but some of the larger ones (Fig. 2) show selective weathering with a great number of small pits on the surface, concentrated mainly in their central part. This would



Fig. 3. Massive greenstone with diffuse fragmental or pillow structure. Grundværsnavaren. The fragments are 10 to 15 centimetres across.

appear to be due to a higher content of carbonate minerals in the interior of the pillows.

A light to medium green colour is typical for the greenstone, pillows as well as groundmass. Mineralogically, it consists of varying amounts of albite, epidote, actinolite and chlorite and minor amounts of sphene and ore minerals. Carbonate is present in some specimens. The carbonate is mainly calcite but occasionally an ankeritic dolomite is present together with the calcite.

The chemistry of the greenstone has been investigated by the analysis of major elements in 3 specimens; these are shown in Table 1. Some trace elements of two of these rocks are listed in Table 2.

DARK CRYSTALLINE LIMESTONE AND MARBLE

According to the cross-section shown in Plate I, all carbonate rocks belong to one and the same stratigraphical unit. This interpretation seems probable but it cannot be proven beyond doubt.

The carbonate belt from Omnøy to Stakkøy in the central part of the area consists of fine-grained, dark and mostly dolomitic crystalline rocks. This is also true for rocks adjacent to the greenstones east of Skålvær, although in this case the calcite content is higher. In the eastern (Grundvær) and western (Kilvær-Tåvær) belts the carbonate rocks are generally calcitic, coarser grained and of a pale grey colour. As far as grain-size and colour are concerned, this is reflecting the increase in metamorphic grade outwards from the central parts of the Skålvær area. Also north of Kilværfjorden the marbles are gen-

Table 1. Chemical composition of greenstones, Skålvær¹ compared with average Storøya greenstone² and Skei greenstone², Leka, and with average ocean floor basalt³ and average island arc tholeiite⁴

Wt %	72-40	72-08	72-24	Storøya greenstones	Skei greenstones	Average Ocean Floor Basalt	Average Island Arc Tholeiite
SiO ₂	51.18	49.03	49.76	45.78	49.72	49.61	52.86
TiO ₂	0.64	1.78	1.57	2.77	1.47	1.43	0.83
Al ₂ O ₃	15.07	15.18	14.38	17.47	16.76	16.01	16.80
Fe ₂ O ₃	0.19	0.78	1.26	5.49	2.49	} 12.63 ⁵	} 11.45 ⁵
FeO	7.81	9.36	9.77	6.78	7.78		
MnO	0.12	0.19	0.19	0.11	0.17	0.18	
MgO	9.47	6.72	7.99	4.19	5.45	7.84	6.06
CaO	10.53	11.72	9.33	9.34	4.71	11.32	10.52
Na ₂ O	3.25	3.09	4.00	3.39	3.61	2.76	2.08
K ₂ O	0.23	0.12	0.29	0.85	0.24	0.22	0.44
H ₂ O-	0.04	0.05	0.00	0.19	0.22		
H ₂ O+	1.69	1.56	1.57	2.29	3.32		
CO ₂	0.03	0.74	0.11	1.69	3.64		
P ₂ O ₅	0.01	0.08	0.09	n.d.	n.d.	0.14	
Total	100.26	100.40	100.31	100.04	100.58		

¹ Analyst: P.-R. Graff, Geol. avd., Norges geologiske undersøkelse.

² Average of 9 Storøya greenstones and 5 Skei greenstones, Leka, calculated from Prestvik (1974).

³ From Cann (1971).

⁴ From Pearce (1975).

⁵ Total iron as Fe₂O₃.

Specimen localities:

72-40: Grunnværsnavaren (Coordinates on 1 : 100 000 map H 17: 1°28' E. of Oslo, 65°49')

72-08: Lamskinnet (1°28' E, 65°51,5' N)

72-24: Ovnskjæret (1°28' E, 65°50,5' N)

Table 2. Trace element data of two greenstones, Skålvær¹, compared with average data of Storøya and Skei greenstones, Leka², and with average ocean floor basalt³ and low potassium tholeiite⁴

Specimen	Rb	Sr	Ba	Zr	V	Ni	Co	Cu	Zn	Cr	Y
72-08	0	135	0	105	300 ⁵	45	30 ⁵	0	98	158	33
72-40	3	77	30	32	200 ⁵	102	60 ⁵	18	61	399	16
Storøya greenstones	19	410	125	220	300	90	40	55	-	-	-
Skei greenstones	10	115	45	65	385	30	35	60	-	-	-
Average OFB	1	130	14	95	-	97	-	77	-	297	29
Average LKT	5	207	-	52	-	-	-	-	-	160	19

¹ Analyses performed at Kjem. Avd., Norges geologiske undersøkelse, X-ray fluorescence method by G. Faye & M. Ødegård.

² Average of 8 Storøya greenstones and 5 Skei greenstones according to Prestvik (1974).

³ From Cann (1971).

⁴ From Pearce (1975).

⁵ Semi-quantitative determination by optical spectrography.

Specimen localities:

72-08 and 72-40, see Table 1.



Fig. 4. Impure (?) marble with lensoid fragments of calcite marble. Grundvær.

erally grey, coarse-grained, calcitic rocks in accordance with the increasing metamorphic grade to the north.

Mineralogically the dark, fine-grained variety is composed of dolomite + calcite + muscovite \pm chlorite \pm quartz + pyrite + black organic 'dust'. The light grey marbles contain the same minerals with the exception of the black dust and in most cases with biotite replacing chlorite. The change from a dolomitic rock-type to a more calcitic one seems to be gradual. A support for this view that the light grey, coarse marbles have been transformed from the dark carbonate rocks in the central area by metamorphic processes is found in the Grundvær area where fragments or 'nodules' of dark carbonate with organic material are locally found as remnants within the light marble. The carbonate in these dark fragments is mainly calcite.

Types transitional between the dark and light marbles are also found in other localities, for example on Sørvær (north of Kilvær fjorden) where the dark carbonate rocks have been only partially recrystallized, adjacent to quartz veins and in irregular patches, to a lighter-coloured coarse marble.

In the Grundvær area and on some small islands north of Skålvær, a rock-type composed of carbonate lenses in a carbonate groundmass (Fig. 4) is met with. Quartz lenses or pebbles of quartz have also been observed in a few cases. This rock-type is occasionally transitional into conglomerates described below and in the writer's opinion this proves that at least some of the marbles are metamorphosed calc-arenites.



Fig. 5. Calcareous mica schist with scattered pebbles and fragments of marble. Slätterøy, N. of Skålvær.

DOLOMITE CONGLOMERATE AND METAGREYWACKE

Typical conglomeratic rocks are present only on the islands north of Skålvær. No sharp distinction can be drawn, however, between these normal conglomerates and calcareous mica schist with scattered boulders (Fig. 5) in other parts of the map area. The groundmass is largely the same and the pebbles or boulders vary only in abundance, not in type.

Fine-grained, grey-coloured dolomite or metalimestone constitutes the dominant boulder type; in many localities it is the only rock-type present. Clast size varies considerably from small fragments up to cobbles and boulders 20–30 cm across. The boulders are frequently lens-shaped and usually orientated with their longest axis within the schistosity (Fig. 5) although no preferred orientation has been detected. In a few cases quartz or quartzite fragments represent additional clast material. Granitoid pebbles have been observed on one small islet north of Skålvær.

As already mentioned (p. 16) the dolomite pebbles are usually of a somewhat paler colour than is typical for the dolomite and metalimestone described from the stratigraphically underlying unit. Similar types have been observed, however, and it must be concluded that the boulder material is of relatively local provenance and most probably derived from the subjacent metalimestone unit. The granitoid boulders are of a red to grey, medium-grained rock-type and are composed of heavily sericitized feldspar (probably both K-feldspar and plagioclase), quartz, muscovite and biotite (partly altered to chlorite). This rock-type is similar in its strong alteration to the predominant rock-type

in the granitoid massif of Vega, some 20 km to the south. No safe conclusion can be drawn, however, about the origin of these pebbles.

The conglomerate groundmass consists of the same minerals as in the calcareous mica schist, mainly quartz, calcite, micas (occurring as biotite porphyroblasts in some rocks), chlorite, epidote and feldspar (mostly saussuritized plagioclase). Tourmaline and ore grains, commonly pyrite, are the usual accessories. Aggregates of quartz and some aggregates rich in calcite may represent recrystallized rock fragments.

The calcareous mica schist with or without boulders is occasionally laminated or banded, but the usual type is a rather massive rock (Fig. 5) with variations from strongly schistose to almost unfoliated. Judging from composition and structure it seems probable that the rock is a metamorphosed, strongly calcareous, lithic greywacke (Pettijohn 1957) or a calcarenite with transition to true conglomerate.

DARK PHYLLITE AND MICA SCHIST

Phyllite and mica schist form a stratigraphical unit above the calcareous mica schist or metagreywacke (Plate I, cross-section). On a smaller scale, dark phyllite is also intercalated in the metagreywacke unit.

The most common rock-type in this formation is a schistose or fissile dark grey or black phyllite. In some parts of the area a later crenulation cleavage is strongly developed. Especially in its northern parts the formation is represented by typical mica schists with a pronounced foliation. Mineralogically a certain content of carbonaceous matter is typical for the dark phyllite variants, giving a black streak. Quartz is present in considerable amounts in all types of phyllite. Plagioclase, usually albite, is also generally present in small amounts. The relative occurrence of other minerals is partly dependent on the position of the locality within the area and also on the changing metamorphic grade (p. 25). Muscovite, chlorite and biotite are common minerals in the central part of the area, while garnet, chloritoid and staurolite are present in the easternmost districts. Epidote, sphene, tourmaline and pyrite are common accessories. This phyllitic formation probably represents a metamorphosed argillite deposited in a marine environment and generally under somewhat reducing conditions.

QUARTZ KERATOPHYRE

White to grey, fine-grained rocks which probably represent metamorphosed quartz keratophyre are encountered in 4 subareas within the Skålvær area:

1. Buøy and adjoining islands south of Skålvær.
2. Brenna islands, north-west of Skålvær.
3. Kjeøy-Slåtterøy in the Skogsholmen area.
4. The small island Årbrauten, north of Kilværfjorden.

The rocks in question are partly quartz-rich, banded rocks (Fig. 6) and it



Fig. 6. Banded, metamorphosed quartz keratophyre. Hestøy, NE of Skogsholmen.

Table 3. Alkalies and silica content of quartz keratophyres, Skälvær area¹

Weight %	SiO ₂	Na ₂ O	K ₂ O	Specimen no.
1.	74.39	3.10	3.05	72-16
2.	73.87	6.80	0.75	72-32
3.	83.12	4.43	0.73	73-44

¹ Analyst P.-R. Graff, Geol. Avd., Norges geologiske undersøkelse.

Localities:

1. 72-16: Buøy (1°27' E of Oslo, 65°51' N)
2. 72-32: Hestøy (1°20' E, 65°49' N)
3. 73-44: Årbrauten (1°18' E, 65°52' N)

is difficult in the field to distinguish them from normal, metasedimentary quartzites. Banding such as that shown in Fig. 6, is less pronounced on Buøy, but intercalations of metasediments (phyllite and a dolomite layer) indicate a supracrustal origin also for this occurrence.

Quartz, muscovite, biotite and the accessories sphene, apatite and ore minerals are readily identified in thin-section. Albite is present, but because of a lack of twinning the amount cannot be easily determined. Partial chemical analyses of 3 specimens from different localities (Table 3), however, show that the amount of albite must be considerable. The dominance of Na₂O over K₂O in two of the specimens is probably valid for most rocks of this group in the area. Specimen 1 is somewhat atypical in that it has an unusually high muscovite content. The other two are comparable with most published analyses of quartz keratophyres from the Norwegian Caledonides (see Gustavson 1969, pp. 80-85 for a review). The banded varieties most probably

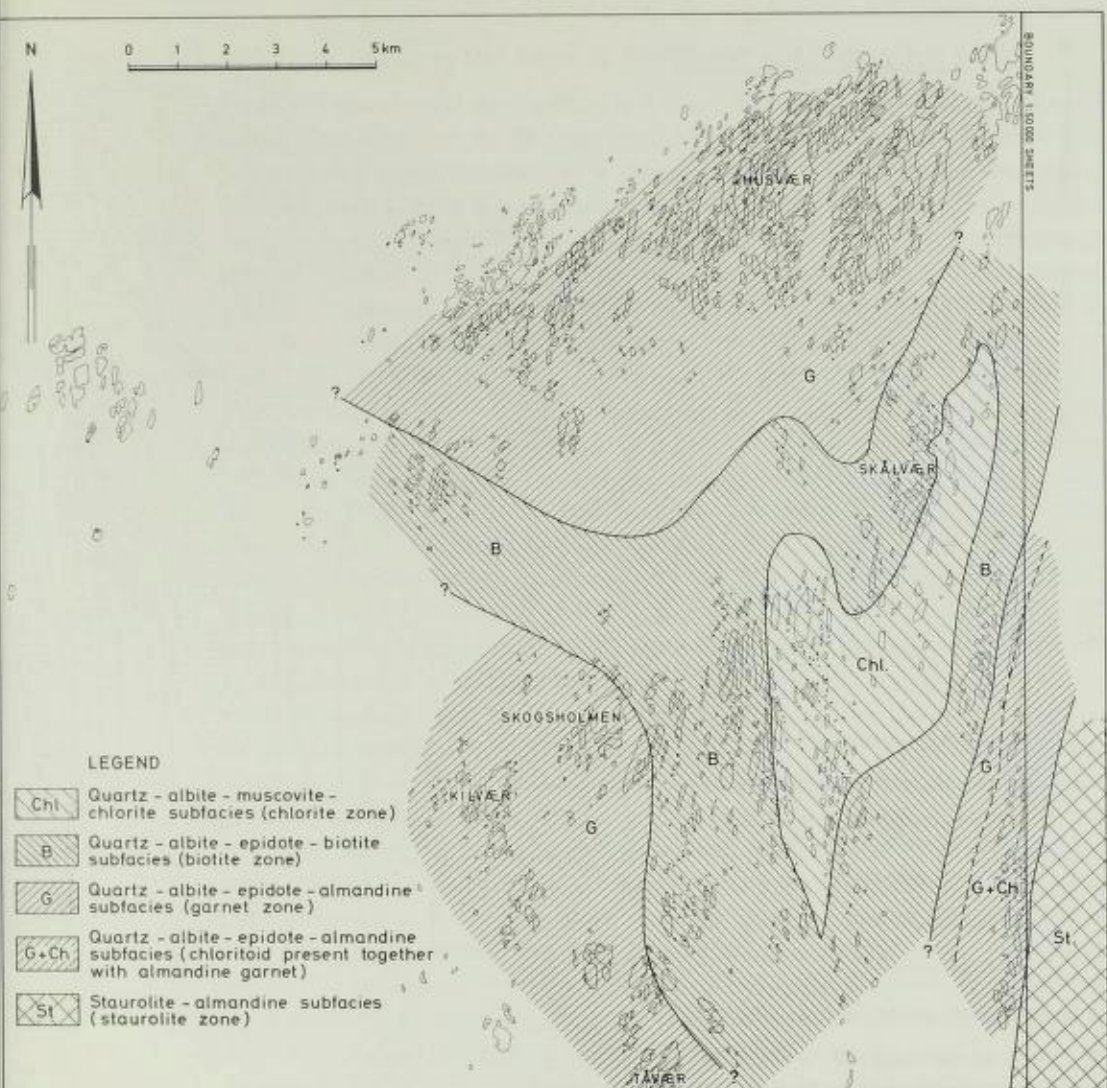


Fig. 7. Metamorphic facies distribution within the Skälvær area.

represent tuff material, whereas the more massive, poorly banded types (Buøy) may conceivably be lavas. Carbonate pebbles in the rock in a couple of localities in the Skogsholmen area show that incorporation of terrigenous sedimentary material may have occurred locally.

INTRUSIVE ROCKS

Within the low-grade area, *metagabbro* is the only intrusive rock-type, except for some rare dyke rocks of uncertain composition which will not be described here.

The metagabbros occur as lenses of different size in the metasedimentary

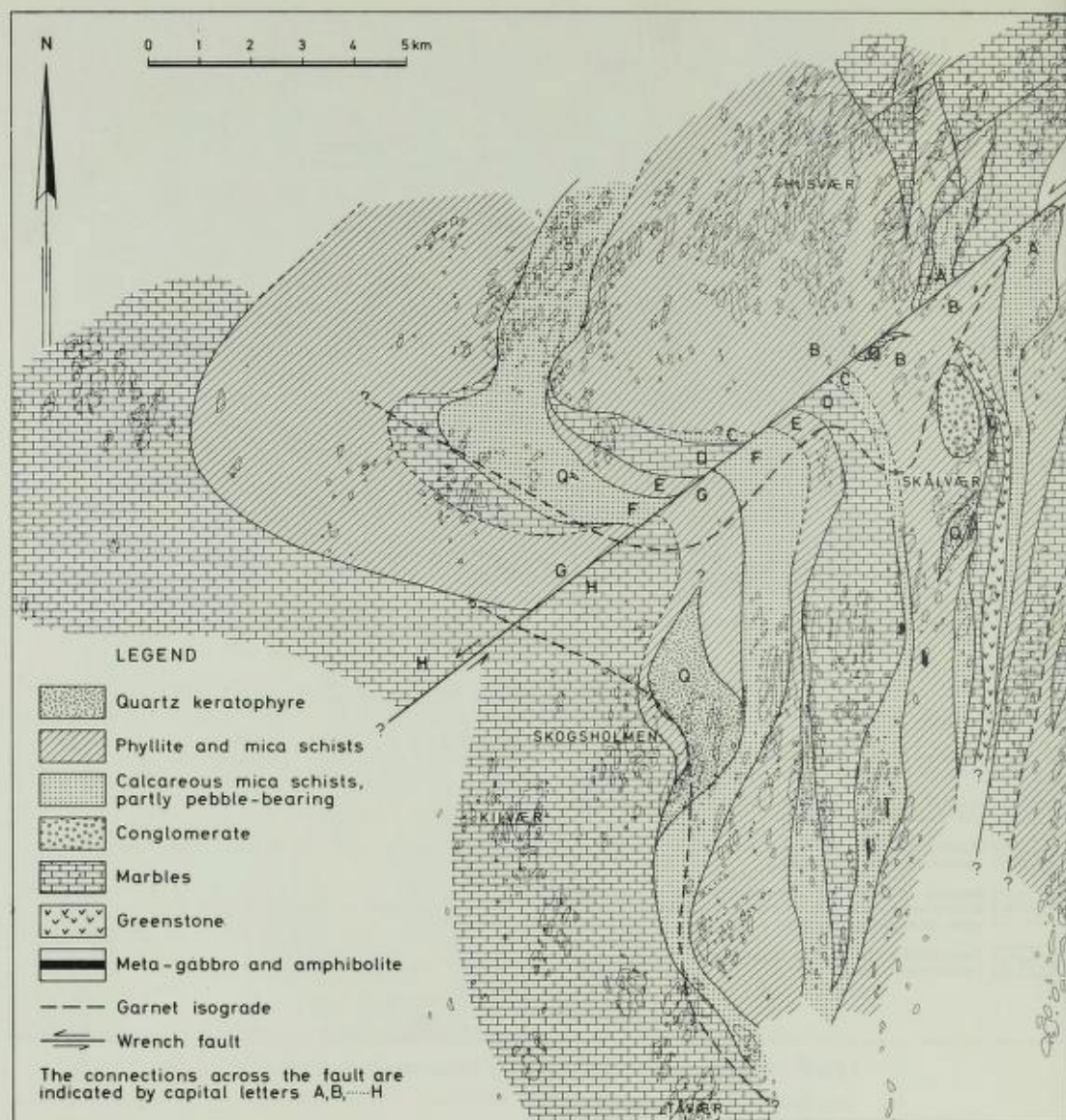


Fig. 8. Interpretation of the geological relationships in the Skålvær and neighbouring areas.

sequence. The lenses are usually small but occasionally form the major part of islands several hundred metres long in the strike direction. Except for the lens shape the rock is very similar to the greenstones but lacks the pillow structure and is always massive and usually coarser grained. The mineral assemblage is the same as in the greenstones: albite, chlorite, actinolite, epidote minerals, calcite and minor amounts of quartz and ore minerals.

A few dykes, from 0.5 to 2 m in thickness, with an appearance similar to the metagabbros have been observed on the northern tip of Skogsholmen and on islands north of Skogsholmen.

Relations between the areas of low-grade and high-grade rocks

From the petrological descriptions it is clear that the metamorphism is lowest in the central part of the Skålvær area, increasing outwards on all sides. The metamorphic facies distribution is shown in Fig. 7. The rocks of the central belt are metamorphosed in the muscovite–chlorite subfacies. The outward increase in metamorphic grade is especially well demonstrated in the eastern part of the map area, with the successive appearance of the biotite, garnet (chloritoid) and staurolite zones. It is noteworthy that chloritoid, which is considered stable throughout the entire greenschist facies of the Barrow-type facies series (Winkler 1965), does not appear here until well into the garnet zone.

Relations to the west and south are less distinctive because of the extensive occurrence of carbonate rocks and the greater distances between the islands, but nevertheless there is a clear tendency towards increasing metamorphic grade also in these directions. The situation to the north, in the strike direction, is of special interest; the author's interpretation of the relationship is shown in Fig. 8. In this reconstruction, a NE–SW fault line is inferred along Kilværfjorden. In general, the rocks north of this fault line are metamorphosed to a higher grade than those in the central Skålvær area. The presence of low-grade rocks just north of the fjord in Sørvær does show, however, that the differences in metamorphic grade are not a consequence of the inferred faulting. There does, in fact, seem to be a general and progressive increase in metamorphism to the north. Except for the greenstones, which have not been detected north of Kilværfjorden, all rock-types from the central area can also be recognized in the northern area, but in a higher metamorphic condition. The dark carbonate rocks of the central area, for example, have been transformed into pale grey, medium- or coarse-grained marbles in the north. In Sørvær (Plate I), transitions between darker, fine-grained and lighter, recrystallized marble can be observed. Phyllites and mica schists with muscovite–chlorite or biotite–muscovite parageneses south of Kilværfjorden are replaced to the north by garnet–mica schists or gneisses. Most important from a stratigraphical point of view is that the calcareous mica schists can be traced into the higher grade areas; this also includes the characteristic carbonate pebble-bearing variant of the schist, an observation which confirms that the same lithostratigraphical sequence is present in the high-grade as in the low-grade areas.

With regard to igneous rocks, these are less frequent in the northern area. Metamorphosed quartz keratophyre has been detected in only one locality on the north side of the fjord, on the small island Årbrauten (Plate I and Fig. 8). Metagabbro bodies are present, as amphibolite, to the north, but are generally smaller than in the central area.

From the structural point of view no significant differences between the central Skålvær area and adjoining areas have been detected.

Correlation of the Skålvær sequence with other areas and discussion of age relations

The medium- to high-grade rocks which surround the Skålvær sequence are very common rock-types in the southern Helgeland region and belong structurally to the Helgeland Nappe Complex. As no tectonic break can be detected, the low-grade rocks must also belong to this nappe. A correlation of the low-grade rocks with the established sequence in other areas can therefore also form a basis for stratigraphical correlations of the high-grade rocks. Such correlations have hitherto been almost impossible or at least very speculative.

So far, very few attempts to determine the probable age of the high-grade sequences have been made. By comparison with the partly fossiliferous Sulitjelma sequence, Bugge (1948) suggested an Upper Cambrian to Lower Ordovician age for the succession of the Rana area. A similar age was assumed, with due reservations, by Ramberg (1967) for the Kongsfjell Group in the Bleikvassli area, NW of Lake Røsvatn (Fig. 1). For the most part, however, such correlation has been restricted to the general assumption that high-grade rocks in Nordland are probably Cambro-Silurian in age (Holtedahl 1953; Strand 1960).

In the present area, according to the most plausible interpretation the greenstone with pillow structures is the lowermost, and probably oldest, member of the Skålvær sequence. In the central Norwegian Caledonides basic volcanics are known to occur mainly at two levels, one in the Lower Ordovician (Tremadocian) and represented by the Støren Group greenstones and its equivalents, and another in the Middle Ordovician (Llanvirn or Llandeilian) which is locally andesitic, e.g. the Hølonda porphyrite (Vogt 1945) of the Lower Hovin Group in the Trondheim Region.

In a description of the Leka area, situated some 90 km to the south of Skålvær, Prestvik (1974) distinguished two greenstone formations with different chemistry and stratigraphical position: the Storøya Formation of pillowed greenstone was correlated with the Støren greenstone of the Trondheim Region, while the greenstone and quartz keratophyre of the Skei Formation were suggested to be equivalents of the Hølonda porphyrite and Hareklett rhyolite tuff, and of other Middle Ordovician greenstones in the Grong-Snåsa area.

With regard to the 3 Skålvær greenstone analyses, on an alkali-silica diagram these plot in the field for subalkaline compositions (Irvine & Baragar 1971), while on an AFM diagram they do not show any clear separation into either the calc-alkaline or the tholeiitic fields since they plot along the field boundary of Irvine & Baragar. A comparison of the major elements and some trace elements of the Skålvær samples with those of the greenstones from Leka and with the element contents of average ocean floor and island arc volcanics is shown in Tables 1 and 2.

Table 1 shows that the SiO₂, TiO₂, total iron and K₂O contents of the Skålvær greenstones are similar to the average values of the Skei greenstones.

but differ considerably from the values for these oxides in the Storøya greenstones. The MgO values are higher in the Skålvær greenstones than in any of the Leka volcanics but closer to those of the Skei than to the Storøya greenstones. For Na₂O the values correspond equally well with the Skei and Storøya averages, while for CaO there is better correspondence with the Storøya greenstones. It should be noted here that the CaO values for the Skei greenstones are extremely low.

Of the trace elements the values for Zr, Sr, Cr, Nb and Y are most important for classification purposes (Pearce & Cann 1973). None of the present rocks have been analysed for Nb, and Y and Cr have not been determined for the Leka greenstones. A comparison with these rocks is therefore difficult. Sr values of the two Skålvær specimens correlate fairly well with the average of the Skei greenstones, while Sr of the Storøya greenstones is about four times as high. Sr, however, is considerably mobile during metamorphism and should be used with caution (Pearce & Cann 1973, p. 294). It should be remembered here that the Ca content is exceptionally low in the Skei greenstone. Zr values in the two Skålvær analyses are not comparable but both are somewhat closer to those in the Skei Formation than the Storøya. The same is true for Rb and Ba but in both cases the values are considerably lower for the Skålvær greenstones than for the Leka rocks.

The differences between the trace element values for the two analysed Skålvær greenstones are striking and would seem to indicate that specimens 72-08 and 72-40 represent two different magma types. This is evident when they are compared with the values for average ocean floor basalt and low potassium tholeiite (Table 2). Not much can be said from analyses of major and trace elements in only 2 or 3 specimens, but from Zr, Y and Cr in Table 2 and Ti and P in Table 1 it would seem that 72-08 (and 72-24?) is an ocean floor type basalt while 72-40 is low potassium tholeiite. This is also confirmed by plotting in the Pearce & Cann (1973) discriminant diagrams. This distinction is peculiar because as the map, Plate I, shows, the two lavas seem to belong to the same zone of volcanic rocks. Clearly, more analyses from different parts of the zone are needed in order to solve this problem. Although one cannot reach any safe conclusion based on these few analyses, the comparison of the available major and trace element data would, however, tend to suggest that the Skålvær greenstones may perhaps best be correlated with the greenstones of the Skei Formation. On Leka, these greenstones are stratigraphically overlain by greywackes and calcareous sandstone with some black schist and polymictic conglomerate. The greywackes also display graded bedding and some possible load cast structures (Prestvik 1974, pp. 70-73). A broad correlation of this sequence with the Skålvær succession therefore seems reasonable. Although the most typical polymict conglomerate with pebbles of igneous rocks (greenstone, quartz keratophyre, etc.) is absent in the Skålvær area, the metagreywackes, partly calcareous and partly with a conglomeratic development in both areas, point to a fairly similar depositional environment. Marble layers are also present in both areas but they are more abundant in the Skålvær area than on Leka.

On Leka, the quartz keratophyres seem to be more closely associated with the greenstones than is the case in the present area. According to the writer's interpretation, the quartz keratophyres occur as a separate unit in the upper part of the Skålvær sequence. In this respect the relationships are more akin to those of the western Trondheim Region, where the rhyolites and rhyolite tuffs are younger than the Middle Ordovician greenstone and andesite (Vogt 1945; Carstens 1960). In the Hølonde-Hørg district of the Trondheim Region, greywacke-sandstones and shales have been described by Chaloupsky (1970) from the Krokstad Group (Middle Ordovician) and the Lower Sandå Group (Upper Ordovician). Polymict conglomerate or breccia are described from both groups. Similar lithologies are met with in other parts of the Trondheim Region (Roberts et al. 1970).

Lithologies similar to those in the Skålvær sequence have been described from the Hattfjelldal area east of the Helgeland Nappe Complex (Strand 1953, 1955). These rocks are situated structurally within the Köli part of the Seve-Köli Nappe and link up with low-grade rocks of the Grong area (Foslie & Strand 1956). The stratigraphy of the Köli rocks has been comprehensively described from the Björkvatten - Virisen area of Sweden (Fig. 1) by Kulling (1933, 1955, 1958). Recent investigations, especially by Zachrisson (1964, 1969), have made possible the correlation of areas to the south and west (towards the Norwegian border) with the Björkvatten - Virisen stratigraphy. Correlations with the western Trondheim Region were proposed by Gee & Zachrisson (1974).

Although situated within different structural units, it seems possible to correlate the Skålvær greenstone with parts of the Seima greenstones of S. Västerbotten (Kulling 1933). This fits in with a correlation of the Skålvær metagreywackes and conglomeratic rocks with the Gilliks Group. Rocks probably corresponding to the Gilliks Group are also present in the Hattfjelldal area (Strand 1963).

According to Kulling (1972, p. 244) certain fossil findings in the Gilliks Group 'lead to the conclusion that the Gilliks Group rocks are probably not older than Caradocian. It may be mentioned that the Slättdal-Vojtja rocks above the Gilliks Group are Upper Ashgillian'. In accordance with this, a correlation of the Skålvær conglomerate and metagreywackes with the Lower Sandå Group (as defined by Chaloupsky 1970) seems to be probable. This view corresponds roughly with earlier correlation of the Gilliks conglomerates with the Volla Conglomerate (Kulling 1955). If the conglomerate of the Skålvær area is an approximate time-equivalent of the Volla Conglomerate of the Hølonde-Hørg area, then the quartz keratophyre may be more or less the same age as the Grimsås Rhyolite (Vogt 1945). As the acid volcanics are the uppermost formation in the Skålvær sequence, however, a precise correlation of this unit is difficult. In the Västerbotten area of Sweden for instance, there are acid volcanics also in the Silurian, e.g. the Stekenjokk Quartz-keratophyres of the Lasterfjäll Group (Zachrisson 1964, 1969). A summary of the various proposed correlations is shown in Table 4.

Table 4. Tentative correlation of S. Helgeland low-grade and high-grade sequences with the successions from some other areas in the central part of the Scandinavian Caledonides

Helgeland Nappe Complex (this paper)		Leka	Central Västerbotten (Kulling	Western Trondheim region (Vogt		
Skålvær area	High-grade part	Prestvik (1974)	1933, 1955, 1958, 1972)	1945) ¹		
?			Viris quartzite Lövfjäll phyllite Broken phyllite and sandst. (F) ²	Sandå shale and sandstone Lyngstein conglomerate.	Horg Group	Llandoverly
Quartz keratophyllite mica schist tagreywacke dolomite conglomerate.	Mica schist and gneisses Calcareous mica sch. and calcareous conglomerate.	Greywackes and calcareous sandst. with dark schist and congl. layers.	Slättdal limest. (F) ² Vojtja conglom. Gilliks Group	Hovin sandstone Grimås rhyolite Volla congl. Tømme beds (F) ² Esphaug & Hareklett rhyolite tuffs Svartjern limest. Krokstad sandst. and shale Stokkvola congl. ³	Upper Hovin Group	Ashgill
Dolomite and quartzite marbles	Marbles				Lower Hovin Group	Caradoc
Limestone	(Amphibolites)	Skei greenstone and quartz keratophyre	Seima greenstones	Hølanda andesite. Hølanda limest. ² Hølanda shale Breccia. Langeland slate (F) ²		Llandeilo
?		Feldspathic sandstone Marble				Llanvirn
	Serpentinite conglomerate Quartzite	Polymict conglomerate	Rotik serpentinite congl. Quartzite congl.	Venna congl.		Arenig
	Rørskar amphibolites	Storøya greenst., agglomerate		Støren greenst.	Støren Group	Tremadoc
	Mica schists and gneisses with some marbles	Pelitic rocks and marble (Solsemøyene)		<i>Tectonic bound.</i> ⁴ Schists and gneisses	Gula Group	Cambro-Ordovician? ⁴ or Cambrian

Adjustments have been made because of new fossil evidence.

¹Dated by fossils (F).

²According to Roberts (1975).

³According to Gale & Roberts (1974).

Turning to the high-grade rocks of the Helgeland Nappe Complex, a direct continuation of the Skålvær sequence in the strike direction to the north has already been described. For other parts of the nappe complex, correlation is more difficult. The presence of dolomite or limestone conglomerate in association with calcareous mica schist of the type described from Skålvær in various places within the Helgeland Nappe Complex may form a basis for further

correlation of these and adjoining rocks with parts of the Skålvær sequence (Table 4). In the eastern parts of the nappe complex (Gustavson & Grønhaug 1960; Gustavson 1973), the dunite conglomerate of Rörskarakselen ('R' on Fig. 1) may be a metamorphosed equivalent of the Lower Ordovician serpentine conglomerate of Otta (Strand 1951) and of a similar conglomerate occurring in the Ro Series of the Björkvatten-Virisen area (Kulling 1933, 1958). In the latter area the serpentine conglomerate is frequently associated with quartzite conglomerate. In the dunite conglomerate localities at Rörskarakselen, a quartzite is present immediately east of the conglomerate and can be followed for some kilometres to the north-east. A correlation of this dunite conglomerate/quartzite association with the serpentine and quartzite conglomerates of the Ro Series would seem quite reasonable.

Some 3 to 4 km west of the Rörskarakselen dunite conglomerate thick and extensive amphibolite layers occur within the succession. The present author has suggested that these might possibly represent metamorphosed lava (Gustavson 1973, p. 29). The presence of serpentinite bodies in the vicinity of the amphibolite layers may indicate a position relatively low in the stratigraphical column here, as serpentinitic intrusions tend to occur mainly in the older part of the sequence (Strand 1960, p. 176). It is also possible that the amphibolites of Rörskaret may be equivalent to the Lower Ordovician Storen greenstones of the Trondheim Region.

Although the preceding discussion has intended to show that a better correlation of the high-grade rocks of the Helgeland region now appears possible, much more work is required from the high-grade areas before a detailed and reliable stratigraphy can be presented. Table 4 must therefore be considered as rather tentative. The most difficult problem in future work will obviously be the positioning within the stratigraphical column of the considerable thicknesses of mica schists and gneisses. Present evidence would seem to indicate that these rocks occur both in the upper and in the lower part of the succession. For the lowermost parts of the high-grade succession (mica gneisses and marbles) a Precambrian age should also be considered.

Strand (1960) divided the eugeosynclinal rocks of the Norwegian Caledonides into two facies types: the Trondheim Region facies and the Nordland facies. Typical of the former are metasediments of greywacke-type and abundant basic volcanics, while thick sequences of metalimestones, dolomites and iron ore horizons are most characteristic of the latter. Strand (1972), however, also noted that, 'Volcanic rocks also occur in the Nordland sequences, especially in the lower parts, while rather thick limestones occur in the upper part of the sequence in the Trondheim region. There is perhaps no fundamental difference between the two type sequences'. The present work would appear to provide support for this latter reservation: because of their transitions into a typical Nordland facies sequence and their structural connection to the Helgeland Nappe Complex, the low-grade metavolcanics and metasediments of the Skålvær area, with their undoubted Trondheim region characteristics, provide some form of link between the two facies types.

Conclusions

The most important conclusions which can be drawn from the present study are as follows:

1. The low-grade rocks of the Skålvær area belong to the Helgeland Nappe Complex and not to a lower tectonic unit, i.e. Köli, which might be suggested from earlier knowledge of the S. Helgeland Region (Strand 1960).
2. Correlation of the low-grade sequence with Ordovician sequences in Central Västerbotten and in the western Trondheim Region seems probable.
3. Direct connections between low-grade and medium- to high-grade sequences in the coastal area show that at least parts of the high-grade sequence probably belong to the Ordovician.
4. From the stratigraphical correlations, it follows that the Helgeland Nappe Complex and the Seve-Köli Nappe Complex are to some extent composed of the same formations, although these are usually in a considerably higher metamorphic grade in the Helgeland Nappe Complex.
5. The Skålvær area may form a link between the Trondheim Region facies and the Nordland facies of eugeosynclinal deposits as defined by Strand (1960).

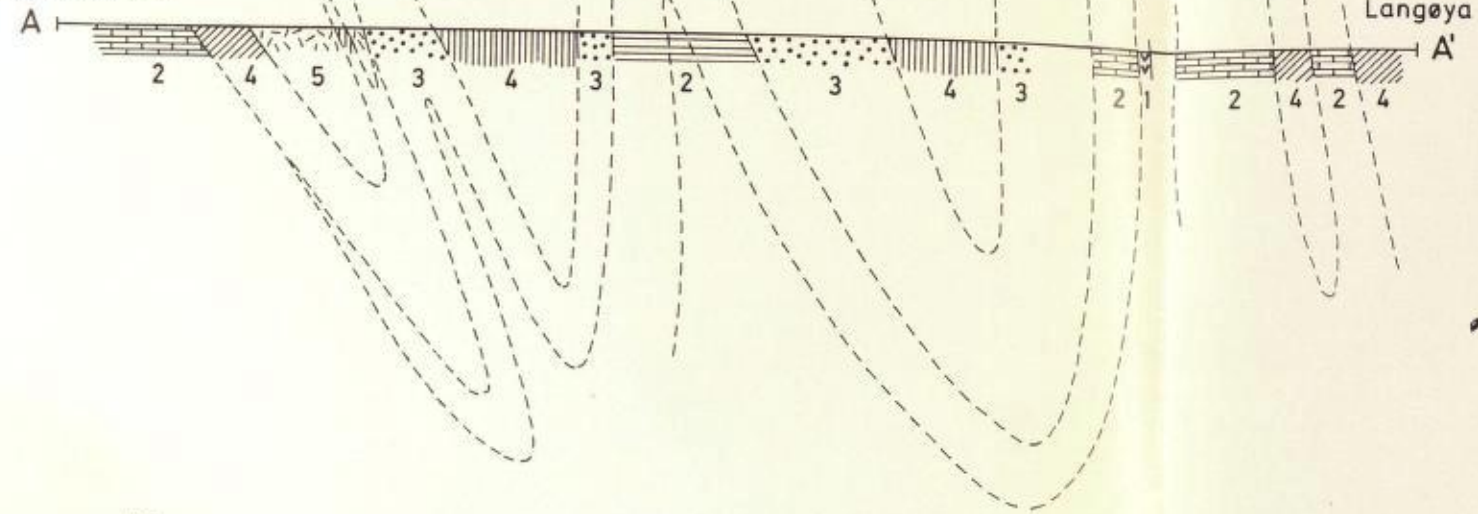
Acknowledgements. – I am greatly indebted to Dr. David Roberts for his critical comments and correction of the English in the first draft of the manuscript. I also wish to thank Professor Trygve Strand and Dr. George Gale for constructive criticism of the manuscript.

REFERENCES

- Birkeland, T. 1958: Geological and petrological investigations in northern Trøndelag. *Norsk geol. Tidsskr.* 38, 327–420.
- Bugge, J. A. W. 1948: Rana Gruber. Geologisk beskrivelse av jernmalmfeltene i Dunderlandsdalen. *Norges geol. Unders.* 171, 149 pp.
- Cann, J. R. 1971: Major element variations in ocean-floor basalts. *Phil. Trans. Roy. Soc. (London)* A 268, 495.
- Carstens, H. 1960: Stratigraphy and volcanics of the Trondheimsfjord area, Norway. *Norges geol. Unders.* 212b, 22 pp.
- Chaloupsky, J. 1970: Geology of the Holonda-Hulsjøen area, Trondheim Region. *Norges geol. Unders.* 266, 277–304.
- Foslie, S. & Strand, T. 1956: Namsvatnet med en del av Frøyningsfjell. *Norges geol. Unders.* 196, 82 pp.
- Gale, G. H. & Roberts, D. 1974: Trace element geochemistry of Lower Palaeozoic basic volcanics and its tectonic implications. *Earth Planet. Sci. Letters* 22, 380–390.
- Gee, D. G. & Zachrisson, E. 1974: Comments on stratigraphy, faunal provinces and structure of the metamorphic allochthon, central Scandinavian Caledonides. *Geol. Fören. Stockholm Förh.* 96, 61–66.
- Gustavson, M. 1966: The Caledonian mountain chain of the Southern Troms and Ofoten areas. Part I. Basement rocks and Caledonian metasediments. *Norges geol. Unders.* 239, 162 pp.
- Gustavson, M. 1969: The Caledonian mountain chain of the Southern Troms and Ofoten areas. Part II. Caledonian rocks of igneous origin. *Norges geol. Unders.* 261, 110 pp.
- Gustavson, M. 1972: The Caledonian mountain chain of the Southern Troms and Ofoten areas. Part III. Structures and structural history. *Norges geol. Unders.* 283, 56 pp.

- Gustavson, M. 1973: Borgefjell. Beskrivelse til det berggrunnsgeologiske gradteigskart J 19 - 1 : 100 000. *Norges geol. Unders.* 298, *Skrifter* 8, 43 pp.
- Gustavson, M. 1975: Helgelandsflesa. (Bedrock map, scale 1 : 100 000). *Norges geol. Unders.*
- Gustavson, M. & Gronhaug, A. 1960: En geologisk undersøkelse på den nordvestlige del av kartblad Borgefjell. *Norges geol. Unders.* 211, 26-74.
- Holtedahl, O. 1953: Norges geologi. Bind I. *Norges geol. Unders.* 164, 583 pp.
- Irvine, T. N. & Baragar, R. A. 1971: A guide to the Chemical Classification of the Common Volcanic Rocks. *Can. Journ. Earth Sci.* 8, 523-548.
- Kollung, S. 1967: Geologiske undersøkelser i sørlige Helgeland og nordlige Namdal. *Norges geol. Unders.* 254, 95 pp.
- Kulling, O. 1933: Berggrunden inom Björkvattnet-Virisenområdet i Västerbottenfjällens centrala del. *Geol. Fören. Stockholm Förh.* 55, 167-422.
- Kulling, O. 1955: Den kaledoniska Fjällkedjans berggrund inom Västerbottens län. *Sveriges geol. Unders. Ser. Ca.* 37, 101-296.
- Kulling, O. 1958: Om begreppen Voitjakonglomerat, Rokonglomerat och Mesketlava i Västerbottenfjällen. *Geol. Fören. Stockholm Förh.* 80, 226-234.
- Kulling, O. 1972: The Swedish Caledonides. In: Strand, T. & Kulling, O.: *Scandinavian Caledonides*, 149-285. Wiley - Interscience, London.
- Myrland, R. 1972: Velfjord. Beskrivelse til det berggrunnsgeologiske gradteigskart I 18 - 1 : 100 000. *Norges geol. Unders.* 274, 30 pp.
- Nicholson, R. & Rutland, R. W. R. 1969: A section across the Norwegian Caledonides; Bodø to Sulitjelma. *Norges geol. Unders.* 260, 86 pp.
- Nissen, A. L. 1965: En petrografisk-mineralogisk undersøkelse i området syd for Majavann, spesielt granaters sammensetning under regional metamorfose. *Norges geol. Unders.* 234, 103-159.
- Nissen, A. L. 1974: Mosjøen. Beskrivelse til det berggrunnsgeologiske gradteigskart I 17 - 1 : 100 000. *Norges geol. Unders.* 307, *Skrifter* 12, 29 pp.
- Pearce, J. A. 1975: Basalt geochemistry used to investigate past tectonic environments on Cyprus. *Tectonophysics* 25, 41-67.
- Pearce, J. A. & Cann, J. R. 1973: Tectonic setting of basic volcanic rocks determined using trace element analyses. *Earth and Planet. Sci. Letters* 19, 290-300.
- Pettijohn, F. J. 1957: *Sedimentary Rocks* Sec. ed. Harper & Brothers, New York.
- Prestvik, T. 1972: Alpine-type mafic and ultramafic rocks of Leka, Nord-Trøndelag. *Norges geol. Unders.* 273, 23-24.
- Prestvik, T. 1974: Supracrustal rocks of Leka, Nord-Trøndelag. *Norges geol. Unders.* 311, 65-87.
- Ramberg, I. B. 1967: Kongsfjellområdets geologi, en petrografisk og strukturell undersøkelse i Helgeland, Nord-Norge. *Norges geol. Unders.* 240, 152 pp.
- Rekstad, J. 1917: Vega. Beskrivelse til det geologiske generalkart. *Norges geol. Unders.* 80, 85 pp.
- Roberts, D. 1975: The Stokkvola conglomerate — a revised stratigraphical position. *Norsk geol. Tidsskr.*, in press.
- Roberts, D., Springer, J. & Wolff, F. C. 1970: Evolution of the Caledonides in the northern Trondheim region, Central Norway: a review. *Geol. Mag.* 107, 2, 133-145.
- Rutland, R. W. R. & Nicholson, R. 1965: Tectonics of the Caledonides of part of Nordland, Norway. *Quart. Journ. Geol. Soc.* 121, 73-109.
- Strand, T. 1951: The Sel and Vågå map areas. *Norges geol. Unders.* 178, 116 pp.
- Strand, T. 1953: Geologiske undersøkelser i den sydøstligste del av Helgeland. *Norges geol. Unders.* 184, 124-141.
- Strand, T. 1955: Sydøstligste Helgelands geologi. *Norges geol. Unders.* 191, 56-70.
- Strand, T. 1958: Greenschists from the south-eastern part of Helgeland, Norway, their chemical composition, mineral facies and geological setting. *Norges geol. Unders.* 203, 112-129.
- Strand, T. 1960: The pre-Devonian rocks and structures in the region of Caledonian deformation. In Holtedahl, O. et al.: *Geology of Norway*. *Norges geol. Unders.* 208, 170-278.
- Strand, T. 1963: Noen stratigrafiske aldersspørsmål i Grongfeltet og i den sydøstligste del av Helgeland. *Norges geol. Unders.* 223, 294-297.

Skogsholmen

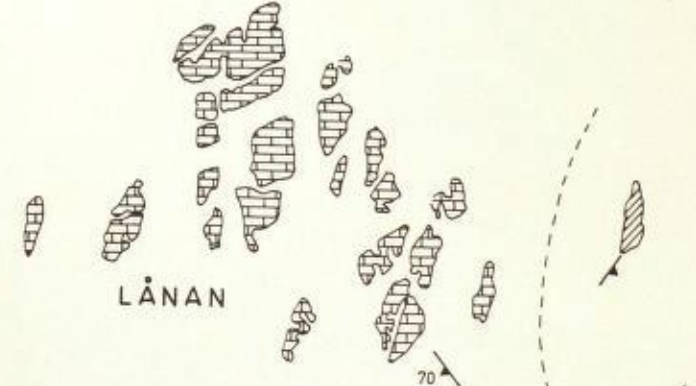


Langøya

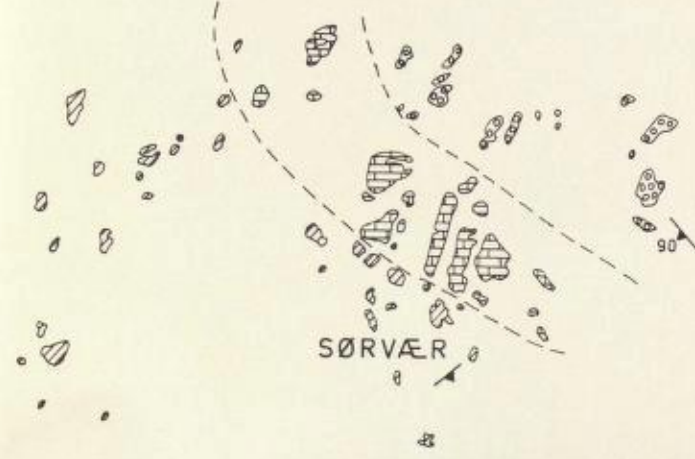
N



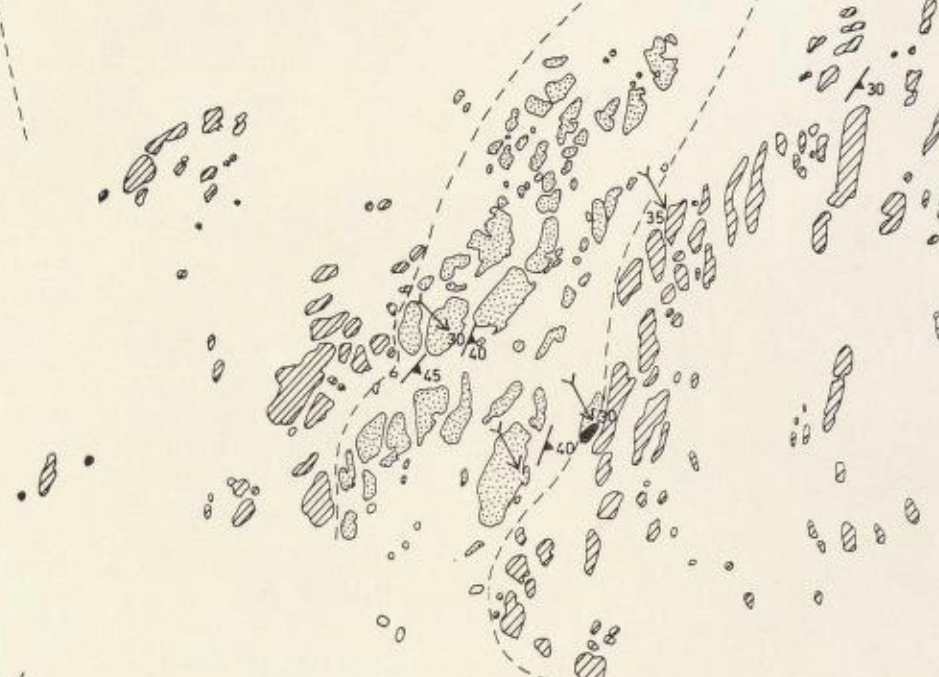
LÅNAN



SØRVÆR



Årbrauten



Husvæn



Brenna



Ørnøyene

SKÅLVÆR



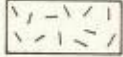


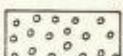
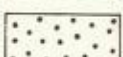

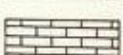
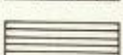

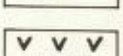
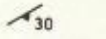


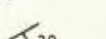
Buøy



RDEN

KILVÆRFJORDEN

LEGEND

- 5  Quartz keratophyre
- 4  Mica schists and gneisses, frequently garnet-bearing
- 4  Dark phyllite and mica schist (without garnet)
- 3  Conglomerate
- 3  Calcareous meta-greywacke, partly pebble-bearing
- 3  Calcareous mica schist or gneiss
- 2  Grey calcite and dolomite marble, medium or coarsegrained
- 2  Dark, finegrained marble, frequently dolomitic
-  Meta-gabbro and amphibolite
- 1  Greenstone
-  30 Strike and dip of foliation, usually parallel to bedding
-  Vertical foliation
-  15 Fold axis, angle of plunge shown
-  30 Strike and dip of bedding

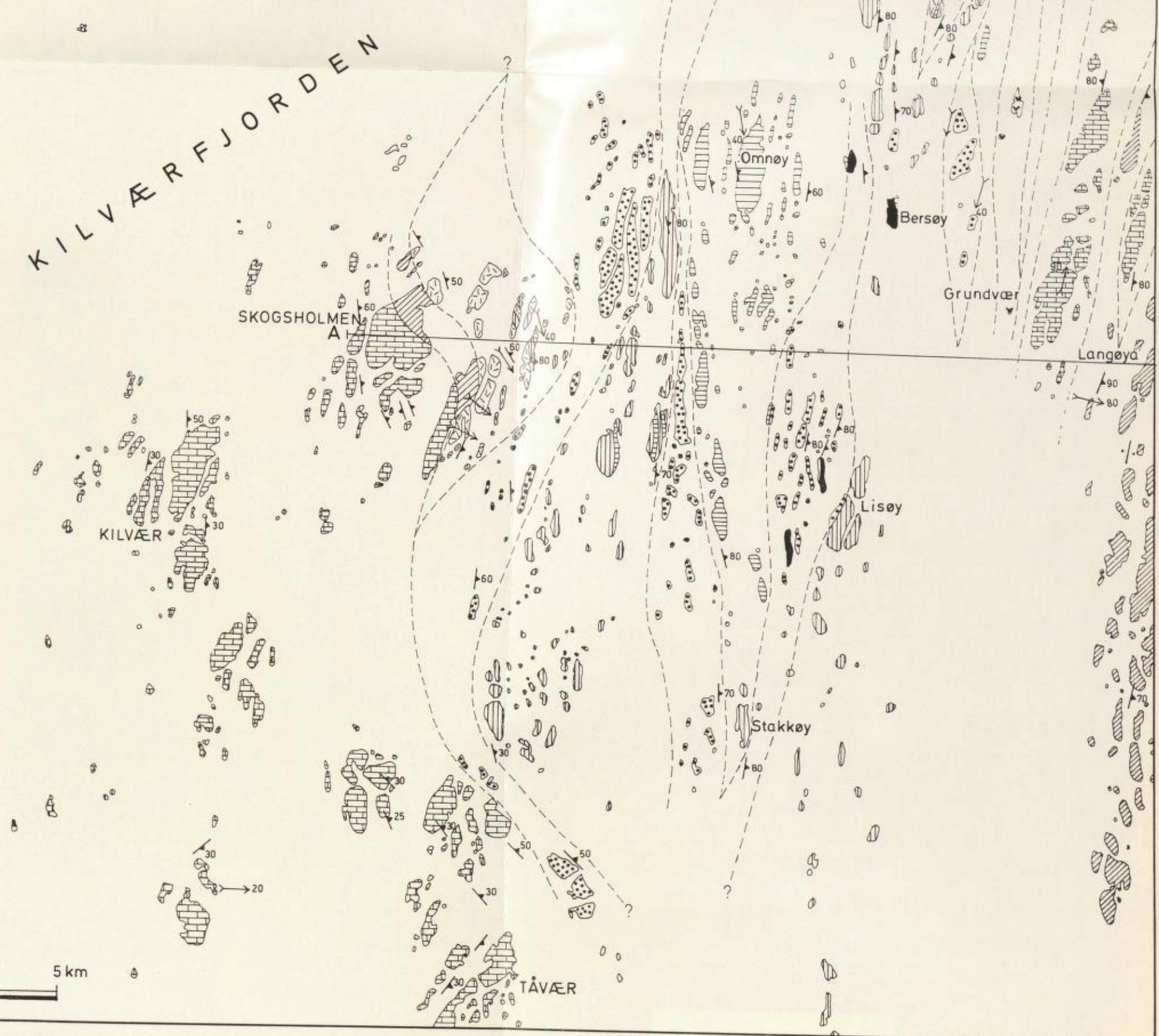


Plate I. Geological map of the Skålvær area and cross section showing the interpreted structural interrelationships of the main lithological units.

- Strand, T. 1972: The Norwegian Caledonides. In Strand, T. & Kulling, O.: *Scandinavian Caledonides*. Wiley-Interscience, London.
- Vogt, T. 1945: The geology of part of the Hølanda-Hørg district, a type area in the Trondheim Region. *Norsk geol. Tidsskr.* 25, 449-527.
- Winkler, H. G. F. 1965: Die Genese der metamorphen Gesteine. Springer Verlag, Berlin. Heidelberg.
- Zachrisson, E. 1964: The Remdalen syncline. Stratigraphy and tectonics. *Sveriges geol. Unders. Ser. C 596*, 33 pp.
- Zachrisson, E. 1969: Caledonian geology of Northern Jämtland - Southern Västerbotten. Köli stratigraphy and main tectonic outlines. *Sveriges geol. Unders. Ser. C 644*, 33 pp.
- Zachrisson, E. 1973: The westerly extension of Seve rocks within the Seve-Köli Nappe Complex in the Scandinavian Caledonides. *Geol. Fören. Stockholm Förh.* 95, 243-251.

Faint, illegible text at the top of the page, possibly a header or introductory paragraph.

Determination of Major and Trace Elements in Rocks Employing Optical Emission Spectroscopy and X-ray Fluorescence

GJERT CHR. FAYE & MAGNE ØDEGÅRD

Faye, G. Chr. & Ødegård, M. 1975: Determination of major and trace elements in rocks employing optical emission spectroscopy and X-ray fluorescence. *Norges geol. Unders.* 322, 35-53.

An optical emission spectrometric method for major element determination and an X-ray fluorescence method for the determination of trace elements are described.

The first method combines a tape machine with a direct reader and uses samples and synthetic standards which have been 'isoformed' by dilution (1 to 12) with Li tetraborate containing Sr tetraborate and Co oxide and fusion. The major element results obtained by this nearly matrix independent method are used in the correction for matrix effects in the trace element procedure where the samples and synthetic standards are diluted by mixing with Li tetraborate (2 to 1) before fusion. The synthetic standards are made from pure chemicals and processed in the same manner as the samples. Matrix effects are corrected for by means of absorption coefficients. Methods of correction based on the use of scattered background or incoherently scattered tube lines (Compton scatter) as intensity reference are also investigated and discussed.

The major elements determined are Si, Al, Fe, Ti, Mg, Ca, Na, K, and Mn. At present the trace element programme includes Zr, Y, Sr, Rb, Zn, Cu, Ni, Cr, and Ba; the programme can easily be extended to include other elements.

Results obtained for major and trace element abundances on some international reference samples and for trace elements in synthetic samples having major element composition quite different from that of the standards are presented.

G. Chr. Faye and M. Ødegård, Geological Survey of Norway, P.O. Box 3006, N-7001 Trondheim, Norway

1. Introduction

From the 1920's and onwards the use of spectrochemical methods for the analysis of geologic material was for a long time concerned with, and confined to, determination of minor or trace constituents. Goldschmidt & Thomassen (1924) used X-ray spectrography for the determination of rare earths and other minor constituents of minerals, and later Goldschmidt and co-workers (Goldschmidt 1930 a, b; Goldschmidt & Peters 1931 a, b, 1932 a, b, c, d, 1933 a, b, c, 1934; Goldschmidt et al. 1933, 1934; Minami 1935; Strock 1936; Noll 1934; Engelhardt 1936) applied both X-ray and optical emission spectrography in the study of the distribution of many minor elements in the earth's crust and in meteorites. By using cathode layer, and very pure carbon electrodes purified by a method very similar to that later described by Gatterer (1941), Goldschmidt was able to detect very low concentrations of many elements by D.C. arc spectrography.

The determination of major constituents by spectrochemical methods was

regarded as less interesting because the high degree of accuracy generally required for such analyses was difficult to attain. Spectrochemical carbon arc methods for determining the major constituents of geologic material were, however, described by Jaycox (1947) and Kvalheim (1947) and further discussed and modified by Ahrens (1954).

The development of direct readers (spectrometers) for industrial metal analysis in the 1940's (Saunderson et al. 1945) was later followed by the introduction of such instruments in slag and rock analysis. Kvalheim & Vestre (1959) applied the ARL Production Control Quantometer to a carbon arc method for determining the major constituents of rocks, and Danielsson et al. (1959) developed the Tape machine for spark analysis of powdered samples of rocks etc., and combined it with a direct reader. This combination has been extensively used by C.R.P.G., Nancy (Govindaraju 1960, 1963, 1965; Roubault et al. 1960, 1964) especially for the analysis of granites, and by Danielsson (1967) for general use in geology and geochemistry. Scott et al. (1969) used the cathode layer carbon arc method in combination with a direct reader for the determination of low concentrations of different elements in soils, etc. Other examples of the use of direct readers in optical spectrochemical analysis of geologic material are given in a paper by Mitchell (1969).

A new era in X-ray analysis began in the late 1940's, mainly due to the work of Friedman & Birks (see Jenkins 1974) and the introduction of Geiger counters. The result was X-ray fluorescence spectrometers, frequently used nowadays for both major and trace element determinations. Because of the instrumental precision of present day direct readers (optical spectrometers and X-ray fluorescence spectrometers) the analyst can concentrate his attention on sample preparation, the selection of suitable spectral lines, the control of the processes occurring in the source of element-characteristic frequency emission (arc, spark, fluorescing sample), and mathematical corrections, in order to achieve maximum accuracy.

Danielsson et al. (1959) used the word 'isoformation' for sample preparations such as dilution and/or fusion which aim at the elimination or reduction of 'matrix effects' (inter-element effects). Unsatisfactory analytical results due to inter-element effects can also be corrected by the use of more or less complicated calculations (see e.g. Birks 1971). Access to a computer for such corrections is a necessity.

The analytical methods, systems or routines to be chosen or developed in different laboratories depend on the equipment available and the analytical tasks in question. At the Geological Survey of Norway the direct readers available are an ARL Production Control Quantometer combined with a Tape machine, and a Philips X-ray fluorescence spectrometer. The analytical problems include the determination of major, minor and trace constituents of minerals, rocks and similar materials, as well as ores. Accuracy is generally more important than speed, but a reasonable analytical speed is also important.

These requirements have led to a routine which is a combination of a quantometer method, in use for many years, with an X-ray fluorescence (XRF)

method. Since the major constituents are still easily determinable after considerable dilution, the samples and standards are diluted and fused with a borate flux and the major elements thereafter determined with the combined Tape machine/Quantometer. The trace constituents are determined by X-ray fluorescence. To avoid too much loss of radiation intensity the samples are, in this case, fused with only a small amount of Li tetraborate. Because of the slight dilution, matrix effects from the major elements can be significant. However, the contents of major constituents are known from the quantometric analysis, and accordingly the matrix effects can be corrected for by using calculations which take into account the influence of the major elements according to their concentrations and absorption coefficients.

2. Major constituents

The constituents SiO_2 , Al_2O_3 , Fe_2O_3 , TiO_2 , MgO , CaO , Na_2O , K_2O and MnO are determined in a variety of geologic material with the ARL Quantometer combined with a tape machine. The method is very similar to the one used by Danielsson et al. (1961) for slags. Fe_2O_3 , CaO , TiO_2 and K_2O are sometimes determined by X-ray fluorescence, using the same material as prepared for the quantometric determinations, i.e. 1 part of the sample is diluted with 12 parts of borate flux and fused. By this 'isofomation' matrix effects become negligible.

2.1 PREPARATION OF STANDARDS AND SAMPLES

One advantage of preparation by dilution and fusion is that the selection of suitable and reliable standards offers no real problem. Synthetic standards covering the concentration ranges of interest can be readily made from pure chemicals and treated in the same way as the samples.

The synthetic standards referred to in this paper are mixtures of 'specpure' oxides or carbonates. Carbonates are used for Na, K and Ca, oxides for Al, Fe, Mg, Ti and Mn. A powder of high purity natural quartz which has been leached with acids is used for Si. These substances are brought to stoichiometric composition by drying or ignition before being mixed. The hygroscopic oxides Al_2O_3 and MgO are ignited for some hours at 1100°C to render them sufficiently stable.

The dilution and fusion procedure is as follows:

0.25 g of finely pulverized sample or standard is mixed with 3 g of borate flux containing 60% lithium tetraborate, 30% strontium tetraborate and 10% cobalt oxide. The mixture is transferred quantitatively to a non-wettable PtAu crucible, which is placed in a quartz dish and left for 5 minutes in a furnace at 1000°C . Usually 4 or more samples are fused simultaneously. After 5 minutes the crucibles are removed from the furnace and left to cool. The melt is loosened from the crucible and ground for one minute in a steel swing mill together with 0.5 g of Standard grade Whatman cellulose powder. The substance is now ready for the Tape machine, or X-ray analysis.

In certain cases agate or tungsten carbide swing mills are used to prevent contamination of the sample. In addition graphite crucibles can be substituted for platinum crucibles. A furnace for continuous fusion performance instead of batch operation, using graphite crucibles, has been described by Roubault et al. (1964) and Govindaraju (1965).

Sulphides tend to form a separate insoluble phase in the borate flux. Samples containing sulphur are therefore ignited, the ignition loss is recorded, and fusion is thereafter carried out in the normal way.

Carbon present in the sample as amorphous carbon, graphite or some other reducing compound may cause problems when heated in a platinum crucible, not only because of the well-known risk of platinum carbide formation, but also because of the possibility of reduction to the elemental form of elements which can readily alloy with platinum and thus escape determination. The alloying process seems to be reversible for many elements. These elements may be extracted again by other samples and thus cause erroneous analytical results.

This kind of loss or gain is in most cases negligible, but alternate heating and hydrochloric acid treatment of crucibles used for borate fusion, followed by analysis of the elements thus extracted, showed that the alloying possibility is real and should be considered when very accurate analyses are required.

2.2 QUANTOMETER ANALYSES

2.2.1 *Line programme*

Since the permanently installed line programme of the quantometer was intended for both arc and spark work, and with some emphasis on arc methods, our choice of suitable lines for spark work is limited to some extent. For tape machine determination of the major elements in rocks the following lines were chosen:

Reference lines:

Co	3518 Å
Li	4972 Å
Sr	4876 Å

Analysis lines:

Si	2881 × 2 Å	Mg	2795 Å	
Si	2514 Å	Ca	3179 Å	
Al	3944 Å	Ca	4454 Å	
Al	3092 Å	Na	3302 × 2 Å	
Fe	4404 Å	K	4044 Å	
Fe	2966 Å	K	7664 Å	(Interference filter and optical fibre)
Ti	3242 × 2 Å	Mn	2801 × 2 Å	
Mg	2779 × 2 Å	Mn	2593 Å	

The choice of reference elements and lines has been based on experience and statistical studies. Li 4972 is used as the reference line for Na 3302, K 4404

and K 7664, Sr 4876 for Ca 4454, and Co 3518 for Ca 3179 and the lines of the remaining elements. The two lines for each of the elements Si, Al, Fe, Ca and Mg usually give very similar, often identical, results. For K and Mn the lines K 7664 and Mn 2593 were found to be more reliable than K 4044 and Mn 2801.

2.2.2 Instrumentation

The equipment used for the quantitative determinations at NGU is:

ARL 7200 S Production Control Quantometer
with digital voltmeter and printer.
Primary slit: 38 microns.
Secondary slits: 75 microns.

ARL Tape machine, somewhat modified.
Tape: Edaplast spectrotape.
Tape speed: 20 cm/second.

Source: ARL No. 4600.

Conditions: 15000 V, sparks per second.

Automatic termination by the Co-integration
(i.e. Co-integrator reads 50 mV). The corresponding
exposure time is approximately 25 seconds.

2.2.3 Calculations

Because of the extensive isoformation by dilution and fusion, the calculation or reading of concentrations from the intensity data recorded by the printer is a relatively simple process since matrix effects need not be considered. However, the data handling involved — conversion of the intensity data to intensity ratios, plotting and construction of a number of analytical calibration curves, and the reading of the percentages — is a time-consuming process which, with considerable advantage, can be left to a computer. At the Geological Survey this is done by basing the computer programme on an analytical evaluation function according to a simple equation of the second order. The intensity data of standards and samples to be analysed is punched on cards and fed to the computer.

An additional advantage of a computer is that the analytical results can be produced on punched cards. These punched cards serve two purposes. They are used for the mathematical matrix corrections in the determinations of the trace constituents of the same sample (see later), and they are also convenient for various statistical studies.

2.2.4 Precision and accuracy

The precision measured under favourable conditions during a short period of time is often better than the precision experienced when the analytical results

Table 1. Precision of the quantometer/tape machine method obtained on 10 fusions of one sample (upper part of Table). Lower part shows precision of the instrument obtained on 10 determinations of one fused sample

	SiO ₂	Al ₂ O ₃	Fe ₂ O ₃	TiO ₂	MgO	CaO	Na ₂ O	K ₂ O	MnO
Mean (10)	47.50	13.68	16.61	1.94	7.23	7.99	2.41	2.31	0.264
s	0.39	0.12	0.13	0.028	0.058	0.042	0.048	0.077	0.0052
s _r (%)	0.8	0.9	0.8	1.4	0.8	0.5	2.0	3.3	2.0
Mean (10)	47.43	13.74	16.73	1.98	7.30	8.15	2.44	2.34	0.263
s	0.66	0.05	0.13	0.027	0.11	0.020	0.049	0.073	0.0048
s _r (%)	1.4	0.4	0.8	1.4	1.5	0.2	2.0	3.1	1.8

Table 2. Results obtained with the quantometer/tape machine method on USGS reference samples

	SiO ₂	Al ₂ O ₃	Fe ₂ O ₃	TiO ₂	MgO	CaO	Na ₂ O	K ₂ O	MnO	
G-2	68.5	14.7	2.4	0.46	0.65	1.80	4.00	4.35	0.02	NGU
	69.11	15.40	2.65	0.50	0.76	1.94	4.07	4.51	0.03	Recom. val.
GSP-1	67.6	15.0	4.2	0.64	1.05	1.95	2.75	5.30	0.03	NGU
	67.38	15.25	4.33	0.66	0.96	2.02	2.80	5.53	0.04	Recom. val.
AGV-1	59.0	17.6	6.8	1.06	1.40	4.80	4.20	3.00	0.10	NGU
	59.00	17.25	6.76	1.04	1.53	4.90	4.26	2.89	0.10	Recom. val.
BCR-1	53.0	13.9	14.0	2.27	3.50	6.75	3.35	1.75	0.20	NGU
	54.50	13.61	13.40	2.20	3.46	6.92	3.27	1.70	0.18	Recom. val.

Table 3. Precision for the quantometer/tape machine method obtained under routine work conditions

	SiO ₂	Al ₂ O ₃	Fe ₂ O ₃	TiO ₂	MgO	CaO	Na ₂ O	K ₂ O
Mean (10)	48.8	13.7	5.39	0.69	6.40	10.0	1.14	2.65
s	0.70	0.27	0.23	0.038	0.25	0.17	0.031	0.18
s _r (%)	1.4	2.0	4.3	5.5	3.9	1.7	2.7	6.8

Table 4. Precision and accuracy for the quantometer/tape machine method obtained on Argillaceous Limestone 1A/1b

	SiO ₂	Al ₂ O ₃	Fe ₂ O ₃	TiO ₂	MgO	CaO	Na ₂ O	K ₂ O
Mean (30)	5.20	4.12	1.58	0.164	2.16	41.16	0.33	0.77
s	0.13	0.14	0.19	0.033	0.11	0.43	0.041	0.12
s _r (%)	2.5	3.4	12.0	20.6	5.1	1.0	12.4	15.6
Recom. val.	4.92	4.16	1.63	0.16	2.19	41.32	0.39	0.71

are collected from routine work over a long period of time. This observation is not uncommon in quantometry.

The precision to be expected under favourable conditions for the quantometric method of this paper is demonstrated in Table 1. The upper part of the Table shows the precision when 10 fusions of the same rock sample are

analysed by the quantometer within about a quarter of an hour. This precision may be regarded as the optimum precision of the quantometer/tape machine method. The lower part of the Table shows the corresponding precision for 10 runs of one fused sample which give the precision of the instrument. From the Table it can be concluded that under favourable conditions the spread of the results is due mainly to instrumental fluctuations. The accuracy obtainable under favourable conditions is shown in Table 2. The results for the four USGS standard samples were obtained from single runs of samples and synthetic standards, all within a short period of time.

Precision and accuracy of this quality cannot be expected for normal routines. For such routines Tables 3 and 4 must be regarded as more realistic. These Tables are based on the analysis of 3 check samples which were intermingled in an analytical routine programme run for a couple of months on a large number of samples ranging in composition from nearly pure limestone to silicate rock.

One silicate rock sample and the NBS Argillaceous limestone standards 1A and 1b were chosen as check samples. The 1b sample was used for SiO_2 only, and 1A for the other components. The check samples (sometimes only one) were analysed about once a day as part of the routine programme. Since the NBS samples are also well known standards, Table 4 gives not only the precision but also a measure of the accuracy obtained.

2.3 DETERMINATION of Fe, Ti, Ca AND K BY X-RAY FLUORESCENCE

The powder prepared for the tape machine is also well suited for X-ray determination of the major elements Fe, Ti, Ca and K. The dilution with borate flux reduces the matrix effect considerably. Acceptable results can therefore be obtained even without the use of reference elements. Since Co is added to the flux this element can readily be used as reference for the Fe determination even though the concentration of Co is high compared with that of iron.

Analytical calibration curves were based on the same synthetic standards as used for the quantometer procedure, and the net intensities of the $K\alpha$ lines were measured. The results obtained on G-2, GSP-1, AGV-1 and BCR-1 are given in Table 5. All determinations are made with a W tube. A LIF (200) crystal was used for Fe and Ti, and an EDT crystal for Ca and K. For Fe a scintillation counter was used and a flow counter for the other elements.

3. Trace constituents

In the procedure described here trace constituents are determined by X-ray fluorescence analysis of samples fused with a relatively small amount of borate flux. Because of the slight dilution, matrix effects are present and must be corrected for. This correction makes use of absorption coefficients and the analytical results from the quantometric determination of the major elements.

The trace elements dealt with in this paper are Zr, Y, Sr, Rb, Zn, Cu, Ni,

Table 5. Results obtained by X-ray fluorescence analyses (NGU) of powders prepared for the tape machine. Recommended values by Flanagan (1973)

Sample	Fe ₂ O ₃ %	TiO ₂ %	CaO %	K ₂ O %	
Granite	2.77	0.47	1.84	4.40	NGU
USGS G-2	2.65	0.50	1.94	4.51	Recom. val.
Granodiorite	4.35	0.65	2.11	5.40	NGU
USGS GSP-1	4.33	0.66	2.02	5.53	Recom. val.
Andesite	6.80	1.06	5.08	2.91	NGU
USGS AGV-1	6.76	1.04	4.90	2.89	Recom. val.
Basalt	13.15	2.24	7.04	1.80	NGU
USGS BCR-1	13.40	2.20	6.92	1.70	Recom. val.

Cr and Ba. These were the elements included in an analytical routine procedure originally worked out for the study of basic rocks. Extension of the analytical programme, however, causes no great problems and, as will be seen later, the method is also readily applicable to samples with compositions differing very much from that of basic rocks.

3.1 PREPARATION OF STANDARDS

The reasons for the choice of synthetic standards rather than natural standards for the major elements are equally valid for the trace elements. The standards were therefore made up from specpure chemicals, the purity of which was checked by optical emission spectrography and XRF. Since the original analytical task was the study of basic rocks the composition of the synthetic base mixture was chosen to approximate that of a greenstone (metabasalt).

The base mixture was made by mixing 55% quartz, 15% Al₂O₃, 10% Fe₂O₃, 10% CaCO₃, 5% MgO and 5% Na₂CO₃. By admixture of 1% of each of the minor elements (in form of oxides) to this base and successive dilution, a synthetic standard series ranging down to 10 ppm was prepared. These standards are referred to hereafter as 'greenstone standards'.

3.2 PREPARATION OF TEST SAMPLES

The analytical curves or functions used in this work are based on intensity measurements obtained for the greenstone standards. In order to test the effectiveness of the matrix correction method used for matrices differing more or less from the greenstone matrix, 8 synthetic test samples were prepared. These were samples containing 1000 ppm and 100 ppm of each of the trace elements in the following very different matrices:

a) a synthetic granite matrix; b) a quartz matrix; c) an Al₂O₃ matrix; and d) a Fe₂O₃ matrix.

The granite matrix had the following composition: 75% quartz, 13% Al₂O₃, 2% Fe₂O₃, 5% K₂CO₃ and 5% Na₂CO₃.

The 8 test samples are referred to as Gr 1000 and Gr 100, Si 1000 and Si 100, Al 1000 and Al 100, Fe 1000 and Fe 100.

3.3 FUSION OF STANDARDS AND SAMPLES

In order not to lose too much of the X-ray intensity the fusion process uses only a minimum amount of flux, the main purpose being to obtain a degree of isoformation of standards and samples by decomposition of the mineral constituents.

The fusion procedure chosen is as follows:

4 g of finely powdered sample or standard is mixed with 2 g $\text{Li}_2\text{B}_4\text{O}_7$ for 1 minute in a Spex mixer. The mixture is transferred to a non-wettable PtAu crucible and heated to melting over a burner. The crucible is then left in a furnace at 1000°C for 5 minutes. If the melt does not loosen easily from the crucible after cooling, the crucible is reheated and quenched in cold water. After cooling the melt is ground in an agate swing mill for 1 minute. The resultant powder is placed in sample cups and after manual pressing is ready for analysis. This method of fusion, by which most rock samples are effectively decomposed, is rapid and well suited for routine analyses of the minor constituents. The test samples of quartz, Al_2O_3 and Fe_2O_3 seemed, however, not to be completely decomposed.

3.4 X-RAY LINE PROGRAMME

The X-ray analysis is carried out without the use of reference elements. The lines used and their interference and background characteristics are listed below.

	Interferences	Background
Zr $\text{K}\alpha$	Sr $\text{K}\beta_1$	Sloping
Y »	Rb $\text{K}\beta_1$	»
Sr »	none	»
Rb »	»	»
Zn »	»	Flat
Cu »	Tube line (W $\text{L}\alpha_1 - 1$)	»
	Tube line (contamination)	
Ni »	Tube line (contamination)	»
	Rb $\text{K}\beta_1$ 2nd order	
	Y $\text{K}\alpha$ 2nd order	
Cr »	Tube line (contamination)	»
	V $\text{K}\beta_1$	
Ba $\text{L}\beta_2$	Tube line (Cr $\text{K}\alpha - 1$)	»

$\text{K}\alpha$ lines are used for all elements except Ba. Ba $\text{K}\alpha$ cannot be used because of its short wavelength, and the $\text{L}\alpha_1$ -line is disturbed by Ti $\text{K}\alpha$, especially in the case of basic rocks due to their relatively high Ti content. Ba $\text{L}\beta_1$ suffers interference from Ce $\text{L}\alpha_1$, and thus the best choice is Ba $\text{L}\beta_2$. For the Ba determination a Cr tube is used. With this tube Ba $\text{L}\beta_2$ is also stronger than Ba $\text{L}\beta_1$.

since only the β_2 line is excited by $\text{CrK}\alpha$. A disadvantage is that the $\text{CrK}\alpha$ tube line also, to some extent, interferes with $\text{BaL}\beta_2$. In some cases a W tube was used for the Ba determination, although the intensity was observed to be only about one third that obtained with a Cr tube. In a great many rock-types, however, the Ba content is also large enough to allow a good determination with a W tube.

Interferences from lines belonging to elements present in the sample (see list) are corrected for by means of correction factors. For each analytical line with interferences this factor is calculated from measurements on standards containing only the interfering element in an otherwise pure greenstone base. The factor to be used for the calculation of the correction is the ratio of the net reading at the position of the analytical line and the net reading of the analysis line of the interfering element. The interference on $\text{NiK}\alpha$ from the second order lines of $\text{YK}\alpha$ and $\text{RbK}\beta$ can be removed by the use of a discriminator.

Tube lines originating from the tube material (W and Cr) or its contents of impurities (Cu, Ni, Cr) represent another type of interference. A correction factor for such interference was derived from measurements at the line position and its background position for a blank represented by a fused pure greenstone base. Similar measurements on the fused bases used for the different test samples confirmed that this correction factor is nearly matrix independent.

Since the analytical method is based on net intensities, background measurements and corrections are necessary. For lines having sloping background, i.e. those of Zr, Y, Sr and Rb, measurements were made on both sides of the line and the average taken as the true background. Measuring only one background is less reliable because the change of background with wavelength is matrix dependent. Background disturbances by elements like Th, U and Pb, which have lines in the wavelength region used, might cause trouble if present, and should be checked for.

The interference from $\text{VK}\beta_1$ on $\text{CrK}\alpha$ is serious when the V-content is high, but is difficult to correct for because $\text{TiK}\beta_1$ interferes with $\text{VK}\alpha$. In this case V was checked for by emission spectrography.

3.5 INSTRUMENTATION

All measurements were carried out on a Philips PW 1540 X-ray spectrometer operated at 40 kV and 18 mA. For Ba a Cr tube and flow counter were used, and a W-tube and scintillation counter were used for all the other elements. The analysing crystal was LiF (200). The counting time was 100 seconds for all measurements.

3.6 MATHEMATICAL CORRECTION FOR MATRIX EFFECTS USING ABSORPTION COEFFICIENTS

The analytical curves of the procedure described are constructed for the greenstone matrix only and are straight lines according to the analytical function

$$c_{\text{X (greenstone)}} = k_{\text{X (greenst.)}} \cdot I_{\text{X (greenst.)}} + b_{\text{X (greenst.)}}$$

where c_X is the concentration of element X, I_X the net measurement of the intensity of the analysis line of element X, and k_X and b_X are constants. b is in most cases zero, and $I/k = \frac{dI}{dc}$ is the sensitivity of the procedure.

Because of difference in absorption, the readings I_X of element X in other matrices must be converted to corrected readings which allow use of the greenstone analytical functions.

The absorption of the primary radiation is normally of minor importance and can be neglected. The element-characteristic fluorescent radiation, on the other hand, undergoes significant matrix dependent absorption on its way out of the sample. The magnitude of this absorption expressed by the total mass absorption coefficient of the matrix in question, relative to that of the greenstone matrix, is the factor used in this paper for the above-mentioned conversion of readings. A thorough treatment of this subject has been given by Hower (1959), Müller (1964) and others. The total mass absorption coefficient can be calculated by use of available Tables of absorption coefficients. It is the sum of the products of mass absorption coefficient and weight fraction of each element making up the matrix, as shown in Table 7 for the greenstone matrix.

Manual correction calculation of this kind is time-consuming. The calculation is, however, well suited for electronic data processing, and a computer programme was therefore written for this purpose. The computer is simply fed with the net X-ray intensity readings for the trace elements and the analytical results for the major elements. All other information, mass absorption coefficients, weight ratio of sample to flux and the constants k and b of the analytical functions are built-in parameters in the computer programme.

Different Tables of mass absorption coefficients are available (Heinrich 1966; Jenkins & De Vries 1970; Liebafsky 1971). For this work the Tables by Heinrich were chosen. One advantage of these Tables is that they give directly the coefficients for the most frequently used lines. $Ba L\beta_2$ is not covered by the Tables and the required interpolation for this wavelength was made on the basis of wavelength raised to the 2.8 power. The constancy of the ratio of the coefficients of two neighbouring fluorescence lines (Fairbairn & Hurley 1971) was taken as a measure of the quality of the mass absorption coefficients. This ratio is, for Rb and Sr, shown in Table 6, which also lists all the mass absorption coefficients used in the present work.

Fusion of synthetic samples containing different carbonates and in different amounts showed that CO_2 was completely removed from the samples. From Table 7 it is seen that loss of volatiles from the sample during fusion is not taken into consideration, nor is the increase in concentration of the major elements caused by such losses or change in the weight ratio sample to flux. Calculations show that this way of calculation gives the same final result as if the calculation had used major element concentrations based on ignited sample, and which also takes into consideration the change in weight ratio sample to flux. By the latter method of calculation the concentrations of trace elements must be reduced to the basis of original sample weight. Typical trace

Table 6. Mass absorption coefficients (Heinrich)

λ	ZrK α	YK α	SrK α	RbK α	ZnK α	CuK α	NiK α	CrK α	BaL β_2	Ratio
Z	0.787	0.830	0.876	0.927	1.436	1.542	1.659	2.291	2.404	$\mu_{\text{Rb}}/\mu_{\text{Sr}}$
Si	9.5	11.0	12.8	15.0	50.4	61.4	75.2	183.8	211.1	1.172
Al	7.6	8.9	10.3	12.0	40.7	49.6	60.7	149.0	171.2	1.165
Fe	49.9	57.7	66.8	78.0	256.3	311.1	379.6	113.0	129.4	1.168
Ti	32.3	37.3	43.3	50.5	166.8	202.6	247.3	597.0	681.6	1.166
Mg	6.0	7.0	8.1	9.5	32.4	39.5	48.4	119.1	136.9	1.173
Ca	25.1	29.0	33.7	39.3	130.5	158.6	193.7	469.2	537.8	1.166
Na	4.6	5.4	6.3	7.3	24.8	30.3	37.2	91.4	105.1	1.159
K	22.0	25.5	29.5	34.5	115.0	139.8	171.0	415.4	476.4	1.169
Mn	45.2	52.2	60.5	70.5	232.0	281.6	343.6	100.5	115.1	1.165
O	1.9	2.2	2.6	3.1	10.5	12.9	15.8	39.4	45.3	1.192
C	0.7	0.8	0.9	1.1	3.8	4.6	5.7	14.2	16.4	1.222
Li	0.1	0.1	0.1	0.1	0.4	0.5	0.6	1.5	1.7	1.000
B	0.4	0.4	0.5	0.6	2.1	2.5	3.1	7.9	9.1	1.200

Table 7. Computation of mass absorption coefficients for fused greenstone standards

4 g standard (greenstone): 55% SiO₂, 15% Al₂O₃, 10% Fe₂O₃, 5.60% CaO, 5% MgO, 2.92% Na₂O + (6.48% CC, 2 g flux: 100% Li₂B₄O₇)

Absorbing element	Percentage	ZrK α	YK α	SrK α	RbK α	ZnK α	CuK α	NiK α	CrK α	BaL β_2
Si	25.70	2.442	2.827	3.290	3.855	12.953	15.780	19.326	47.237	54.253
Al	7.94	0.603	0.707	0.818	0.953	3.232	3.938	4.820	11.831	13.593
Fe	6.99	3.488	4.033	4.669	5.452	17.915	21.746	26.534	7.899	9.045
Ca	4.00	1.004	1.160	1.348	1.572	5.220	6.344	7.748	18.768	21.512
Mg	3.02	0.181	0.211	0.245	0.287	0.978	1.193	1.462	3.597	4.134
Na	2.17	0.100	0.117	0.137	0.158	0.538	0.658	0.807	1.983	2.281
O	43.70	0.830	0.961	1.136	1.355	4.589	5.637	6.905	17.218	19.796
	93.52	8.648	10.016	11.643	13.632	45.425	55.296	67.602	108.533	124.614
Li	8.20	0.008	0.008	0.008	0.008	0.033	0.041	0.049	0.123	0.139
B	25.20	0.102	0.102	0.128	0.154	0.537	0.640	0.793	2.022	2.329
O	66.21	1.258	1.457	1.721	2.053	6.952	8.541	10.461	26.087	29.993
	100.0	1.368	1.567	1.857	2.215	7.522	9.222	11.303	28.232	32.461
4/6 base:		5.765	6.677	7.762	9.088	30.283	36.864	45.068	72.355	83.076
2/6 flux:		0.456	0.522	0.619	0.738	2.507	3.074	3.768	9.411	10.820
		6.221	7.199	8.381	9.826	32.790	39.938	48.836	81.766	93.896

elements do not contribute appreciably to the absorption, and in the calculations referred to trace elements have been treated as non-absorbing.

3.7 CORRECTION OF MATRIX EFFECTS BY USING SCATTERED PRIMARY RADIATION AS A REFERENCE

Scattering of the primary tube spectrum consists of coherent and incoherent scattering. The power of the scattering is strongly dependent on matrix and wavelength. Based on this dependency different methods have been proposed and used for the correction of matrix effects (see e.g. Andermann & Kemp 1958; Cullen 1962; Kalman 1962; Taylor & Andermann 1971; Clark & Mitchell 1973). A certain wavelength has to be selected as intensity reference,

Table 8. Precision of the X-ray method (upper part of Table). Precision of the instrument (lower part of Table)

	Zr	Y	Sr	Rb	Zn	Cu	Ni	Cr	Ba
Mean (ppm)	128.3	37.7	303.8	69.8	93.4	35.3	59.8	183.6	234.3
s (ppm)	2.45	1.49	2.57	2.62	2.59	3.43	3.26	3.31	25.8
s _r (%)	1.9	4.0	0.8	3.8	2.8	9.7	5.5	1.8	11.0
Mean (ppm)	124.8	38.4	309.1	71.2	94.5	35.4	59.7	183.2	234.1
s (ppm)	1.40	1.58	3.35	2.30	2.12	4.55	2.06	2.30	16.2
s _r (%)	1.1	4.1	1.1	3.2	2.2	12.9	3.5	1.3	6.9

but the choice of wavelength has been much discussed in the literature. The use of coherently scattered tube lines were advised against by Reynolds (1963), whereas incoherently scattered lines (Compton peaks) have generally been recommended as more suitable. The results shown in Table 10 were obtained by use of the incoherently scattered MoK α tube line as reference line for Rb and Sr. The results appear to be fairly promising.

When a W tube is used, however, there are no suitable incoherently scattered tube lines available. In this case it was therefore decided to make use of a background wavelength and, since at short wavelengths incoherently scattered radiation is supposed to be strong compared to coherently scattered radiation, the background at $2\theta = 17^\circ$, corresponding to a wavelength of 0.59 \AA , was chosen. This background was used as intensity reference for all the trace elements of this work, and the results are listed along with those based on other calculation procedures in Table 9.

3.8 PRECISION

The precision of the method was investigated by analysing 10 fusions of one greenstone sample. The precision of the instrument was tested by analysing one fused sample 10 times. The results of the measurements are shown in Table 8. There seems to be no significant difference between the precision of the method and that of the instrument.

3.9 DETECTION LIMITS

If the limit of detection, C_L , is taken as the concentration corresponding to a measurement $x_L = \bar{x}_b + 3s_b$, where \bar{x}_b is the mean and s_b the standard deviation of the background reading, then

$$C_L = \frac{3}{S} \cdot \sqrt{\frac{R_b}{T_b}}$$

where S is the slope of the analytical calibration curve in $\frac{\text{counts per second}}{\text{ppm}}$ (= sensitivity).

R_b = True background counting rate

T_b = Counting time on the background

The calculation gives the following limits of detection in a greenstone matrix.

Table 9. Summary of results on trace elements

	Zr ppm	Y ppm	Sr ppm	Rb ppm	Zn ppm	Cu ppm	Ni ppm	Cr ppm	Ba ppm	
Granite USGS G-2	397	7	624	201	122	32	5	0	1585	Unfused, uncorrected
	407	5	609	203	98	37	5	0	1813	Fused, uncorrected
	316	6	499	160	99	18	0	0	1715	Unfused, corrected
	335	4	501	168	81	31	4	0	1976	Fused, corrected
	384	5	573	192	92	35	5	0	1708	Scattered b.g. at 17.0 as reference
	300	12	479	168	85	11.7	5.1	7	1870	Recommended values
Granodiorite USGS GSP-1	610	29	283	267	134	58	14	3	1064	Unfused, uncorrected
	698	25	271	271	108	36	7	0	1210	Fused, uncorrected
	534	25	248	234	118	33	9	4	1222	Unfused, corrected
	624	23	242	243	97	32	6	0	1350	Fused, corrected
	701	26	272	273	108	36	7	0	1216	Scattered b.g. at 17.0 as reference
	500	30.4	233	254	98	33.3	12.5	12.5	1300	Recommended values
Andesite USGS AGV-1	254	17	724	64	93	101	17	6	942	Unfused, uncorrected
	234	13	715	70	88	64	15	6	1089	Fused, uncorrected
	244	16	695	61	89	71	15	8	1035	Unfused, corrected
	228	13	696	68	86	62	15	7	1206	Fused, corrected
	243	14	740	72	91	66	16	7	1127	Scattered b.g. at 17.0 as reference
	225	21.3	657	67	84	59.7	18.5	12.2	1208	Recommended values
Basalt USGS BCR-1	164	27	280	33	114	14	7	15	535	Unfused, uncorrected
	158	28	280	35	105	12	7	21	570	Fused, uncorrected
	202	33	345	40	138	9	16	19	593	Unfused, corrected
	195	34	344	44	128	14	9	24	658	Fused, corrected
	196	34	345	44	129	14	9	26	703	Scattered b.g. at 17.0 as reference
	190	37.1	330	46.6	120	18.4	15.8	17.6	675	Recommended values
Biotite CRPG Mica-Fe	526	26	0	1240	968	0	10	65	58	Unfused, uncorrected
	579	3	0	1374	847	0	13	56	83	Fused, uncorrected
	871	43	0	2040	1581	0	36	74	64	Unfused, corrected
	940	5	0	2222	1360	0	21	63	94	Fused, corrected
	882	5	0	2093	1289	0	20	85	127	Scattered b.g. at 17.0 as reference
	-	-	6	2300	1350	4	35	90	140	Recommended values
Granite CRPG CRGR	214	19	729	201	78	586	55	63	873	Unfused, uncorrected
	267	9	691	205	70	358	64	77	924	Fused, uncorrected
	183	16	622	172	67	328	43	69	950	Unfused, corrected
	232	8	604	179	61	314	56	84	1014	Fused, corrected
	254	9	659	195	66	341	61	73	881	Scattered b.g. at 17.0 as reference
	180	19	550	175	60	345	55	110	1050	Recommended values
Larvikite ASK-1	607	40	868	100	74	17	137	29	917	Unfused, uncorrected
	737	39	797	99	101	14	113	22	978	Fused, uncorrected
	546	36	782	90	67	13	121	34	1028	Unfused, corrected
	676	36	732	92	93	13	104	25	1107	Fused, corrected
	732	39	792	100	100	14	112	22	972	Scattered b.g. at 17.0 as reference
	(400)	-	(680)	(85)	(105)	(7)	(110)	(40)	(1130)	Recommended values

(Continued opposite)

W-tube:

Element	S	R _i	C _L (ppm)
Zr	2.2	1079	4.5 ppm
Y	2.3	1020	4.2 »
Sr	2.2	875	4.0 »
Rb	2.1	781	4.0 »
Zn	1.9	405	3.2 »
Cu	1.3	477	5.0 »
Ni	1.5	312	3.5 »
Cr	0.8	55	2.8 »
Ba	0.03	34	58 »

Cr-tube:

Ba	0.08	84	34 »
----	------	----	------

3.10 RESULTS AND DISCUSSION

The results obtained on the international reference samples as well as on the synthetic test samples are given in Table 9. The samples named Larvikite ASK-1 and Schist ASK-2 are internordic geological reference samples. The recommended values for these are based on very few determinations and are therefore put in parentheses. Values near the detection limit should not be considered when evaluating which method is to be preferred.

The Table shows the necessity of some form of matrix effect correction. Mathematical matrix correction on fused samples seems to be superior to the other methods; furthermore, the importance of fusion seems to increase with increasing wavelength.

As regards Zr there are disagreements for GSP-1 and CRGR. By comparison with the values obtained by a number of analysts (Flanagan 1973) on this material, however, our values fall well within the range of values obtained in other laboratories. For synthetic test samples the mathematical correction method gives good results for Zr, Sr and Rb in all matrices, and for Zn, Cu and Ni in all matrices except Fe₂O₃ where the results are about 20–25% too high (exception: Cu in Fe 100). It should be remembered, however, that Fe₂O₃ is an exceptional matrix compared to greenstone, thus having a very large correction factor. As far as Cr and Ba in the Fe₂O₃ matrix are concerned, it is difficult to explain why the Ba values are higher than the Cr values. Enhancement from Fe on Cr and Ba would be expected to influence Cr more than Ba.

The method of scattered background cannot be used when an absorption edge for a matrix element lies between the analytical line and the measured scattered background position. This is clearly demonstrated for Cr and Ba in Fe 100 and Fe 1000. Otherwise, scattered background seems to give acceptable results.

Results obtained by use of the MoK α Compton peak for Sr and Rb determinations are shown in Table 10. Good results are obtained on unfused as well as

Table 10. Results obtained by using the MoK α Compton peak as matrix correction

Sample	Rb (ppm)			Sr (ppm)		
	Fused sample	Unfused sample	Recom. values, respectively correct values	Fused sample	Unfused sample	Recom. values, respectively correct values
G-2	160	166	168	482	505	479
GSP-1	235	248	254	233	245	233
AGV-1	62	60	67	658	693	657
BCR-1	41	42	46.6	322	347	330
Mica-Fe	2091	2130	2300	-	-	6
CRGR	170	176	175	584	623	550
Larvikite	87	93	(85)	686	736	(680)
Schist	187	181	(175)	115	108	(100)
GR 100	94		100	96		100
GR 1000	986		1000	998		1000
Al 100	99		100	101		100
Al 1000	1007		1000	1018		1000
Si 100	95		100	98		100
Si 1000	996		1000	989		1000
Fe 100	87		100	92		100
Fe 1000	939		1000	952		1000

fused samples. The Compton peak correction factor established for Sr and Rb can be used also for the elements Zr, Y, Zn, Cu and Ni since the factor is nearly identical for all these elements.

The elements Y, Sr and Rb have good sensitivity ($\frac{dI}{dc}$) with a Mo-tube, which has a suitable K α Compton peak to be used for matrix correction. Zr, Zn, Cu and Ni, however, have better sensitivity with a W-tube, but this tube gives no suitable Compton peak. A combination of two tubes could therefore be used, a W-tube for measuring analytical lines and backgrounds, and a Mo-tube for establishing the correction factor. The elements Cr and Ba can in many cases be analysed even without matrix corrections, since their correction factors vary only slightly with the matrix.

Acknowledgements. - The writers are indebted to Director Aslak Kvalheim for valuable help and advice during the preparation of this paper. Ola Kihle has assisted in the writing of computer programs and George Gale and David Smith have reviewed the manuscript.

REFERENCES

- Ahrens, L. H. 1954: *Quantitative Spectrochemical Analysis of Silicates*, 122 pp. Pergamon Press, London.
- Andermann, G. & Kemp, J. W. 1958: Scattered X-rays as internal standards in X-ray emission spectroscopy. *Analyt. Chem.* 30, 1306-1309.
- Birks, L. S. 1971: X-ray spectroscopy: Recent advances and current capabilities in quantitative analysis. *Colloq. Spec. Int. XVI*, Heidelberg, Plenary lectures and reports, 13-27.
- Clark, N. H. & Mitchell, R. J. 1973: Scattered primary radiation as an internal standard in X-ray emission spectrometry: Use in the analysis of copper metallurgical products. *X-ray Spectrometry* 2, 47-55.
- Cullen, T. J. 1962: Coherent scattered radiation internal standardization in X-ray spectrometric analysis of solutions. *Analyt. Chem.* 34, 812-814.

- Danielsson, A. 1967: Spectrochemical analysis for geochemical purposes. *Colloq. Spec. Int. XIII*, Ottawa, 311-323.
- Danielsson, A., Lundgren, F. & Sundkvist, G. 1959: The tape machine I, II and III. *Spectrochim. Acta* 15, 122-137.
- Danielsson, A., Nilsson, I. & Sundkvist, G. 1961: Spectrochemical slag analysis with the tape technique. *Trans. metall. Soc. A.I.M.E.* 221, 826-831.
- Engelhardt, W. v. 1936: Die Geochemie des Barium. *Chemie der Erde* 10, 187-246.
- Fairbairn, H. W. & Hurley, P. M. 1971: Evaluation of X-ray fluorescence and mass spectrometric analyses of Rb and Sr in some silicate standards. *Geochim. cosmochim. Acta* 35, 149-156.
- Flanagan, F. J. 1969: U.S. Geological Survey standards - II. First compilation of data for the new U.S.G.S. rocks. *Geochim. cosmochim. Acta* 33, 81-120.
- Flanagan, F. J. 1973: 1972 values for international geochemical reference samples. *Geochim. cosmochim. Acta* 37, 1189-1200.
- Gatterer, A. 1941: Zur Reinigung der Kohle für spektralanalytische Zwecke. *Spectrochim. Acta* 2, 49-70.
- Goldschmidt, V. M. 1930a: Über das Vorkommen des Germaniums im Meteoriten von Cranbourne. *Zeitschr. phys. Chemie, A* 146, 404-405.
- Goldschmidt, V. M. 1930b: Über das Vorkommen des Germaniums in Steinkohlen und Steinkohlen-Produkten. *Nachr. Ges. Wiss. Göttingen, Math.-Phys. Kl.*, 398-401.
- Goldschmidt, V. M. & Peters, Cl. 1931a: Zur Geochemie des Galliums. *Nachr. Ges. Wiss. Göttingen, Math.-Phys. Kl.*, 165-183.
- Goldschmidt, V. M. & Peters, Cl. 1931b: Zur Geochemie des Scandiums. *Nachr. Ges. Wiss. Göttingen, Math.-Phys. Kl.*, 257-279.
- Goldschmidt, V. M. & Peters, Cl. 1932a: Zur Geochemie des Berylliums. *Nachr. Ges. Wiss. Göttingen, Math.-Phys. Kl.*, 360-376.
- Goldschmidt, V. M. & Peters, Cl. 1932b: Zur Geochemie der Edelmetalle. *Nachr. Ges. Wiss. Göttingen, Math.-Phys. Kl.*, 377-401.
- Goldschmidt, V. M. & Peters, Cl. 1932c: Zur Geochemie des Bors I. *Nachr. Ges. Wiss. Göttingen, Math.-Phys. Kl.*, 402-407.
- Goldschmidt, V. M. & Peters, Cl. 1932d: Zur Geochemie des Bors II. *Nachr. Ges. Wiss. Göttingen, Math.-Phys. Kl.*, 528-545.
- Goldschmidt, V. M. & Peters, Cl. 1933a: Zur Geochemie des Germaniums. *Nachr. Ges. Wiss. Göttingen, Math.-Phys. Kl.*, 141-166.
- Goldschmidt, V. M. & Peters, Cl. 1933b: Zur Kenntnis der Troilit-Knollen der Meteoriten. *Nachr. Ges. Wiss. Göttingen, Math.-Phys. Kl.*, 278-287.
- Goldschmidt, V. M. & Peters, Cl. 1933c: Über die Anreicherung seltener Elemente in Steinkohlen. *Nachr. Ges. Wiss. Göttingen, Math.-Phys. Kl.*, 371-386.
- Goldschmidt, V. M. & Peters, Cl. 1934: Zur Geochemie des Arsens. *Nachr. Ges. Wiss. Göttingen, Math.-Phys. Kl.*, 11-12.
- Goldschmidt, V. M. & Thomassen, L. 1924: Geochemische Verteilungsgesetze der Elemente III. Röntgenspektrographische Untersuchungen über die Verteilung der seltenen Erdmetalle in Mineralen. *Vid. Selsk. Skr., Mat. naturv. Kl. No. 5*, 1-58.
- Goldschmidt, V. M., Bauer, H. & Witte, H. 1934: Zur Geochemie der Alkalimetalle II. *Nachr. Ges. Wiss. Göttingen, Math.-Phys. Kl.*, 39-55.
- Goldschmidt, V. M., Berman, H., Hauptmann, H. & Peters, Cl. 1933: Zur Geochemie der Alkalimetalle. *Nachr. Ges. Wiss. Göttingen, Math.-Phys. Kl.*, 235-244.
- Govindaraju, K. 1960: Contribution à l'analyse spectrochimique des roches silicatées et des silicates naturels. Dosage des éléments majeurs. *Publ. G.A.M.S.*, 221-246.
- Govindaraju, K. 1963: Nouveaux progrès dans le dosage des éléments majeurs des roches par spectrométrie photoélectrique avec le quantomètre A.R.L. *Publ. G.A.M.S.*, 217-221.
- Govindaraju, K. 1965: Dosage des éléments majeurs des roches silicatées par spectromètre photoélectrique avec le quantomètre A.R.L. *Bull. Soc. fr. Cér.* 67, 25-45.
- Heinrich, K. F. J. 1966: X-ray absorption uncertainty, 296-377, in McKinley, T. D., Heinrich, K. F. J. & Wittry, D. B.: *National Symposium on the Electron Microprobe*, Washington Oct. 1964, 1035 pp. John Wiley & Sons, Inc., New York.
- Hower, J. 1959: Matrix corrections in the X-ray spectrographic trace element analysis of rocks and minerals. *Am. Miner.* 44, 19-32.
- Jaycox, E. K. 1947: Spectrochemical Analysis of Ceramics and other Non-Metallic Materials. *J. Opt. Soc. Am.* 37, 162-165.

- Jenkins, R. 1974: *An Introduction to X-ray Spectrometry*, 163 pp. Heyden, London, New York, Rhein.
- Jenkins, R. & De Vries, J. L. 1970: *Practical X-ray Spectrometry*, 2nd ed., 190 pp, MacMillan and Co. Ltd., London.
- Kalman, Z. H. 1962: Theoretical study of X-ray fluorescent determination of traces of heavy elements in a light matrix. Application to rocks and soils. *Analyt. Chem.* 34, 946-951.
- Kvalheim, A. 1947: Spectrochemical determination of the major constituents of minerals and rocks. *J. Opt. Soc. Am.* 37, 585-592.
- Kvalheim, A. & Vestre, K. S. 1959: Studies on the application of the Noar cellulose pellet arc method to the quantometer. *Colloq. Spec. Int. VIII*, Luzerne, 198-204.
- Liebafsky, H. A. et al. 1971: *X-rays, Electrons and Analytical Chemistry*, 566 pp. John Wiley & Sons, Inc., New York.
- Minami, E. 1935: Gehalte an seltenen Erden in europäischen und japanischen Tonschiefern. *Nachr. Ges. Wiss. Göttingen, Math.-Phys. Kl.*, 155-170.
- Mitchell, R. L. 1969: Trends in applied geochemical and biochemical analysis. *Colloq. Spec. Int. XV*, Madrid, Plenary conferences, 11-23.
- Müller, R. 1964: Die Abhängigkeit der Fluoreszenzintensität von Massenabsorptionskoeffizienten der Matrix bei der Spurenbestimmung durch Röntgenfluoreszenz. *Spectrochim. Acta* 20, 143-151.
- Noll, W. 1934: Geochemie des Strontiums. *Chemie der Erde* 8, 507-600.
- Reynolds, R. C. Jr. 1963: Matrix corrections in trace element analysis by X-ray fluorescence: Estimation of the mass absorption coefficient by compton scattering. *Am. Miner.* 48, 1133-1143.
- Roubault, M., de la Roche, H. & Govindaraju, K. 1960: Sur l'analyse quantitative des roches silicatées naturelles à l'aide du spectromètre à réseau à enregistrement direct. *C. R. Acad. Sci., t. 250*, 2912-2914.
- Roubault, M., de la Roche, H. & Govindaraju, K. 1964: L'analyse des roches silicatées par spectrométrie photoélectrique au quantomètre A.R.L. et son contrôle par des roches étalons. *Sc. de la Terre, t. IX*, 339-371.
- Saunderson, J. L., Caldercourt, V. J. & Peterson, E. W. 1945: A photoelectric instrument for direct spectrochemical analysis. *J. Opt. Soc. Amer.* 35, 681-697.
- Scott, R. O., Burrige, J. C. & Mitchell, R. L. 1969: Direct current arc analysis with a multi-channel direct reader. *Colloq. Spec. Int. XV*, Madrid, Proceedings IV, 387.
- Strock, L. W. 1936: Zur Geochemie des Lithiums. *Nachr. Ges. Wiss. Göttingen, Math.-Phys. Kl.*, 171-204.
- Taylor, D. L. & Andermann, G. 1971: Evaluation of an isolated atom model in the use of scattered radiation for internal standardization in X-ray fluorescence analysis. *Analyt. Chem.* 43, 712-716.

Wavelength Tables:

- General Electric 1959: *X-ray wavelengths for spectrometer*. Cat. No. A 4961 DA., 448 pp.
- Harrison, G. R. 1939: *M.I.T. Wavelength Tables*, 429 pp. John Wiley & Sons, Inc., New York.

The first part of the document discusses the early years of the nation, from the time of the signing of the Declaration of Independence in 1776 to the end of the Revolutionary War in 1783. It covers the challenges faced by the new government, including the lack of a strong central authority and the need to establish a stable political system. The document also mentions the signing of the Constitution in 1787 and the beginning of the federal government under George Washington.

The second part of the document focuses on the period of the early republic, from the 1790s to the 1820s. It describes the political and social changes that took place during this time, including the rise of the Federalist Party and the Democratic-Republican Party. It also discusses the expansion of the United States into new territories and the role of the judiciary in shaping the nation's future.

The third part of the document covers the period of the 1830s and 1840s, a time of rapid westward expansion and the discovery of gold in California. It discusses the impact of the Mexican-American War and the resulting acquisition of new territory. It also mentions the rise of the Whig Party and the Democratic Party, and the growing tensions between the North and the South over the issue of slavery.

The fourth part of the document describes the period of the 1850s and 1860s, a time of intense political and social conflict. It discusses the rise of the Free Soil Party and the Republican Party, and the growing divide between the North and the South over the issue of slavery. It also mentions the outbreak of the Civil War in 1861 and the role of Abraham Lincoln in leading the Union to victory.

The fifth part of the document covers the period of the 1870s and 1880s, a time of Reconstruction and the rise of the Gilded Age. It discusses the challenges of rebuilding the South and the role of the Freedmen's Bureau. It also mentions the rise of the Industrial Revolution and the growth of the economy, as well as the emergence of the Populist Party and the Progressive Movement.

The sixth part of the document describes the period of the 1890s and 1900s, a time of imperial expansion and the rise of the Progressive Era. It discusses the Spanish-American War and the acquisition of new territories, as well as the role of the Progressive Movement in reforming government and society. It also mentions the rise of the Republican Party and the Democratic Party, and the growing tensions between the North and the South over the issue of race.

The seventh part of the document covers the period of the 1910s and 1920s, a time of economic growth and the rise of the New Deal. It discusses the impact of World War I and the role of the federal government in the economy. It also mentions the rise of the Republican Party and the Democratic Party, and the growing tensions between the North and the South over the issue of race.

The eighth part of the document describes the period of the 1930s and 1940s, a time of economic crisis and the rise of the New Deal. It discusses the impact of the Great Depression and the role of the federal government in the economy. It also mentions the rise of the Democratic Party and the Republican Party, and the growing tensions between the North and the South over the issue of race.

The ninth part of the document covers the period of the 1950s and 1960s, a time of social and political change. It discusses the impact of the Cold War and the role of the federal government in the economy. It also mentions the rise of the Democratic Party and the Republican Party, and the growing tensions between the North and the South over the issue of race.

The tenth part of the document describes the period of the 1970s and 1980s, a time of economic growth and the rise of the New Deal. It discusses the impact of the Vietnam War and the role of the federal government in the economy. It also mentions the rise of the Democratic Party and the Republican Party, and the growing tensions between the North and the South over the issue of race.

The eleventh part of the document covers the period of the 1990s and 2000s, a time of economic growth and the rise of the New Deal. It discusses the impact of the end of the Cold War and the role of the federal government in the economy. It also mentions the rise of the Democratic Party and the Republican Party, and the growing tensions between the North and the South over the issue of race.

The twelfth part of the document describes the period of the 2010s and 2020s, a time of economic growth and the rise of the New Deal. It discusses the impact of the 2008 financial crisis and the role of the federal government in the economy. It also mentions the rise of the Democratic Party and the Republican Party, and the growing tensions between the North and the South over the issue of race.

Geochemistry of Dolerite and Metadolerite Dykes from Varanger Peninsula, Finnmark, North Norway

DAVID ROBERTS

Roberts, D. 1975: Geochemistry of dolerite and metadolerite dykes from Varanger Peninsula, Finnmark, North Norway. *Norges geol. Unders.* 322, 55-72.

Dolerite dykes provide the only manifestation of igneous activity in the thick, Riphean to Lower Cambrian, weakly metamorphosed sedimentary sequence of Varanger Peninsula. Major and trace element abundances and ratios from two distinctive generations of mafic dyke, one metamorphosed and cleaved and the other post-metamorphic and fresh, reveal disparate grouping and trends in several variation diagrams. Older metadolerites show an overall major-element compositional similarity with abyssal tholeiites, a relationship which is confirmed by most trace element concentrations and ratios. Certain element abundances, together with the tectonic environment, suggests however that these dykes are representative more of magmas transitional to those producing abyssal and continental tholeiites. The younger dolerites are also subalkaline though less typically tholeiitic than the metadolerites. Comparison of their element contents and ratios reveals calc-alkaline affinities, as well as similarities with data for continental tholeiites. The trend of relative enrichment in Si, Ba, Zr, Rb and alkalis in the dolerites may possibly signify a greater depth of magma generation than that which produced the metadolerites. The petrogenesis of the dyke sets is discussed in the light of the regional geology and recently published K-Ar whole-rock ages which place the dolerites in the uppermost Devonian and date the metadolerites, provisionally, as Riphean.

D. Roberts, Norges geologiske undersøkelse. P.O.Box 3006, N-7001 Trondheim, Norway

Introduction

The geology of Varanger Peninsula in East Finnmark (Fig. 1) has been studied in some detail over the past decade, with emphasis placed on stratigraphical and sedimentological investigations (Siedlecka & Siedlecki 1967, 1971, 1972; Røe 1970; Banks et al. 1971, 1974; Laird 1972; Siedlecka 1972, 1975; Banks & Røe 1974). Tectonic structural observations are principally those of Roberts (1972) and Teisseyre (1972).

As a result of this activity, the essential features of the geology are now fairly clear. In brief, the peninsula is divided more or less in half by a complex, NW-SE-trending, NE-dipping dislocation, the Trollfjord-Komagelv fault-zone (Siedlecka & Siedlecki 1967), along which there has occurred considerable dextral, strike-slip movement (Roberts 1972). South-west of the fault zone is an autochthonous 4000-5000 m-thick succession of shallow water sediments of late Precambrian to Lower Cambrian age, including two Eocambrian (Vendian) tillite formations. This sequence rests unconformably upon Precambrian crystalline basement just to the south-west of Varanger Peninsula.

On the north-east side of the Trollfjord-Komagelv fault-zone is the 9000 m-

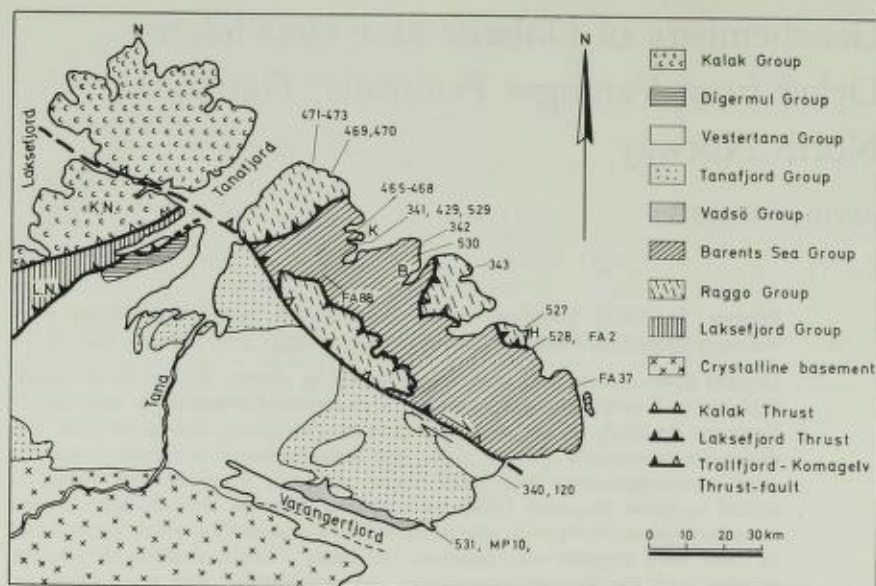


Fig. 1. Geological map of Varanger Peninsula and adjacent areas showing the locations of analysed dolerites and metadolerites. The numbers refer to the samples (Tables 1 and 2). K.N. - Kalak nappe; L.N. - Laksefjord nappe; B - Båtsfjord; K - Kongsfjord; N - Nordkyn; H - Hamningberg. The areas of Raggo Group rocks may include sequences from different allochthonous or parautochthonous units.

thick Barents Sea Group, a sedimentary pile of considered Riphean age; this is overthrust by the equally thick Raggo Group (Siedlecka & Siedlecki 1967, 1972). A lithostratigraphical correlation involving these two groups has been proposed (Siedlecka & Siedlecki 1972), but the validity of this interpretation has been challenged (Laird 1972, Gayer & Roberts 1973). In the alternative scheme of correlation the Raggo sediments are considered as being of Vendian age, and equivalent to the rocks of the Laksefjord Group. Relationships between the different successions (Fig. 1) juxtaposed along the Trollfjord-Komagelv fault zone are the subject of current debate and research.

A significant element in the geological history of Varanger Peninsula is that of dolerite dyke intrusion. Dykes are particularly prominent in the Barents Sea region, north of the fault zone, where they were first recorded by Holtedahl (1918); locally they attain swarm proportions. Towards the south-east they are far less common.

During a tectonic structural investigation of the Barents Sea region by the present author (Roberts 1972), it was found that two main phases of dyke intrusion could be distinguished, one coeval with the major fold-producing deformation and low-grade metamorphic episode (and representing the majority of the dykes), and the other post-dating this regional metamorphism. Dolerites of the older intrusive phase are metamorphosed and cleaved, whereas the younger set are comparatively fresh and unaltered.

Preliminary potassium-argon age determinations have recently been reported on some of the basic dykes (Beckinsale et al. 1975). These appear to indicate

that some 650 m.y. separates the two generations of dyke intrusion noted above, the post-tectonic dolerites showing an uppermost Devonian age. In addition, a third set of dykes has apparently been recognised. These are from an area as yet not visited by the present writer. The significance of these radiometric dates is discussed later.

Field relationships

The metamorphosed dolerite dykes, hereafter referred to as the metadolerites, are particularly common in the multilayered distal-turbiditic parts of the Barents Sea Group, especially around Kongsfjord, but also occur in the allochthonous Raggo Group. Dyke thickness is usually 1 to 3 m, rarely up to 10 m. Characteristically the metadolerites lie parallel or subparallel to the axial surfaces of common, close to tight, mesoscopic folds (D_1), although they are themselves sheared and cleaved by the penetrative slaty cleavage or schistosity axial planar to these folds (Roberts 1972). Dyke strike is consistently ENE-WNW with dips vertical or steep to the SSE in the Barents Sea Group and moderate or steep to the NW in the Raggo Group.

The dykes are green- to brown-weathering, the colour depending on grain-size and thickness; the thinner, finer grained dykes show a distinct green coloration. They have narrow, chilled marginal zones, often display pinch- and swell features or true boudinage, and are locally cut by irregular quartz-chlorite-calcite veinlets and segregations. A pale, green-grey, baked aureole zone is frequently present, especially where the dykes intrude pelites. Field relationships, noted in more detail elsewhere (Roberts 1972), indicate that the dyke intrusion accompanied the main, D_1 , folding episode but pre-dated the actual cleavage development and a late- D_1 differential flattening phase. The possibility that the dykes are pre- D_1 and have been rotated into the plane of D_1 flattening has been considered, but rejected on several grounds. Nevertheless, it cannot be entirely ruled out that some may be pre- D_1 .

The unmetamorphosed dolerite dykes of the present study are quantitatively insignificant, occurring in comparative isolation, and are largely restricted to the south-eastern districts of Varanger Peninsula on both sides of the Trollfjord-Komagelv fault-zone. They clearly post-date the main D_1 folding and regional metamorphic fabric, and trend between NE-SW and N-S. These dykes are generally from 8 to 12 m in thickness, are dark green to almost black and have distinctive chilled marginal facies.

Petrography

The mineralogy and petrography of the fine- to medium-grained *metadolerite* dykes is partially obliterated by a pervasive alteration of the plagioclase and variable chloritization of the constituent mafic minerals, but it is nevertheless possible to recognise the original dominance of primary plagioclase and clinopyroxene and in most cases, the relict ophitic to sub-ophitic texture in the dyke interiors. Towards the margins of several of the dykes, shearing and

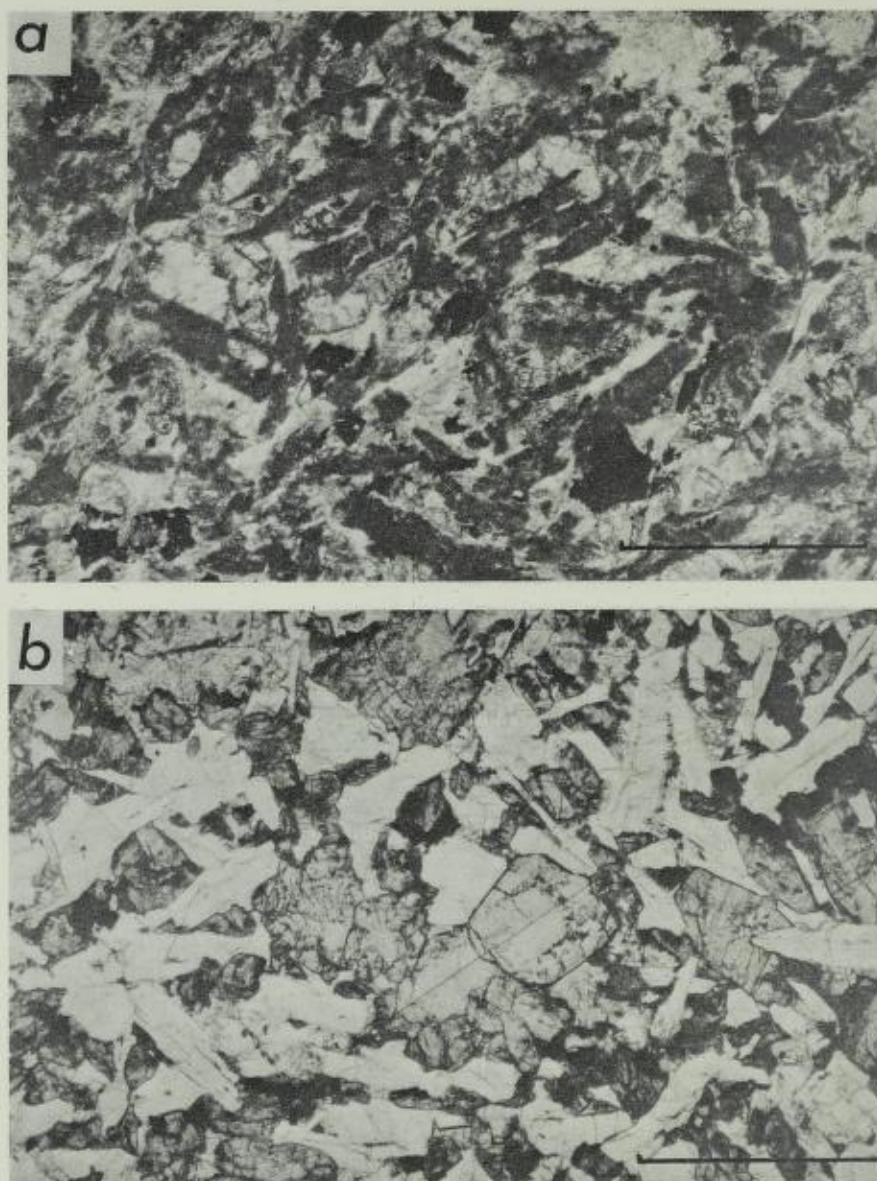


Fig. 2. Photomicrographs of the dykes. (a) Metadolerite. The higher relief clinopyroxene and the strongly altered plagioclase (dark laths) are distinguishable; chlorite and ilmenomagnetite are the only other minerals. Sample no. 467. Scale, 1 mm. Plane polarised light. (b) Dolerite. Sub-ophitic texture of clinopyroxene and plagioclase with some ore mineral grains. Sample no. 340. Plane polarised light. Scale, 1 mm.

alteration have been such that only chlorite, opaques and some amphibole and epidote are definable, with some ghost-like relics of plagioclase laths. Rarely, where chilled zones have escaped alteration, original microporphyritic texture may be observed with randomly oriented microphenocrysts of clinopyroxene, labradorite and opaques set in a brown cryptocrystalline groundmass.

Plagioclase and clinopyroxene are, or were, the most abundant minerals in the metadolerites. The plagioclase is heavily altered (Fig. 2a), frequently to a cloudy brownish product; microgranular epidote can be recognised in some cases, and some saussuritization has been observed. Where alteration is not so advanced, ragged lath-like shapes from 0.5 to 1 mm in length can be distinguished and compositional determinations are possible, the plagioclase falling in the range An_{42} to An_{54} . Towards the north-westernmost part of Varanger Peninsula where the grade of greenschist facies metamorphism is slightly higher, metadolerite dykes in Raggo Group rocks show partial recrystallization features with some plagioclases recrystallized to aggregates of equigranular epidote, quartz and some calcite.

The colourless clinopyroxene has suffered extensive chloritization as well as fragmentation resulting from the late- D_1 deformation. Many of the ragged crystals show wavy extinction. Much of the pyroxene would appear to be augitic, but in some cases low $2V$ angles indicate pigeonite; microphenocrysts from a chilled marginal zone of one dyke are definitely of pigeonite, with $2V$ in the 5° – 15° range.

Chlorite is the principal alteration product of the clinopyroxene. In the finer grained facies of the dykes it may completely pseudomorph the pyroxene, although where deformation has been advanced the original pyroxene shape is impossible to recognise. The chlorite also occurs as veinlets and irregular segregations in the dykes; optical examination and X-ray determinations show it to be ripidolite. Uralitization is less common than might be expected in these metadolerites, tending to be restricted to the areas in the north-west with higher greenschist facies metamorphism, or to the more strongly deformed dykes. Even here the colourless amphibole is not an important mineral, and shows extensive chloritization.

Other, quantitatively insignificant minerals in the metadolerites are ilmenite-magnetite, pyrite, quartz, epidote, calcite and some sphene. In some of the dykes from near Kongsfjord, 5–6 mm-sized pyrite cubes are prominent. Generally, however, the opaque mineral is an ilmenite-magnetite mixture, sometimes present as skeletal grains with alteration of ilmenite lamellae to leucoxene. Minor phlogopitic biotite, partially going over to chlorite, has been found in only one dyke, rimming pyroxene. A minor amount of olivine has been determined in the norms of 3 of the metadolerites, but none has been seen in thin-section.

In contrast to the metadolerites, the younger *dolerite* dykes are either completely fresh or show only minor alteration features (Fig. 2b). Their uniform mineralogy is dominated by plagioclase and clinopyroxene in the general size range 0.5–3 mm and 0.3 to 0.6 mm, respectively, and textures are mostly ophitic or subophitic and rarely glomeroporphyritic. The plagioclase shows albite, Carlsbad and pericline twinning and, locally, oscillatory zoning. Sericitization is encountered in some instances, although the feldspar is usually quite fresh. In one dyke from near Hamningberg, a glomeroporphyritic texture is observed with plagioclase laths occurring in scattered clusters from 3 to

5 mm across. Plagioclase composition in the dolerite dykes in general ranges from An₄₄ to An₆₀.

Clinopyroxene is colourless and occurs as lath-shaped, equant or subhedral crystals dispersed or moulded between the dominant plagioclase. Twinning is common, both simple and polysynthetic, and 'hourglass' wavy extinctions are sometimes observed; occasionally a faint concentric zoning may be distinguished by small differences in extinction angles. Axial angle determinations show that the bulk of the pyroxene is undoubtedly a pigeonite, although an augite phase may also be present either as peripheral zones to pigeonite crystals or as separate individuals.

The clinopyroxene of the dolerites is altered marginally only to a minor degree, and then to a phlogopitic biotite or chlorite rather than to uraltite. Accessory pale green amphibole has been observed in some thin-sections, however. Other accessory minerals in the dolerites are titanomagnetite and minor apatite and calcite.

Chemical composition of the dykes

Major element analyses have been obtained for twenty-four samples, 16 metadolerites and 8 dolerites (Tables 1 and 2). In most cases, specimens were taken from the approximate central part of dykes; additional samples from the margins were collected from three metadolerite dykes for comparison purposes. Trace element concentrations for nineteen of the samples are also presented in the Tables. The major elements Si, Al, Ca, Mg and total Fe were analysed by classical wet chemical methods, while Ti, Mn, Na, K and ferrous iron were determined by the method of Langmyhr & Graff (1965). The trace elements, with the exception of Nb and some Rb determinations were analysed on fused rock powders using a manual Philips 1540 XRF. Niobium and metadolerite rubidium values were determined by XRF using pressed-powder pellets.

The major element data have been plotted on several variation diagrams, all of which have revealed compositional groupings of the two dyke sets. From the alkalis-silica diagram (Fig. 3), both metadolerites and dolerites tend to plot in the subalkaline field (Irvine & Baragar 1971). This was also confirmed by a ternary plot of normative Cpx-Ol-Opx, using the discriminant functions of Chayes (1966).

With alkaline compositions eliminated, the AFM diagram (Fig. 4) serves to show that while the metadolerites are distinctly tholeiitic, though showing no actual tholeiitic trend, the younger dykes plot close to the tholeiitic/calc-alkaline dividing line of Irvine & Baragar (1971). This distinction is confirmed in a SiO₂ vs. *FeO/MgO variation plot, not presented here.

Figs. 5 and 6 show *FeO vs. *FeO/MgO and TiO₂ vs. *FeO/MgO variation and depict definite and disparate trends for both dyke sets. The gentler slopes

* Total iron as FeO.

Table 1. Chemical compositions of the metadolerite dykes

%	465	466	467	468	469	470	471	472	473	529	429	341	342	343
O ₂	45.95	48.08	46.75	46.08	47.76	48.61	45.39	44.71	47.84	47.13	46.21	45.56	45.56	46.75
SiO ₂	14.96	15.04	14.87	14.79	15.09	16.26	13.11	13.37	15.36	14.85	15.06	16.14	14.66	15.30
Al ₂ O ₃	1.49	0.81	1.60	0.65	1.62	2.25	1.89	2.20	1.54	1.09	1.90	4.24	2.82	1.69
FeO	10.86	11.37	11.49	12.00	10.79	9.07	13.27	13.85	10.47	8.47	8.54	9.50	10.49	10.68
MgO	1.73	1.98	1.93	1.73	1.81	1.48	3.39	3.50	1.72	1.38	1.40	2.26	1.95	1.51
CaO	7.35	7.34	7.21	7.04	5.96	6.46	6.43	6.29	7.18	6.75	6.85	6.96	7.50	7.62
Na ₂ O	12.01	7.43	10.07	6.80	10.75	8.62	10.30	9.81	8.52	14.37	14.36	6.27	10.69	10.41
K ₂ O	2.00	2.36	1.80	1.85	2.60	2.49	.17	.13	3.14	.41	.42	2.34	1.54	1.68
Sum	.05	.05	.05	.05	.08	1.12	.13	.07	.10	.05	.01	2.20	1.15	.86
H ₂ O	.23	.21	.23	.29	.02	.20	.23	.21	.24	.25	.16	.20	.21	.20
SO ₃	.06	.06	.07	.08	.08	.07	.16	.18	.09	.08	.08	.11	.11	.09
LOI	3.25	5.17	3.44	8.00	3.18	3.72	5.98	6.35	4.29	4.42	5.28	4.78	3.34	3.23
Total	99.89	99.85	99.46	100.19	99.74	100.35	100.45	100.67	100.49	99.25	100.26	100.56	100.02	100.02
n.o.m.														
	89	65	78	105	121	83	190	208	80	54	56	-	-	-
	36	34	35	39	38	30	56	61	28	28	28	-	-	-
	486	1685	1167	320	371	368	739	656	1135	795	759	-	-	-
	2	2	2	2	3	39	7	5	3	2	2	-	-	-
	107	111	116	110	116	113	151	181	111	100	96	-	-	-
	57	58	60	35	26	40	3	58	49	12	74	-	-	-
	76	62	68	66	55	77	59	56	85	56	73	-	-	-
	191	164	166	161	88	144	122	120	182	220	195	-	-	-
	96	98	68	68	71	292	91	25	61	113	67	-	-	-
	2 ¹	*	1 ¹	6	4 ¹	4	4	4	*	*	*	-	-	-

Below detection limit.

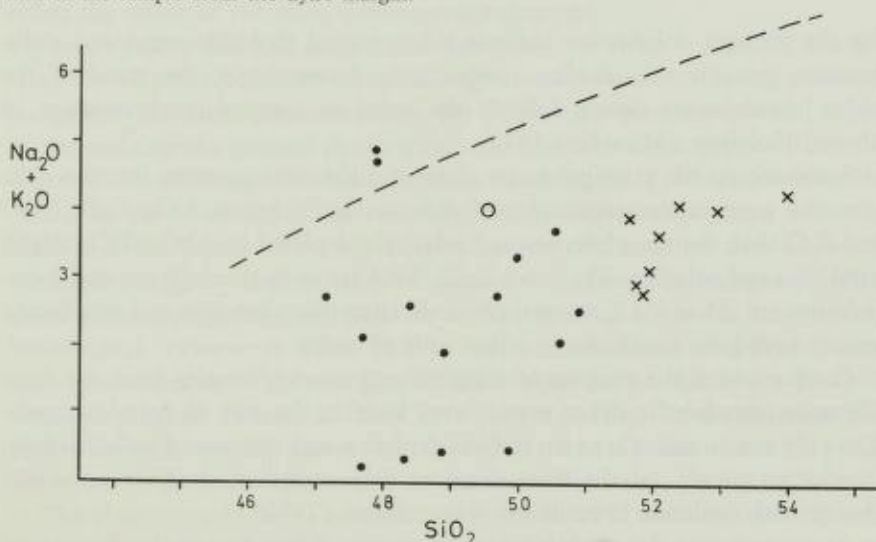
Analysts: Major elements, P.-R. Graff, Norges geologiske undersøkelse.

¹ — analysed by J. R. Cann, University of East Anglia.

Rb and other Nb — O. Lutro, University of Bergen.

All other trace elements, G. C. Faye and M. Ødegård, Norges geologiske undersøkelse.

Samples from the interior and margin of three separate dykes are those of nos. 467-8, 469-70 and 471-2; in each case the higher number is that of the sample from the dyke margin.

Fig. 3. SiO₂ vs. Na₂O + K₂O, wt% volatile-free, variation plot. The dashed line separates alkaline (above) and subalkaline fields (after Irvine & Baragar 1971).

● — metadolerite dykes; x — dolerite dykes; o — dyke sample no. FA88.

Table 2. Chemical composition of the dolerite dykes

wt.%	527	528	531	MP 10	FA 2	FA 37	340	120	FA 88 ¹	530
SiO ₂	52.82	51.61	50.59	50.84	51.24	51.01	50.98	50.92	47.17	46.2
Al ₂ O ₃	15.23	14.79	15.28	14.62	15.17	15.17	14.89	13.09	16.07	15.1
Fe ₂ O ₃	1.08	1.94	2.55	1.95	2.84	1.98	2.73	2.20	1.11	3.4
FeO	9.20	8.89	7.70	8.37	8.47	8.64	7.82	8.24	11.18	9.2
TiO ₂	1.15	1.31	.97	.99	1.28	1.08	1.02	1.07	2.94	2.0
MgO	5.19	5.91	6.99	7.63	5.82	6.78	7.17	8.00	3.96	7.0
CaO	9.07	9.21	10.28	11.20	9.14	9.92	10.65	10.90	8.94	8.2
Na ₂ O	2.76	2.92	2.79	2.20	3.07	2.58	2.34	2.11	2.64	2.3
K ₂ O	1.42	1.01	1.08	.68	1.03	1.00	.68	.64	1.24	2.2
MnO	.18	.27	.20	.20	.21	.19	.21	.18	.23	.2
P ₂ O ₅	.11	.12	.09	.06	.11	.08	.09	.13	.11	.1
L.O.I.	.80	1.26	1.69	1.40	2.03	1.46	1.87	1.81	3.96	2.7
Total	99.37	99.24	100.21	100.14	100.41	99.89	100.45	99.39	99.62	100.0
p.p.m.										
Zr	162	107	73	79	135	194	-	-	120	10
Y	29	24	21	22	21	49	-	-	25	
Sr	235	216	334	230	215	238	-	-	267	3
Rb	49	29	29	23	33	35	-	-	27	
Zn	94	95	77	84	97	123	-	-	90	
Cu	91	103	83	83	104	15	-	-	116	
Ni	29	24	44	49	12	17	-	-	59	
Cr	65	18	97	110	17	71	-	-	51	1
Ba	468	287	950	411	198	256	-	-	186	3
Nb	13	11	4	-	-	-	-	-	-	

¹ — Sample no. FA 88 and possibly sample no. 530 are from another dyke set (see text).

Analysts: Major elements, P.-R. Graff, Norges geologiske undersøkelse.

Nb — O. Lutro, University of Bergen.

All other trace elements, G. C. Faye and M. Ødegård, Norges geologiske undersøkelse.

for the younger dolerite set indicate a less typical tholeiitic trend and a disposition towards calc-alkaline composition. Interestingly, the trend of the older metadolerites closely follows the trend of compositional variation of abyssal tholeiites (Miyashiro 1975).

Summarizing the principal major element differences between the two dyke sets, the younger unmetamorphosed dolerites are richer in SiO₂, CaO, Na₂O and K₂O than the metadolerites and relatively depleted in Al₂O₃, TiO₂, MgO, total iron and volatiles. The mean Fe₂O₃/FeO ratios in the dolerites and metadolerites are .25 and .17, respectively, indicating that alteration and weathering cannot have been significant in either suite of rocks.

Comparison of the analyses of marginal and interior samples from the three different metadolerite dykes reveals very little in the way of definite trends. The only consistencies are seen in CaO depletion and increase of volatiles from interior to margin; of the trace elements only strontium shows a consistent change with depletion towards the dyke margins (Table 1).

An attempt was also made to identify possible differences in the chemistries of metadolerites from the Barents Sea Group and overthrust Raggo Group in view of the importance of the age of the Raggo rocks in the regional strati-

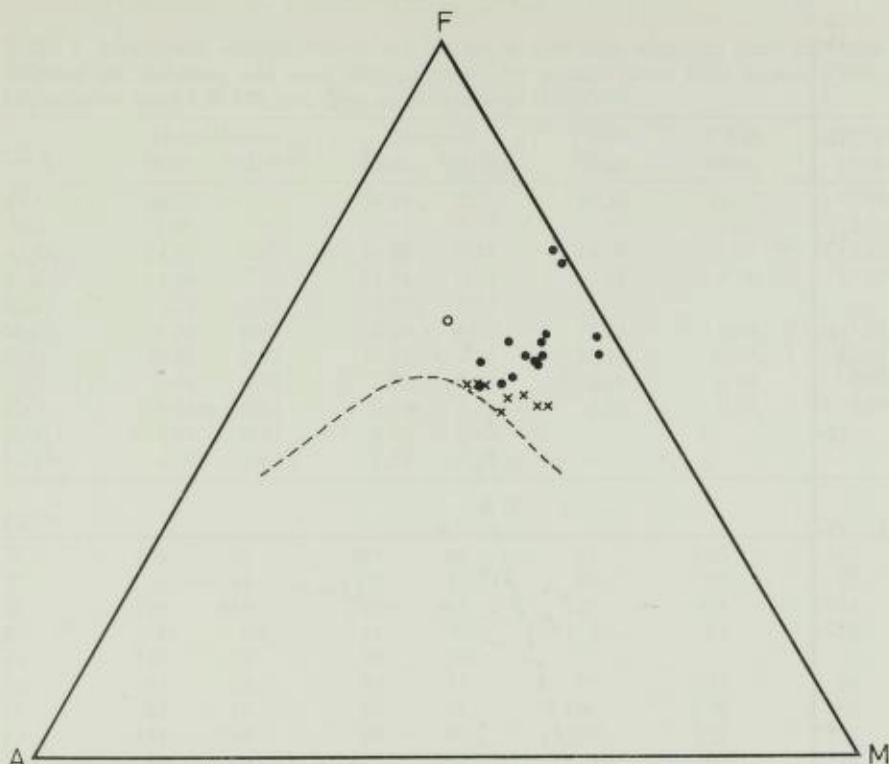


Fig. 4. AFM diagram. The dashed line separates the field of tholeiitic and calc-alkaline compositions (after Irvine & Baragar 1971). Symbols as in Fig. 3.

graphic and structural development, but no distinction could be observed in either the major or the trace element concentrations.

Trace element data and mean values are given in Tables 1, 2 and 3. Considering the elements which are comparatively insensitive to weathering processes and greenschist facies metamorphism, the Y/Nb ratio provides a useful means of determining the general petrological character of magma types (Pearce & Cann 1973). Although Nb determinations are few, the Y/Nb ratios from the metadolerites (mean of < 12) are appreciably higher than those from the dolerite dykes (mean of < 3). This is further confirmation that while the metadolerites have characteristics of abyssal tholeiites, the younger dolerites show a less typically tholeiitic and an increasing alkali character, i.e. they are 'transitional' (Pearce & Cann 1973). Further indications of differing compositional character of the two generations of dyke are provided by a Ti-Zr-Y variation diagram (Pearce & Cann 1973). In this (Fig. 7) the dolerites plot somewhat transitionally across the ocean floor, calc-alkaline and within-plate fields, while the metadolerites fall in the ocean floor and, partly, LKT fields.

The element ratio Sr/Ba plotted as a function of K concentration (Condie et al. 1969) again illustrates the similarity of the older metadolerites to submarine tholeiites (Fig. 8), in spite of the fact that these elements are some of the most mobile during alteration and low-grade metamorphism and have

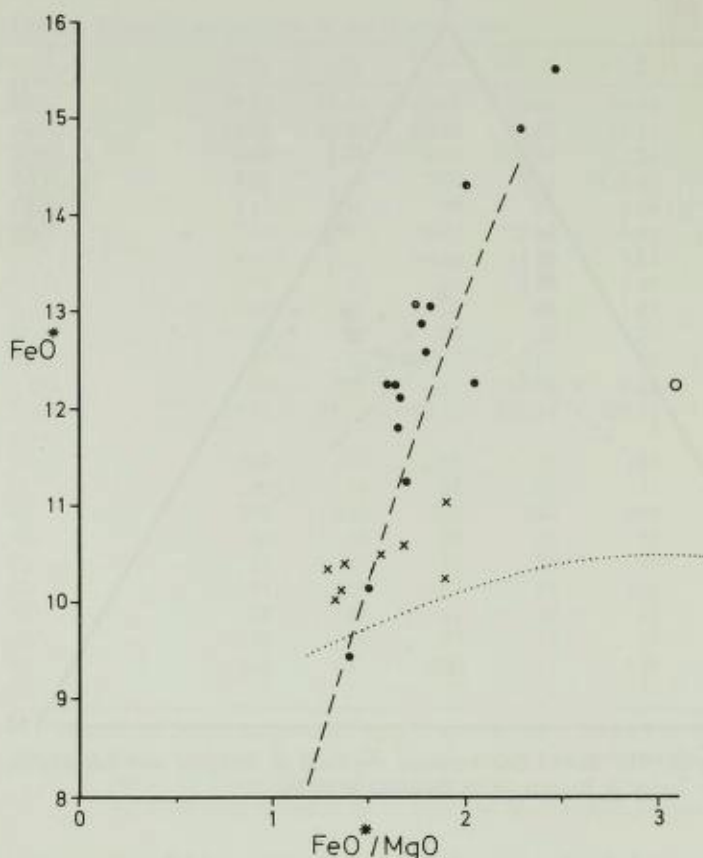


Fig. 5. Variation plot of FeO^* vs. FeO^*/MgO (FeO^* = total iron as FeO), symbols as in Fig. 2. Dashed line — average compositional variation trend of abyssal tholeiites; dotted line — the compositional trend of the Tofua Island (Tonga) tholeiite (both trend lines after Miyashiro 1975).

comparatively high mean values in the present case. Interesting here is the fact that the dolerites occupy the fields of either average continental tholeiites or the Antarctic and Tasmanian tholeiites. Other element ratios plotted on other 'Condie' diagrams show similar distributions for both dyke sets. The K/Rb ratio of ca. 240 for the dolerites compares well with the value of 300 obtained for continental basalts (Gast 1965). The mean Rb content of 3 ppm for the metadolerites is equivalent to the 2 ppm average for abyssal tholeiites (Condie et al. 1969); that for the dolerites, 33 ppm, is close to the average (36 ppm) for continental basalts.

Considering the above petrological affinities, the strontium content in the metadolerite dykes is anomalously high, being over 5 times the mean for abyssal basalts (Pearce & Cann 1973). Although this high average is caused by three particularly Sr-rich samples (Table 1), the generally high values are noted even in the Sr-depleted dyke-margin samples, and it is therefore suggested that this is likely to reflect high primary values in the original

Table 3. Means and standard deviations for major and trace elements from the metadolerites and dolerites, and mean element values for average ocean floor basalts (OFB), calc-alkaline basalts (CAB) and continental tholeiites (CON)

wt. %	Metadolerites		Dolerites		OFB ³	CAB ³	CON ³
	Mean	Std. dev.	Mean	Std. dev.	Mean	Mean	Mean
SiO ₂	46.60	1.16	51.25	0.70	49.56	52.12	48.81
TiO ₂	1.98	0.67	1.11	0.13	1.42	1.07	2.47
Al ₂ O ₃	14.92	0.85	14.78	0.72	16.09	18.07	14.41
Fe ₂ O ₃ ¹	13.69	1.82	11.41	0.38	11.19	9.78	13.20
MnO	0.21	0.06	0.20	0.03			
MgO	6.92	0.49	6.69	0.97	7.69	5.00	5.96
CaO	10.03	2.45	10.05	0.84	11.34	9.67	10.05
Na ₂ O	1.64	0.98	2.60	0.35	2.80	2.95	2.90
K ₂ O	0.43	0.66	0.94	0.27	0.24	0.94	0.95
P ₂ O ₅	0.09	0.04	0.10	0.02			
L.O.I.	4.60	1.44	1.54	0.40			

p.p.m.							
Zr	103	52	125	48	83	106	149
Y	38	11	28	11	28	23	25
Sr	771	418	245	45	121	435	401
Rb	3 ²	0.6	33	9	2.6	23	15
Zn	119	25	95	16			
Cu	43	22	80	33	73	35	99
Ni	67	10	29	15	106	50	68
Cr	159	38	63	39	280	135	139
Ba	95	69	428	274	8.4	260	338
Nb	3.5	2	10	2.5	2.5	3.3	25

¹ Total Fe as Fe₂O₃.

² Excluding sample 470.

³ Taken from Pearce (1973).

magma. The average Sr content of 245 ppm in the dolerites is somewhat lower than the average for continental tholeiites in general (Condie et al. 1969), yet higher than for certain basalts of this type, e.g., some of the Karroo dolerites.

Ba averages of 95 ppm and 428 ppm for the metadolerites and dolerites, respectively, are higher than those for mean abyssal tholeiites and continental basalts, a feature which could bear some relationship to the high strontium values and which is probably also a primary feature of the magmas.

Of the remaining elements, Ni, Cr and Zn are consistently higher in the metamorphosed dykes, whereas Cu shows greater concentrations in the dolerites. Ni values are lower than the averages for both submarine and continental basalts, possibly a reflection of a negligible content of olivine; the higher Ni content, 67 ppm, in the metadolerites may be associated with the higher Ti values and the more abundant ilmene-magnetite in these dykes. The low Ni values in the dolerites may be related to the abundance of pigeonite, rather than augite, in the rock (McDougall & Lovering 1963).

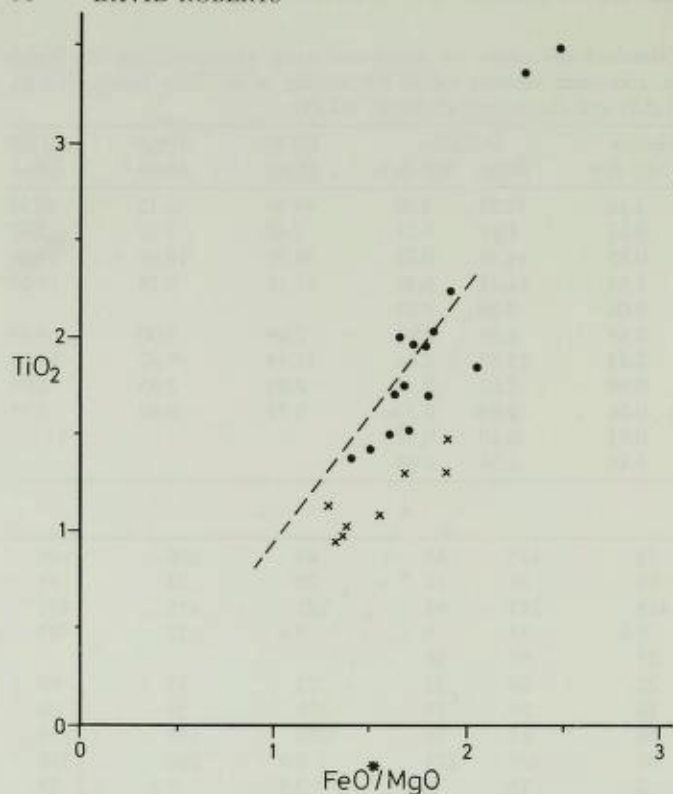


Fig. 6. TiO_2 vs. FeO^*/MgO diagram, symbols as before. The dashed line shows the average trend of compositional variation of abyssal tholeiites (after Miyashiro, 1975).

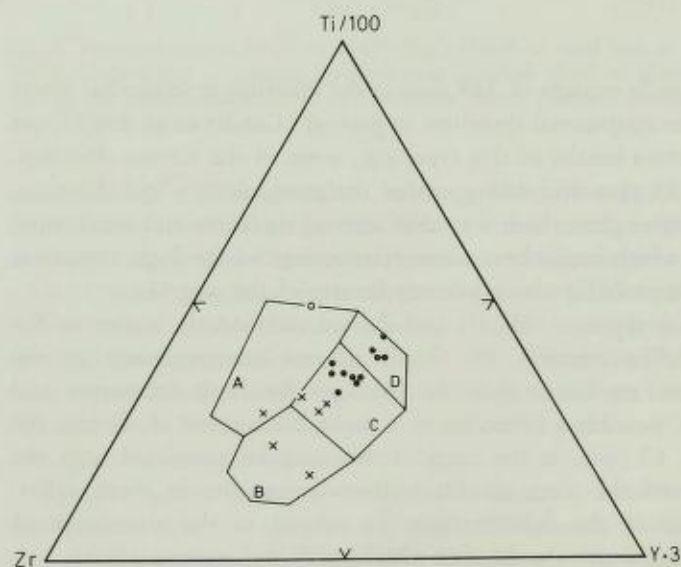


Fig. 7. Ti-Zr-Y plot of the dolerite and metadolerite samples; symbols as in previous figures. The various fields, representative of magma types (after Pearce & Cann, 1973), are as follows: within-plate basalts plot in field A, ocean floor basalts in field C, calc-alkali basalts in fields B and C, low-potassium tholeiites in fields D and C.

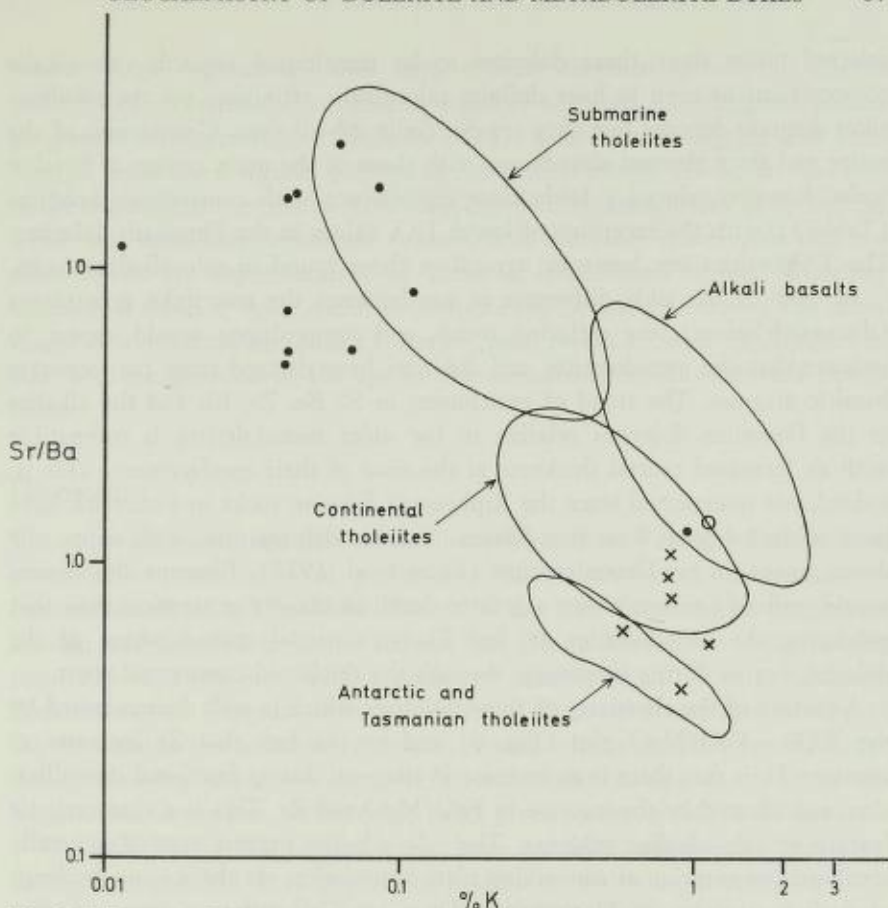


Fig. 8. Sr/Ba vs. % K diagram, showing the fields for some major rock-types (after Condie et al. 1969). The symbols are those of the previous figures.

Petrogenetic considerations

The foregoing presentation of the major and trace element data on variation and discrimination diagrams has revealed notable differences in the groupings and trends between the two dyke generations. The older metadolerites show a reasonably close correspondence to oceanic tholeiites both on element concentrations (Sr and Ba excluded) and on various ratios, in particular the low potassium and niobium values and high K/Rb ratios (Engel et al. 1965). This is in spite of the low-grade greenschist metamorphism, in which both Rb and K as well as Sr and Ba are particularly mobile elements. The possibility that the chemistry of the metadolerites has been modified to some extent by the metamorphism is clearly present. This may account for some of the scatter in certain diagrams, but otherwise there are no consistent trends indicative of element abundance modification by metamorphic processes in these dykes.

The younger dolerite dykes are petrographically more difficult to classify. While tending towards tholeiitic affinities, certain element variation plots and

selected ratios show these dolerites to be transitional towards calc-alkalic compositions or even to have definite calc-alkalic affinities; yet the alkalis-silica diagram denotes that they are decidedly sub-alkaline. Comparison of the major and trace element abundances with those of the main groups of basaltic rocks, however, shows a fairly close equivalence with continental tholeiites (Table 3), with the exception of lower TiO_2 values in the Finnmark dolerites. The TiO_2 values are, however, typical of those found in calc-alkaline rocks.

In view of the wide difference in age between the two dyke generations (discussed below), the differing trends and compositions would appear to indicate that the metadolerites and dolerites have derived from two separate basaltic magmas. The trend of enrichment in Si, Ba, Zr, Rb and the alkalis in the Devonian dolerites relative to the older metadolerites is compatible with an increased crustal thickness at the time of their emplacement. This is, indeed, not unexpected since the Riphean to Silurian rocks in Finnmark have been subjected to at least two phases of major deformation, with nappe-pile development, in pre-Devonian time (Sturt et al. 1975). Element abundances would probably reflect either a greater depth of magma generation than that producing the metadolerites or, less likely, a partial contamination of the dolerite magma during its passage through the thickened continental crust.

A feature of the chemistry of these dolerites which is well demonstrated by the $\text{TiO}_2 - \text{FeO/MgO}$ plot (Fig. 6) and by the fact that Zr increases at constant Ti, is that there is no increase in titanium during fractional crystallisation, as indicated by the increase in FeO/MgO and Zr. This is a characteristic feature of calc-alkaline magmas. The calc-alkaline magma type is generally attributed to eruption at converging plate boundaries, yet there is no evidence of such a situation in Finnmark in Devonian/Carboniferous times. A few rocks of this composition have been found at continental edges (J. Pearce, pers. comm.), and it is not impossible that these dolerites were intruded in such an environment. The composition in no way resembles 'hot spot' volcanic rocks, but could be representative of a small class of rocks emplaced in an extensional continental environment not associated with 'hot spot' activity (J. Pearce, pers. comm.). It is interesting here to note that the trends of the various fold episodes on Varanger Peninsula indicate a progressive dextral rotation of the regional maximum shortening direction with time (Roberts 1972). The latest gentle to open warps have NW-SE to E-W axial trends, exactly normal to the c. NNE-SSW dolerite dykes which were undoubtedly intruded in a tensional regime.

By contrast, the chemistry of the metadolerites would, at first glance, appear to signify that the crust underlying the sediments into which these dykes were intruded was thinner in this northernmost Scandinavian region and possibly largely of oceanic character at the time of dyke emplacement, assuming that the magma chemistry is a direct reflection of the physico-chemical conditions and compositions in the lower crust and upper mantle. On the other hand it is clear that these dykes, intruded as they are into a thick pile of Riphean sediments concomitant with deformation, do not represent material from

oceanic ridge (spreading) axes despite their chemical affinity to abyssal tholeiites. This tectonic environment, together with our knowledge of palaeogeographic reconstructions (Siedlecka 1975), would rather suggest that some form of transitional regime, perhaps of continental margin character, was host to the metadolerite intrusion. Reflecting on the high abundances of Sr and Ba, which was considered a primary feature, it is therefore conceivable that the older dykes are representative of rocks of transitional abyssal tholeiite/continental tholeiite type; such hybrid rocks can be intruded during the initial stages of continental break-up (J. Pearce, pers. comm.). Some implications of this, and the question of the age of the metadolerites, are discussed briefly below.

Discussion

The only radiometric age data on the basic dykes from Varanger Peninsula, as noted earlier, are those of preliminary K-Ar whole-rock determinations (Beckinsale et al. 1975). Metadolerites of the type described in the present account and sampled from the Barents Sea Group have given dates ranging from 935 to 1946 m.y. with a preferred mean of c. 1075 m.y., although Beckinsale et al. recognise the unreliability of these particular ages in view of the consistently low potassium contents. A metadolerite sample from the Raggio Group showing the same intrusive/tectonic relationships as those in the Barents Sea Group has, on the other hand, given an age of 542 ± 17 m.y.

The dolerites of the present study have provided rather more consistent dates of around 355 ± 10 m.y., from 6 samples, which is considered a fairly reliable intrusive age (Beckinsale et al. 1975). In addition, these authors have sampled apparently unclesed dykes from the Båtsfjord area which cut the thrust beneath supposed Raggio Group equivalents. These have given K-Ar whole-rock ages averaging about 640 ± 19 m.y.

As yet, this 640 m.y. dyke set has not been studied in detail in the field. The chemistry of these dykes is poorly known although in the present study samples nos. FA88 and possibly 530 may be representatives of this Båtsfjord-type dyke set. These show higher values for titanium and alkalis than the metadolerites. A more detailed study of the chemistry of these particular dykes is planned.

A comparison of the chemical and radiometric data obtained from the Varanger Peninsula dykes, on a wider regional basis, has revealed that the uppermost Devonian dykes are apparently unique in the northern Russo-Fennoscandian region. Siedlecka (1975), in a comprehensive survey of the Russian literature on the Timan-Kanin-Ribachiy region, found no reports of basic dyke ages younger than 500 m.y.; these particular 500 m.y. dykes, dolerites and camptonites, are from the northern Timans (Malkov 1972, Table 1). In the same region, gabbroic rocks were intruded in the period 620-640 m.y., and a metamorphic event is dated at 525-520 m.y. Nearer to Finnmark, there is an isolated K-Ar age of 600 ± 20 m.y. for a dolerite (.32% K) from the Sredniy Peninsula (Bekker et al. 1970).

Turning to central and west Finnmark, metadolerites similar in petrography and intrusive/tectonic relationships to those in the Raggo and Barents Sea Groups are fairly common in the Gaissa, Laksefjord and Kalak nappes (Føyn 1960, Gayer & Roberts 1971, Sturt et al. 1975). Rb-Sr* whole-rock isochrons of 530 ± 50 m.y. (now revised to 515 ± 7 m.y.) and 535 ± 60 m.y. have been obtained for the cleavage in the autochthon (Pringle 1972) and in the Laksefjord nappe (Sturt et al. 1975), respectively; these dates may also roughly correspond to the dyke intrusion ages, although some of the dykes could be of earlier, pre-deformation, Vendian emplacement.

The problem of the two suggested Laksefjord/Raggo/Barents Sea Group correlation schemes has already been outlined (p. 56). The single 542 ± 17 m.y. date of Beckinsale et al. (1975) for the Raggo metadolerite could possibly be interpreted in favour of similar dyke and deformation ages for the Laksefjord and Raggo Groups. This does not, of course, imply that the sediments of these two groups are necessarily correlatives, although they *may* in fact be of roughly equivalent age. Alternatively, the westernmost part of the Raggo Group, on the basis of biotite porphyroblasts common throughout the nearby Nordkyn Peninsula (Roberts, unpublished results) and also present in the Raggo (Teisseyre 1972), could possibly represent a segment of the Kalak Nappe.

Returning to the matter of the virtually identical structural/dyke-intrusive features displayed by the Raggo and Barents Sea Groups (Roberts 1972), these must now be considered in the light of the Beckinsale et al. 935–1946 m.y. preliminary dates. Clearly, there are seemingly incompatible data here, but *if* the c. 1075 m.y. age is confirmed then this would denote a folding and metamorphic event of about the same age for the Barents Sea Group, an orogenic pulse which would invite comparison with the Carolinian deformation of N.E. Greenland (Haller 1970) and signify an even older age for the Barents Sea Group than has hitherto been suggested (e.g., Siedlecka & Siedlecki 1971, Siedlecki 1975). At the same time, an implication of the chemistry and tectonic setting of these metadolerites would be that we are possibly dealing with an incipient stage of continental break-up in the period 1100–950 m.y. B.P. There is no evidence from the younger dolerites, on the other hand, either from the chemistry or from the regional geology, of a comparable megatectonic movement in uppermost Devonian time. It must be stressed once again, however, that the above assumptions are based on the results of the preliminary K-Ar studies, the oldest dates of which are the most suspect; moreover, they are not strictly compatible with what we know of the geology of Ribachiy (Siedlecka 1975) or of the character and age of deformation throughout Finnmark. Further radiometric work on the dykes and on the metasediments should certainly help to resolve several of these fundamental problems.

* Based on $^{87}\text{Rb} : \lambda = 1.39 \times 10^{-11} \text{yr}^{-1}$.

Acknowledgements. - I wish to thank Dr. G. H. Gale for helpful and stimulating discussion at all stages during the work, and Drs. J. A. Pearce, W. L. Griffin and G. H. Gale for their constructive criticism of the manuscript. An earlier draft was also read by Drs. A. Siedlecka and S. Siedlecki. The bulk of the analytical work was carried out by P.-R. Graff, G. C. Faye and M. Odegård, Norges geologiske undersøkelse; O. Lutro (Bergen) and Dr. J. R. Cann (East Anglia) provided additional data and check analyses; some of the samples or analyses were donated by Drs. R. D. Beckinsale, A. Siedlecka and S. Siedlecki. To all these persons I am greatly indebted.

REFERENCES

- Banks, N. L., Edwards, M. B., Geddes, W. P., Hobday, D. K. & Reading, H. G. 1971: Late Precambrian and Cambro-Ordovician sedimentation in East Finnmark. *Norges geol. Unders.* 269, 197-236.
- Banks, N. L., Hobday, D. K., Reading, H. G. & Taylor, P. N. 1974: Stratigraphy of the Late Precambrian 'Older Sandstone Series' of the Varangerfjord area, Finnmark. *Norges geol. Unders.* 303, 1-15.
- Banks, N. L. & Roe, S.-L. 1974: Sedimentology of the Late Precambrian Golneselv Formation, Varangerfjorden, Finnmark. *Norges geol. Unders.* 303, 17-38.
- Beckinsale, R. D., Reading, H. G. & Rex, D. C. 1975: Potassium-argon ages for basic dykes from East Finnmark: stratigraphical and structural implications. *Scott. J. Geol.* (in press).
- Bekker, Y. R., Negrutsa, V. Z. & Poleyaya, N. I. 1970: Age of glauconite horizons and the upper boundary of the Hyperborean in the eastern part of the Baltic Shield. *Doklady Akad. Nauk. SSSR*, 193, 80-83.
- Chayes, F. 1966: Alkaline and subalkaline basalts. *Amer. J. Sci.* 264, 128-145.
- Condie, K. C., Barsky, C. K. & Mueller, P. A. 1969: Geochemistry of Precambrian diabase dikes from Wyoming. *Geochim. Cosmochim. Acta*, 33, 1371-1388.
- Engel, A. E. J., Engel, C. G. & Havens, R. G. 1965: Chemical characteristics of oceanic basalts and the upper mantle. *Geol. Soc. Am. Bull.*, 76, 719-734.
- Foyn, S. 1960: Tanafjord to Laksefjord. In Aspects of the geology of Northern Norway. Guide to Excursion A3. *Norges geol. Unders.* 212a, 45-55.
- Gast, P. W. 1965: Terrestrial ratio of potassium to rubidium and the composition of the Earth's mantle. *Science* 147, 858-860.
- Gayer, R. A. & Roberts, J. D. 1971: The structural relationships of the Caledonian nappes of Porsangerfjord, West Finnmark, N. Norway. *Norges geol. Unders.* 269, 21-67.
- Gayer, R. A. & Roberts, J. D. 1973: Stratigraphic review of the Finnmark Caledonides, with possible tectonic implications. *Proc. Geol. Assoc.* 84, 405-428.
- Haller, J. 1970: Tectonic map of East Greenland (1 : 500,000). *Medd. om Grønland* 171, 5, 1-286.
- Holtedahl, O. 1918: Bidrag til Finnmarkens geologi. *Norges geol. Unders.* 84, 1-314.
- Irvine, T. N. & Baragar, W. R. A. 1971: A guide to the chemical classification of the common volcanic rocks. *Canad. Jour. Earth Sci.* 8, 523-548.
- Laird, M. G. 1972: Sedimentation of the ?Late-Precambrian Raggo Group, Varanger Peninsula. *Norges geol. Unders.* 278, 1-12.
- Langmyhr, F. J. & Graff, P.-R. 1965: A contribution to the analytical chemistry of silicate rocks: a scheme of analysis for eleven main constituents based on decomposition by hydrofluoric acid. *Norges geol. Unders.* 230, 1-128.
- Malkov, B. A. 1972: Petrology of the gabbroid dykes of the Northern Timans. (In Russian). *An SSSR, Komi Branch, Izd. Nauka*, 127 pp.
- McDougall, I. & Lovering, J. P. 1963: Fractionation of chromium, nickel, cobalt and copper in a differentiated dolerite-granophyre sequence at Red Hill, Tasmania. *Geol. Soc. Australia Jour.* 10, 325-328.
- Miyashiro, A. 1975: Classification, characteristics and origin of ophiolites. *J. Geol.* (in press).
- Pearce, J. A. 1973: *Some relationships between the geochemistry and tectonic setting of basic volcanic rocks.* Unpubl. Ph.D. thesis, Univ. of East Anglia.
- Pearce, J. A. & Cann, J. R. 1973: Tectonic setting of basic volcanic rocks determined using trace element analyses. *Earth Planet. Sci. Letters* 19, 290-300.

- Pringle, I. R. 1972: Rb-Sr age determinations on shales associated with the Varanger Ice age. *Geol. Mag.* 109, 465-472.
- Roberts, D. 1972: Tectonic deformation in the Barents Sea region of Varanger Peninsula, Finnmark. *Norges geol. Unders.* 282, 1-39.
- Roe, S.-L. 1970: Correlation between the Late Precambrian Older Sandstone Series of the Varangerfjord and Tanafjord areas. *Norges geol. Unders.* 266, 230-245.
- Siedlecka, A. 1972: Kongsfjord Formation - a Late Precambrian flysch sequence from the Varanger Peninsula. *Norges geol. Unders.* 278, 41-80.
- Siedlecka, A. 1975: Late Precambrian stratigraphy and structure of the north-eastern margin of the Fennoscandian Shield (East Finnmark - Timan region). *Norges geol. Unders.* 316, 313-348.
- Siedlecka, A. & Siedlecki, S. 1967: Some new aspects of the geology of Varanger Peninsula (Northern Norway). *Norges geol. Unders.* 247, 288-306.
- Siedlecka, A. & Siedlecki, S. 1971: Late Precambrian sedimentary rocks of the Tanafjord-Varangerfjord region of Varanger Peninsula, Northern Norway. *Norges geol. Unders.* 269, 246-294.
- Siedlecka, A. & Siedlecki, S. 1972: Lithostratigraphical correlation and sedimentology of the Late Precambrian of Varanger Peninsula and neighbouring areas of East Finnmark, Northern Norway. *XXIV Intern. Geol. Congress, Montreal*, 6, 349-358.
- Siedlecki, S. 1975: The geology of Varanger Peninsula and stratigraphic correlation with Spitsbergen and North-east Greenland. *Norges geol. Unders.* 316, 349-350.
- Sturt, B. A., Pringle, I. R. & Roberts, D. 1975: The Caledonian nappe sequence of Finnmark, northern Norway, and the timing of orogenic deformation and metamorphism. *Bull. Geol. Soc. Am.* 86, 710-718.
- Teisseyre, J. H. 1972: Geological investigations in the area between Kjolnes and Trollfjorden (Varanger Peninsula). *Norges geol. Unders.* 278, 81-92.

Possible Mesozoic Mantle Plume Activity beneath the Continental Margin of Norway

TORE TORSKE

Torske, T. 1975: Possible Mesozoic mantle plume activity beneath the continental margin of Norway. *Norges geol. Unders.* 322, 73–90.

Based on recent geological and geophysical information from the Norwegian/Greenland Sea and North Sea areas, and on earlier geomorphological information interpreted in terms of regional drainage pattern evolution, it is concluded that the More-Jotunheimen and Norrbotten-Troms uplands may be erosional remnants of two large, pre-Tertiary, mantle plume-generated domal uplifts. These were centred on the adjacent parts of the present continental shelf and slope, where linear gravity highs and elongate sedimentary troughs may represent mantle plume-generated mafic intrusions and rifts. The mantle plume activity probably occurred in Mesozoic time, possibly in the Jurassic, long before the onset of Early Tertiary ocean-floor spreading in the Norwegian/Greenland Sea area. The inferred rifts and intrusions appear to form a northern extension of pre-splitting tectonic activity along the present North American and north-west European Atlantic margins.

Tore Torske, Institutt for biologi og geologi, Universitetet i Tromsø, P.O. Box 790, N-9001 Tromsø, Norway

Introduction

Dome-shaped crustal uplifts, with ensuing rifting, volcanism and formation of tectonic triple junctions, are currently regarded as surface manifestations of mantle plume activity beneath the lithosphere (Morgan 1971; Wilson 1972, 1973; Burke & Whiteman 1973). In a typical evolutionary sequence mantle plume-generated uplifts develop through rifting, with the formation of three crestral rifts meeting at triple junctions designated 'rrr' ('rift-rift-rift') junctions, into spreading 'RRR' junctions (Burke & Whiteman 1973). Continental triple junctions are considered to have developed into diverging, accreting lithospheric plate margins causing continental break-up and ocean-floor spreading (Burke & Dewey 1973). An example is the Afar RRR junction in Ethiopia, with active spreading on the Red Sea and Gulf of Aden arms and incipient spreading on the Ethiopian Rift arm (Burke & Whiteman 1973). These rifts form the diverging, accreting margins of the Arabian, Nubian and Somalian lithospheric plates (Darracott et al. 1973).

In other examples only two arms of a triple junction reach the spreading stage, while the third rift forms the 'failed' arm of a 'RRr' triple junction (Burke & Whiteman 1973). The occurrence of triple junctions with two or even three 'failed' arms has also been suggested (Burke & Whiteman 1973; Burke & Dewey 1973; Naylor et al. 1974; Whiteman et al. 1975). Examples of mantle plume-generated uplifts without associated rifting are the Rhodesia and Vaal swells in southern Africa (Burke & Wilson 1972), the Adamawa

uplift in equatorial Africa (Burke & Whiteman 1973) and the Colorado Plateau in North America (Wilson 1973).

Morgan (1971) considered mantle plume activity to be the driving force of lithospheric plate motion. Wilson (1972) and Burke & Dewey (1973) have suggested that divergent plate motion is initiated following the emplacement of axial dykes in crestral rifts on swells above mantle plumes, and that accreting plate margins develop from rifts in the lithosphere linking neighbouring plume tops in the asthenosphere. Burke & Wilson (1972), in proposing the average lifetime of individual mantle plumes to be of the order of 100 m.y., ascribed the changing patterns and rates of plate motion to the influence of changing competition among shifting arrays of plumes of different ages and of variable intensities of activity.

The present paper presents evidence suggesting that, in mainland and off-shore Norway, two instances of mantle plume-generated doming and rifting preceded the Early Tertiary initiation of active ocean-floor spreading in the Norwegian/Greenland Sea. It is concluded that the present uplands in the Møre-Jotunheimen and Troms-Norrbotten areas may be remnants of the suggested domal uplifts, and that the Mesozoic sedimentary troughs on the Norwegian continental shelf and slope were formed as a result of rifting associated with them. These events may be integrated into the post-Palaeozoic geotectonic history of the North European-North American region.

Ocean-floor spreading in the North Atlantic-Arctic region

The final closing of the Palaeozoic proto-Atlantic ocean in Late Palaeozoic time by continental collisions of Africa, North America and South America (Coney 1973) completed, together with the collision between the European/Russian and Siberian platforms (Hamilton 1970; Ostenso 1973), the assemblage of the universal Pangaeans continent (Dietz & Holden 1970); Europe and North America had already collided at an earlier stage (Coney 1973). The Mesozoic re-organization and the subsequent renewal of lithosphere plate motion, causing the break-up of Pangaea (Dietz & Holden 1970), constitute the geotectonic point of departure for the currently continuing ocean-floor spreading and continental drift in the North Atlantic-Arctic region.

Active ocean-floor spreading in the North Atlantic commenced about 180 m.y. ago when Africa separated from North America (Le Pichon 1968; Dietz & Holden 1970; Vogt et al. 1970; Pitman & Talwani 1972; Bott 1973a; Burke & Dewey 1973; Laughton 1975).

In the Early Cretaceous (120 m.y. ago), ocean-floor spreading produced a widening split between the Grand Banks of Newfoundland and the Iberian Peninsula, and at the same time opened up the Bay of Biscay by a counter-clockwise rotation of Iberia with respect to Europe (Laughton 1975). This rotation stopped in the Late Cretaceous (80 m.y. ago), and active spreading is then thought to have started along an axis running north-westwards from the Bay of Biscay into the Labrador Sea (Laughton 1975). As the Labrador Sea

started to develop, Greenland, Europe and Iberia formed parts of a single plate separating from North America (Laughton 1971, 1975).

In the Arctic Ocean area, complex lithospheric plate motion involving divergent, convergent and transform plate interactions appears to have started in the early Mesozoic (Ostenso 1973, 1974), although the Beaufort Sea area of the Canadian Basin possibly had been in existence as an ocean basin (the Hyperborean Sea) since the Early Palaeozoic (Churkin 1969, cited in Ostenso 1973). Spreading in the Arctic Ocean was originally proceeding from the Alpha Ridge but switched to the Nansen Ridge about 47 m.y. ago, thereby splitting off the Lomonosov Ridge from Eurasia as a strip of continental crust, which now separates the Canadian Basin from the Siberian Basin (Ostenso 1973, 1974). In Mesozoic time the spreading axis in the Arctic Ocean may have been coupled to the Labrador Sea spreading axis by a major fracture zone, the Wegener fault (Wilson 1963, Burke & Dewey 1973).

South of Greenland the Cape Farewell triple junction (Pitman & Talwani 1972; Burke & Dewey 1973), possibly initiated in the Jurassic, became a RRR junction with active spreading on all three arms in the Late Palaeocene. This caused Greenland to become a separate plate by being split off from Europe along a spreading axis which opened up the Norwegian/Greenland Sea (Avery et al. 1968; Vogt et al. 1971; Johnson et al. 1972; Pitman & Talwani 1972; Bott 1973a; Ostenso 1973; Laughton 1975).

Greenland rejoined the American plate when a change in spreading pattern in the Middle Eocene (42/47 m.y. ago) stopped further opening of the Labrador Sea. Simultaneously, relatively minor changes affected the local North Atlantic, Norwegian/Greenland Sea and Arctic Ocean spreading centres.

Since the Middle Oligocene no major changes in spreading pattern are known to have occurred in the North Atlantic-Arctic region (Phillips & Luyendyk 1970; Vogt et al. 1971; Johnson et al. 1972; Bott 1973a; Ostenso 1973, 1974; Laughton 1975).

The Norwegian/Greenland Sea area and its spreading history

Within this oceanic province, the Mid-oceanic Ridge is segmented into the Kolbeinsey Ridge between Iceland and the transverse Jan Mayen Fracture Zone (Fig. 1), Mohn's Ridge between the Jan Mayen and Greenland Fracture zones and the Atka (or Knipovich) Ridge between the Greenland and the Spitsbergen Fracture zones (cf. Talwani & Eldholm 1974). This stretch of the Mid-oceanic Ridge separates the Norwegian Basin, to the south-east, from the Greenland Basin, to the north-west. Both these basins are bordered on their landward sides by a continental slope and shelf.

Structurally important physiographic elements within the Norwegian Basin are (Fig. 1): the Vøring Plateau, a relatively deep oceanward protrusion from the Norwegian continental slope; the Jan Mayen Ridge, a narrow micro-continental strip extending southwards from the volcanic Jan Mayen Island towards the Iceland-Faeroe Plateau (Johnson et al. 1972); and the Aegir

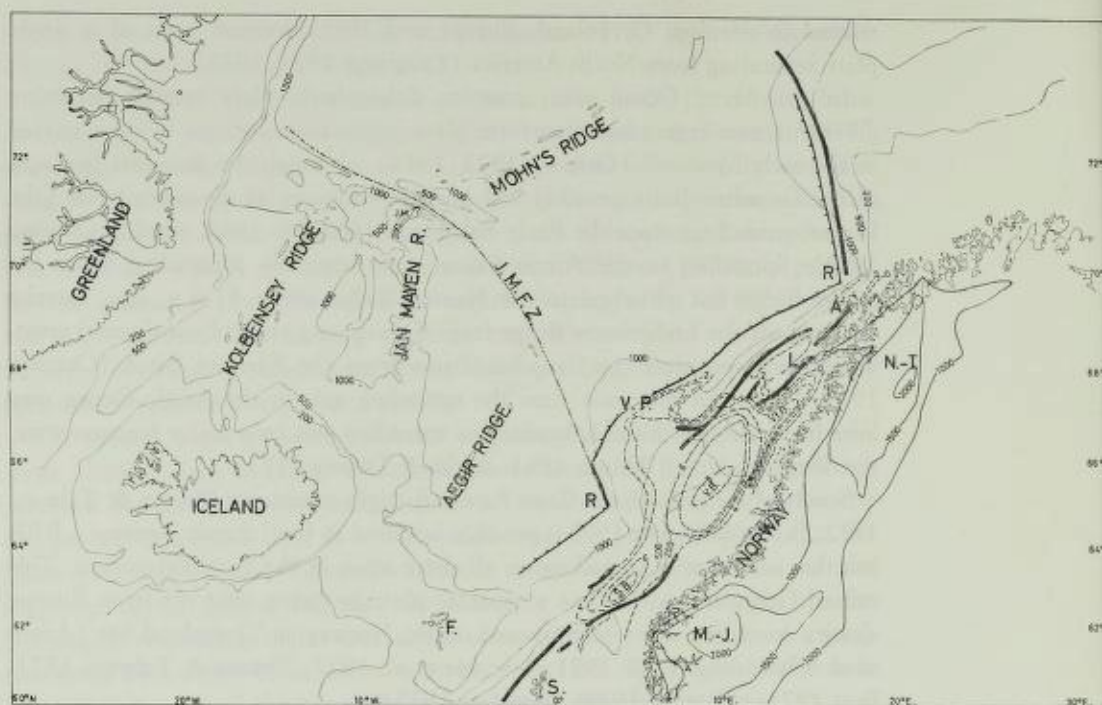


Fig. 1. Map of the Norwegian/Greenland Sea area (Redrawn after Talwani & Eldholm 1972 and Talwani & Grønlie, in press; Mercator projection).

A — Andoya; F — the Faeroes; J.M. — Jan Mayen island; J.M.F.Z. — Jan Mayen Fracture Zone (dash-dot line); L — Lofoten; M.-J. — Møre-Jotunheimen upland area; N.-T. — Norrbotten-Troms upland area; R — continental margin re-entrants; S — Shetland; S.B. — Stadt Basin; V.B. — Vøring Basin; Vf.B. — Vestfjord Basin; V.P. — Vøring Plateau. Thin, continuous lines: 200-, 500- and 1000-fathom isobaths.

Dashed, numbered lines on Norwegian continental margin are approximate isopach contours of pre-Tertiary sediments with thickness in km (adapted from Talwani & Eldholm 1972, Figs. 13 and 15). Thick, ticked line: ?oceanic crust/continental crust boundary along the Norwegian continental margin. Short, thick lines: linear gravity highs on Norwegian and Barents shelf edges and slopes. Numbered contours on mainland Scandinavia: 'enveloping surface' (modified after Gjessing 1967; heights in metres a.s.l.).

Ridge, a NNE-SSW trending chain of abyssal seamounts in the southern half of the Norwegian Basin (Hinz & Moe 1971) representing an extinct, buried ocean ridge/rift valley structure (Eldholm & Windisch 1974).

Active ocean-floor spreading in the Norwegian/Greenland Sea area started about 60 m.y. ago, according to interpretations of magnetic anomalies in terms of the geomagnetic time scale of Heirtzler et al. (1968); anomaly no. 24 (c. 60 m.y. old) is the oldest magnetic anomaly identified in segments of oceanic crust immediately adjacent to continental crust in this area (Avery et al 1968; Talwani & Eldholm 1972, 1974).

North of the Jan Mayen Fracture Zone, spreading has apparently always proceeded from Mohn's Ridge. In the area between the Iceland-Faeroe Plateau and the Jan Mayen Fracture Zone, ocean-floor spreading has been more complex: in the first period of active spreading, from c. 60 to c. 42 m.y. ago,

the Aegir Ridge was the spreading axis (Vogt et al. 1970). Later (cf., Laughton 1975, p. 187), the spreading centre migrated westwards, eventually initiating spreading beneath the Greenland continental margin and thereby splitting off a chip of continental crust, overlain by a thick sedimentary pile, which now forms the Jan Mayen Ridge (Fig. 1; Johnson & Heezen 1967). A further, but so far unconfirmed, westward migration of the spreading centre has been inferred to explain the asymmetrical position of the presently active Kolbeinsey Ridge between the continental Jan Mayen Ridge and the Greenland continental margin (Talwani & Eldholm 1972, Bott 1973a).

The Jan Mayen Fracture Zone (Fig. 1) forms a belt, up to 75–100 km broad (Avery et al. 1968, Johnson 1968), transecting the oceanic crust between Norway and Greenland and consisting of en échelon fault scarps and ridges with small intervening deep basins containing up to more than 2 km of sediments (Johnson & Heezen 1967; Eldholm & Windisch 1974). The island of Jan Mayen, with the active volcano Mt. Beerenberg (Gjelsvik 1970; Siggerud 1972) occurs within the zone. The Jan Mayen Fracture Zone can be inferred to represent the fossil trace of transform faults between the offset spreading axes abutting against it (Fox et al. 1969); the Aegir and Mohn's ridges during the period from about 60 to about 42 m.y. ago (or later; cf. Laughton 1975), and the Mohn's and Kolbeinsey ridges from about 10 m.y. ago (Hinz 1975).

The Vøring Plateau, between about 66° and 68.5°N, forms a large oceanward protrusion (surface area > 21,000 km²; Johnson et al. 1968) from the continental slope off Norway at roughly the 1,000 fathom depth level. Its structure and origin have been variously interpreted. The Plateau is dissected by a NE–SW trending buried escarpment (Talwani & Eldholm 1972, 1974). The inner, south-eastern portion of the Plateau consists of up to 9 km of Mesozoic and Cenozoic, and possibly also late Palaeozoic, sediments deposited on a basement inferred to be of continental type (Talwani & Eldholm 1972; Sellevoll 1973, 1975). The outer, north-western portion of the Vøring Plateau has up to c. 1 km of Cenozoic sediments overlying a basement interpreted as either oceanic (Talwani & Eldholm 1972, 1974) or continental (Hinz 1972). Talwani & Eldholm (1972, 1974) considered that the Vøring Plateau escarpment marks the boundary between landward continental crust and oceanward oceanic crust, created by Early Tertiary ocean-floor spreading.

The Norwegian continental margin

Talwani & Eldholm (1972) divided the continental margin of Norway into three sedimentary provinces (Fig. 1): A) a southern province, south of c. 67°N, including the Stadt and Vøring sedimentary basins with thick accumulations of mainly pre-Tertiary sediments, overlain by thinner Tertiary and Quaternary deposits and wedging out near the coastline; B) the Lofoten–Vesterålen province to the north, characterized by generally having a relatively thin cover of sediments (1 to 2 km thick) but with much thicker (> 4 km)

deposits in a deep sedimentary trough in Vestfjorden (Nysæther et al. 1969); and C) a northern sedimentary province, north of Andøya, with sediment distribution and structures similar to those in the southern province. Just to the north of Andøya a downfaulted trough contains up to 4.8 km of sediments (Sundvor 1971).

Narrow, linear, gravity highs occur along the shelf edge (Fig. 1; Talwani & Eldholm 1972, 1974; Talwani & Grønlie, in press). From the available geophysical evidence, Talwani & Eldholm (1972, 1974) concluded that these anomalies occur in continental crust-type basement and that in places they form structural ridges protruding into the overlying sedimentary rocks. They interpreted the gravity highs as representing dense, metamorphic Precambrian rocks, similar to those underlying the Lofoten area, and suggested that such rocks may form a more or less continuous, long and narrow belt running along the shelf edge from Lofoten all the way to the Lewisian region of NW Scotland where a linear gravity high has, in a general way, been similarly interpreted (Watts 1971). The coinciding of the shelf edge with linear gravity highs was explained by Talwani & Eldholm (1972, 1974) by the tentative assumption that the suggested belt of high-density Precambrian rocks had pre-determined the location of the shelf edge by acting as a landward hinge for the subsidence of the newly formed continental margin after the Early Tertiary opening of the Norwegian Sea.

In the present paper the linear gravity highs along the Norwegian shelf edge are tentatively interpreted as being caused by mafic dykes, genetically related to ?Mesozoic mantle plume activity. In this interpretation the coincidence of the gravity highs with the shelf edge is considered to be a consequence of the Early Tertiary continental splitting in this region having partly followed older zones of weakness in the lithosphere, i.e., parallel to rifts and dyke intrusions associated with older, 'abortive', mantle plume activity.

The linear gravity high along the base of the continental slope off the Barents shelf (Fig. 1; Talwani & Eldholm 1972, 1974; Eldholm & Windisch 1974; Talwani & Grønlie, in press) was tentatively interpreted (Talwani & Eldholm 1972, 1974; Eldholm & Windisch 1974) as representing a deeply buried fracture zone, called the Senja Fracture Zone, produced by shearing during the initial, Early Tertiary opening of the Norwegian/Greenland Sea. An alternative interpretation, tentatively suggested here, is that this linear gravity high, like the ones along the continental margin off Norway, may represent mafic material intruded into the continental crust in connection with (?) Mesozoic mantle plume activity. Later, continental splitting may have occurred along this zone of dilation to produce a fracture zone along a sheared continental margin, bordering the Barents shelf.

Tectonic events in the North Atlantic–Arctic region prior to active ocean-floor spreading in the Norwegian–Greenland Sea

Along and near many of the continental margins created by the onset of ocean-floor spreading in the North Atlantic–Arctic Region, continental break-up was heralded by early tectonic events involving rifting and basin sedimentation with or without igneous activity. Such events, a synopsis of which is presented below, appear to have preceded the opening of the ocean basins by up to several tens of millions of years.

Hallam (1971) presented evidence showing that the southern North Atlantic experienced a period of rifting some 50 m.y. before the actual continental separation in that area. Such pre-opening tectonism produced Triassic (c. 230–220 m.y. ago) rifts with thick sedimentary piles and basic dyke intrusions along the Atlantic continental border of North America from Alabama to Labrador (King 1959; Coney 1973; Vogt 1973).

Rifting, and perhaps minor spreading (van der Linden 1975), took place in the Labrador Sea in the Jurassic, during the initial development of what was later to become the Cape Farewell Triple Junction (Pitman & Talwani 1972).

The basement of the Rockall Trough (Bott & Watts 1971), south-east of the continental Rockall Plateau (Scrutton 1972), can be interpreted as oceanic crust or as thinned and subsided continental crust underlying a thick pile of sediments, assumed to have been deposited in an early Red Sea-type trough formed contemporaneously with the initial split further south, along the eastern shelf of North America.

Along the continental shelf and margin north of Scotland, sedimentation during the Mesozoic was probably largely controlled by contemporaneous faulting along older 'Caledonian' NNE directions (Bott & Watts 1971). The Faeroe–Shetland Trough was in existence before the onset of Tertiary ocean-floor spreading (Bott 1975), and probably formed by rifting simultaneously with the Rockall Trough on oceanic or thinned continental crust in the Early Mesozoic. It has been inferred to be bordered by continental crust both to the north-west and the south-east (Bott 1973a, 1975), but it has also been considered that the basement to the north-west of the flanking Faeroe–Shetland escarpment may be oceanic (Talwani & Eldholm 1972, 1974).

Fault activity during the Mesozoic, mostly pre-Mid Jurassic in age, formed a complex, NE–SW trending sedimentary trough in the Moray Firth, Scotland (Bacon & Chesher 1975). Faulted Mesozoic basins also occur on the Shetland–Orkney shelf and in the Minch (Bott 1975), and active graben downfaulting in the North Sea during this period (Whiteman et al. 1975; Ziegler 1975) produced the complex North Sea System of interlinked troughs (Naylor et al. 1974; Whiteman et al. 1975).

Bott (1975) suggested that the Stadt and Vøring basins, on the Norwegian continental margin, are NE-ward extensions of the Faeroe–Shetland Trough; and Whiteman et al. (1975) have suggested that the Stadt and Vøring basins, the Faeroe–Shetland Trough and the Northern North Sea Trough form the

three 'failed' arms of a Late Palaeozoic–Early Mesozoic rrr triple junction. The Middle/Upper Jurassic to Lower Cretaceous sedimentary rocks on Andøya in Vesterålen were deposited during periods of downfaulting in Middle Jurassic and Early Cretaceous times, and were subject to further faulting in the Early Tertiary (Dalland 1975). The Andøya sediments form a small, landward extension of the much larger and thicker, NW–SE trending sedimentary basin to the east and north of the island (Sundvor 1971; Talwani & Eldholm 1972; Dalland 1975). In Trøndelag, central Norway, the occurrence of several hundred boulders of Middle Jurassic sedimentary rocks in Beitstadfjorden, a tributary to the inner Trondheimsfjord, has suggested the presence of a small, downfaulted, Mesozoic sedimentary basin in this area (Ofstedahl 1972).

Thick Mesozoic and (?) Late Palaeozoic sedimentary deposits in downfaulted troughs, parallel to the later-established continental margin, thus appear to occur more or less continuously along the Atlantic coast of North America and its pre-drift continuation along the continental margin of north-western Europe. These sedimentary troughs include the Rockall, Minch and Faeroe–Shetland (West Shetland Basin of Naylor et al. 1974 and Whiteman et al. 1975) troughs on the British continental margin, and the Stadt, Vøring, Vestfjord and Andøy sedimentary basins on the Norwegian continental margin. In a pre-drift reconstruction of the Greenland/Norwegian Sea area, the continental Jan Mayen Ridge with its thick sedimentary pile, split off from the Greenland shelf by sea floor spreading from the Kolbeinsey Ridge (or its immediate, unidentified precursor), would fit into the re-entrant in the continental margin south-east of the inner part of the Vøring Plateau (Fig. 1); here it would appear to fill in the gap between the Mesozoic trough deposits of the Faeroe–Shetland Trough and the Vøring Basin (cf. Talwani & Eldholm 1974, Fig. 2).

Successive events of rifting and downfaulting in the Central Graben of the North Sea in Middle Jurassic to Lower Cretaceous times were accompanied by marginal uplifts with ensuing sub-aerial erosion (Ziegler 1975), and large uplifts in the northern parts of the North Sea during the Middle Jurassic are evidenced by the development of major regressive sedimentary facies sequences (Sellwood & Hallam 1974; Ziegler 1975). Regional uplift in the North Sea area is also evidenced by a major, complex unconformity beneath Cretaceous sediments; in the northern North Sea this unconformity constitutes a major trap for oil (Howitt 1974). The concurrence of regional uplifts and Mesozoic rifting in the North Sea area seems, therefore, to be well established.

Mantle plume activity beneath the Norwegian continental margin

REGIONAL TECTONICS AND GEOMORPHOLOGICAL SETTING

Burke & Dewey (1973) have suggested that four, pre-Tertiary, mantle plume-generated triple junctions occur along the Rockall and Faeroe–Shetland troughs, and Naylor et al. (1974) and Whiteman et al. (1975) recorded three in the central and southern parts of the North Sea. Further north, structural features

on the Norwegian continental shelf together with physiographic and geomorphological features of the Norwegian mainland appear to give evidence of early (?Jurassic) mantle plume activity in two additional areas: the Møre-Jotunheimen and adjoining offshore areas in West Norway, and the Troms-Lofoten-Norrbotten area of North Norway and adjoining parts of Sweden. In both areas the inferred mantle plume activity was arrested at an early stage, before the formation of fully developed triple junctions.

The Tertiary oblique uplift of the Scandinavian landmass (Strøm 1948; Holtedahl 1953; Rudberg 1954) has been considered in general terms as a side effect of the opening-up of the Norwegian Sea by ocean-floor spreading about 60 m.y. ago (Ofstedahl 1972; Talwani & Eldholm 1972; Torske 1972; Nilsen 1973). Later marginal subsidence resulted in a large flexural downwarp, with ensuing Tertiary sedimentation on the submerged continental margin with its Mesozoic sedimentary troughs (Holtedahl & Sellevoll 1971; Talwani & Eldholm 1972; Sellevoll 1975).

The physiographical 'enveloping surface' of Norway (Gjessing 1967) shows two elongate highs, one in the Møre-Jotunheimen area and another in the Lofoten-Ofoten-Troms area and adjoining parts of Norrbotten in Sweden. Both highs are in close proximity to areas exposing the deepest crustal sections within the Scandinavian Caledonides and both are situated on the landward side of sharp re-entrants in the continental margin (Fig. 1; Rudberg 1954). Continental margin configurations such as these are often associated with mantle plume-generated triple junctions (cf. Burke & Dewey 1973; Burke & Whiteman 1973).

The Tertiary oblique uplift of the Scandinavian landmass has been regarded as the first major rejuvenating event to occur after a protracted period of denudation (Strøm 1948; Holtedahl 1953, 1960; Rudberg 1954; Gjessing 1967). The character of the landscape which was rejuvenated by the Tertiary oblique uplift has been much debated; a review of the differing opinions and the evidence presented to support them is outside the scope of the present paper, except where they may be directly applied in the present context. Opinions have differed on whether the physiography immediately before the uplift was dominated by a peneplain, by a rolling landscape of old age or whether several peneplains and other erosion surfaces, deriving from older, sequential cycles of erosion were being downgraded simultaneously. Another matter of debate and differing opinions has been the amount and geomorphological significance of subsequent glacial erosion during the Pleistocene ice ages. Reviews have been given by Holtedahl (1953, 1960), Rudberg (1954) and Gjessing (1967).

DEVELOPMENT OF DRAINAGE PATTERNS

Evidence has been presented to show that prior to the Tertiary uplift the main drainage divide in central Scandinavia was further east than at present (Ångeby 1947, 1955), and that the Tertiary uplift displaced the divide westwards, towards the Norwegian coast, from where the renewed erosion displaced it eastwards again.

Holtedahl (1953) pointed out the similar directions of the drainage pattern in central Sweden and that of a number of transverse, glacially eroded troughs along the inner part of the continental shelf in mid-Norway. He speculated that these features could constitute parts of old drainage systems whose missing, intervening portions in mainland Norway had been destroyed by later erosion. Such drainage systems could have been old, pre-Tertiary river valley systems draining the central parts of Scandinavia towards the west-northwest, across the partially or completely downwasted Caledonian mountain chain and into the epicontinental sea between Greenland and Norway. The common orientation of central Swedish rivers and Norwegian, transverse, glacially eroded troughs indicate the possibility that the pre-Tertiary land surface sloped, probably gently, towards the WNW in this region.

A general and regional drainage direction towards the WNW in central Scandinavia would be consistent with the widespread occurrence of retroverse rivers in central Sweden (Hjulström 1936; Rudberg 1954). It is also consistent with the inferred existence of an epicontinental sea in the northern extension of the North Sea depositional basin during Late Palaeozoic and Early Mesozoic times (Talwani & Eldholm 1972; Dunn 1975), since the Baltic Sea area appears to have been subject to continuous subaerial erosion from Late Devonian time to the Late Tertiary formation of the Baltic Sea by epeirogenic subsidence (Martinsson 1960). The present area of the Baltic Sea was drained by major rivers flowing southwards east of Gotland towards the Danzig depression. These relations suggest that, during these periods, the Baltic Shield was a largely positive feature, lacking the present Baltic Sea depression. By implication, the drainage divide may then be inferred to have been displaced eastwards from the orographic axis of the Caledonian mountain chain as denudation of this Early Palaeozoic feature progressed. The question of the pre-Tertiary position of the main drainage divide is closely related to the question of the time of the final downwasting of the orographic Caledonides.

The Tertiary uplift tilted the land-surface towards the ESE, and later Tertiary downwarp along the newly formed continental margin may have resulted in a welt-shaped upland along mid-Norway which was rapidly affected by erosion, guided by bedrock structures to form a subsequent drainage pattern. This would have disrupted the former continuity between the eastern and western parts of the old, WNW-directed drainage pattern. Such a sequence of events on land in mid-Norway may be reflected in the offshore sedimentary sequence by the occurrence of WNW-wards prograded, coalesced deltas well up in the Tertiary sequence between c. $63\frac{1}{2}^{\circ}\text{N}$ and 65°N off the Trøndelag coast (Sellevoll 1975), since a regressive, prograding sequence would be expected to follow an earlier, non-deltaic, transgressive sequence during the waning stages of coastal downwarping in an area with a continuing high rate of sediment influx (Curry 1969). According to the present model the deltaic deposits should consist, to a large extent, of material eroded from the welt-shaped upland during the initial, Tertiary development of the subsequent drainage pattern in this area.

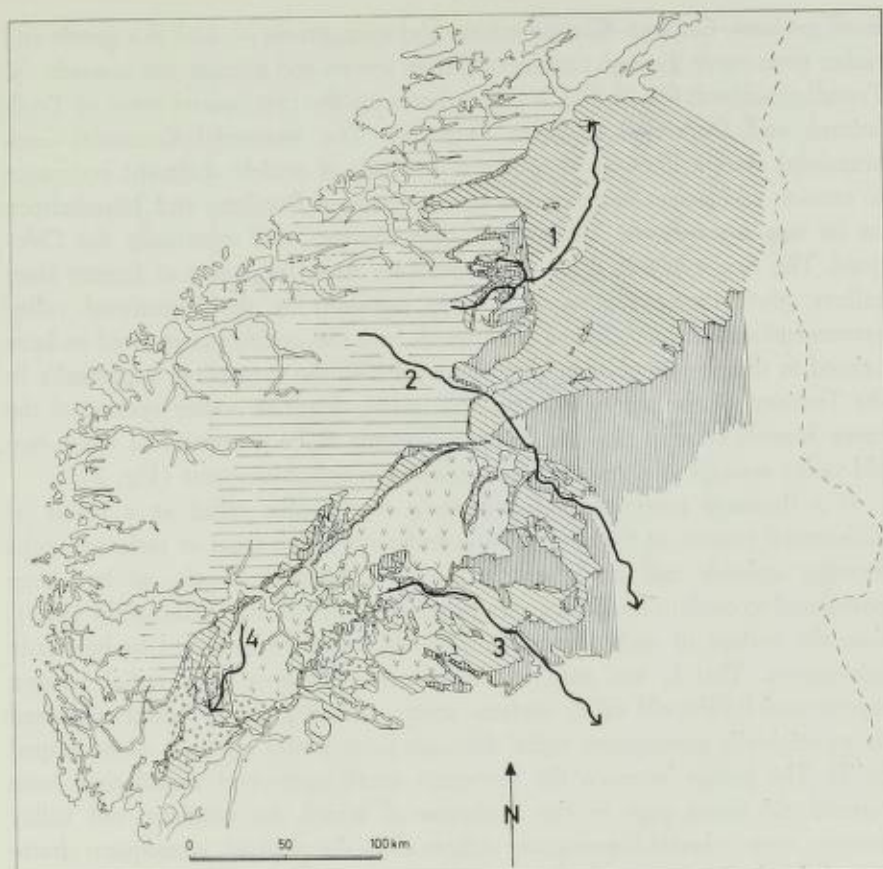


Fig. 2. Sketch map of west-central South Norway showing bedrock geology (simplified after Holtedahl & Dons 1960) and old drainage systems (1-4): 1) Sunndal-Drivdal-Gauldal system (Barrett 1900); 2) Vermedal-Raumadal-Gudbrandsdal system (Ahlmann 1919); 3) Lærdal-Valdres system (Ahlmann 1919); 4) Stalheimsdal-Uppheimsdal-Voss system (Ahlmann 1919).

Ornamented areas: horizontal ruling — northwestern basement gneisses; vertical ruling — sparagmitic rocks; oblique ruling — Cambro-Silurian schists; V-ornament — plutonic igneous rocks; circle ornament — allochthonous, Precambrian crystalline schists and plutonic rocks.

In the Møre-Jotunheimen region the oldest valley systems recognizable in different areas seem to constitute remnants of a radial drainage pattern (Zernitz 1932; Lobeck 1939; Strahler 1969). They are (Figs. 2 and 3): 1) the Sunndal-Drivdal-Gauldal system in Nordmøre and Trøndelag (Barrett 1900); 2) the Vermedal-Raumadal-Gudbrandsdal system in the Romsdal-Oppland area (Ahlmann 1919); 3) the Lærdal-Valdres system in the Sogn-Oppland area (Ahlmann 1919); and 4) the Stalheimsdal-Uppheimsdal-Voss system in the Sogn-Hordaland area (Ahlmann 1919).

These old drainage systems are apparently not of the subsequent type. The Sunndal-Drivdal-Gauldal system runs from the peripheral parts of the basal gneiss area of Møre, across several belts of rocks of varying resistance — base-

ment gneisses, Cambro-Silurian schists and sparagmites — and in a gentle and rather even curve through Cambro-Silurian schists and greenstones towards the Trondheimsfjord. On its way it passes between the two upland areas of Trollheimen and Dovrefjell-Snøhetta (Fig. 3). The Vermedal-Raumadal-Gudbrandsdal system likewise runs across bedrock of widely different resistance to erosion and passes between the upland areas of Rondane and Jotunheimen on its way towards the lowlands of East Norway, and eventually the Oslofjord. The two southern drainage systems are mere fragments of former river valleys; their upper reaches have been captured by the Sognefjord valley system and cannot be followed northwards into the uplands postulated to have existed in this region (Holtedahl 1953) prior to the formation, supposedly in the Tertiary, of the westward-draining, initial, dendritic valley system of the inner Sognefjord area. However, enough seems to be preserved of these two old valley systems to show that they, too, were non-subsequent (Fig. 2).

If a drainage pattern developed on a topographic relief as a result of differential erosion of rocks of varying resistance, with areas of resistant rocks forming uplands and easily eroded rocks forming lowlands, as has been postulated to explain the preserved upland areas of Norway (Holtedahl 1953), then the valleys of such a drainage pattern would be expected to be partly subsequent. This is not seen in the present instances. The radial pattern represented by the old valley systems seems, therefore, to be better explained by an originally consequent, radial drainage pattern of a regional, dome-shaped uplift. The passes between the mountain areas mentioned would then have formed old water gaps in the landscape of which the remnant, old valley systems were inherited, resequent valleys after the original, consequent drainage of the dome.

If the valley systems which guided the positions of the glacially eroded fjords and valleys in West Norway were originally conditioned by fluvial erosion after the Tertiary uplift, then possibly the upper, captured reaches of the older, regionally radiating valleys were elements of a pre-uplift landscape. Indirectly, this suggests that the assumed domal uplift may be pre-Tertiary in age. Rifting in connection with this uplift would lead to rapid erosion of the rift valley margins and to rapid sedimentation in the rift valley.

DOMAL UPLIFTS AND RIFTING

Schneider (1972) introduced the concept of sedimentary stages of development for ocean basins formed by rifting and subsequent ocean-floor spreading. The stages occur in the following sequence: 1) the rift valley stage; 2) the Red Sea stage; 3) the turbidite-fill stage; and 4) the deep-ocean current stage. Only the rift valley stage need concern us here. It is initiated by graben faulting caused by tensional rifting on thermally induced regional uplifts. In broad, regional uplifts several, near-parallel and competing rift systems may form, as for instance in the case of initial Triassic tension and rifting, with competing activities along the present Mid-Atlantic Ridge and the Triassic fault basin system along the east coast of North America from Alabama to Labrador (Schneider 1972).

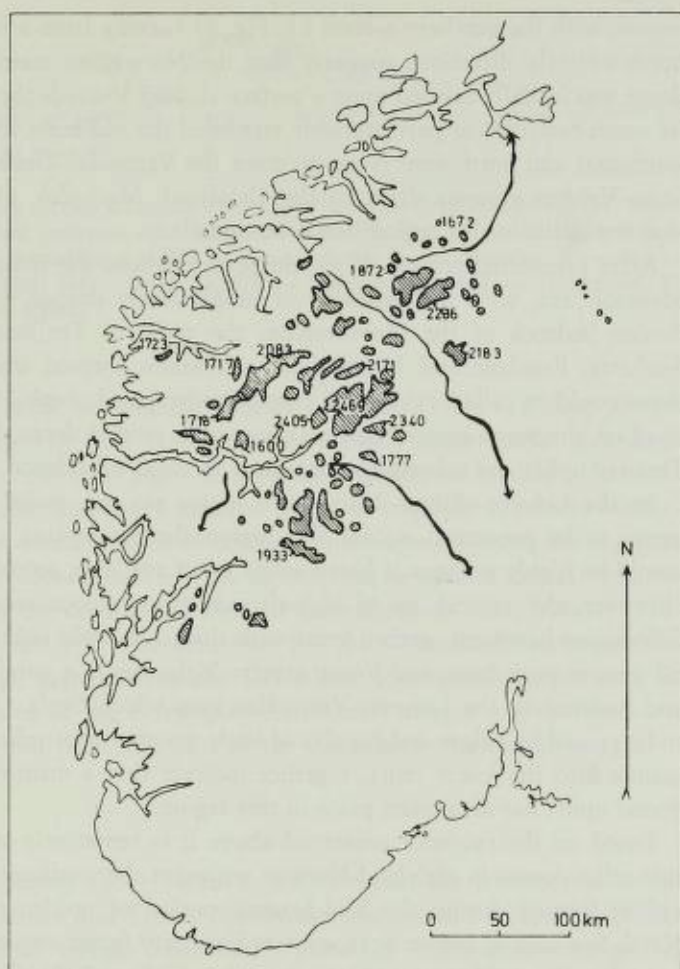


Fig. 3. Upland areas in west-central South Norway higher than 1500 m a.s.l. (lined ornament); summit levels in m a.s.l. Thick lines with arrow-head: old drainage systems (cf. Fig. 2), presumably representing an old, inherited, radial drainage pattern and running through wide, ancient water gaps, dissecting the upland area.

In the rift valley stage the crests of the rift valley walls become drainage divides: the regional drainage is down the gentle outward slopes of the uplift, or dome, away from the centre of uplift, and a local, internal drainage system forms within the rift valley system (Schneider 1972). In relation to the large-scale, crustal geometry and structure such a regional, external drainage must be classified as consequent, and the internal, graben drainage as obsequent. The steep fault scarps along the rift valleys will promote more vigorous erosion by the internal, obsequent drainage than by the external, consequent drainage, and the water divides will migrate away from the rift valleys. Thus the rift crests must be bevelled by erosion.

The old, disrupted, external drainage pattern in the Møre-Jotunheimen

region, with the northern system (1, Fig. 2) curving from a north-easterly to a north-westerly direction, suggests that the Norwegian mainland half of this dome was initially formed upon a surface sloping towards the WNW, and that its south-easternmost part probably straddled the old main watershed between south-east and north-west Norway, since the Vermedal-Gudbrandsdal and the Sogn-Valdres systems drain to the Oslofjord. Machaček (1908) considered that the uplift in this region had been domal.

After protracted erosion of the dome throughout the remaining part of the Mesozoic era, with the exposure of progressively deeper levels in the Caledonian bedrock of the Møre region, the resistant Trollheimen, Dovrefjell-Snøhetta, Rondane and Jotunheimen mountains formed what in a 'classical' dome could be called a dissected cuesta landscape (Lobeck 1939). This developed on the south-eastern half of a maturely eroded dome, later subjected to Tertiary uplift and subsequent, marginal flexural subsidence.

In the Lofoten-Troms-Norrbotten region no old, radial drainage pattern seems to be preserved, so for this region the assumption of a domal uplift would be highly tenuous if based solely upon available geomorphological data. However, the coincidence of high-altitude mountainous areas, deeply eroded Caledonian basement, graben areas with thick Mesozoic sediments, a continental margin re-entrant, and linear gravity highs running parallel to the margin and underneath the Lofoten-Vesterålen area which Sveta (1971) considered to be caused by ridges and cupolas of basic material protruding from the upper mantle into the lower crust, together indicate that a mantle plume-generated domal uplift has also taken place in this region.

Based on the evidence presented above it is tentatively suggested that the two relict domes in mainland Norway represent the south-eastern parts of two uplifts formed during the Mid-Jurassic period of uplifting recorded in the North Sea area in contemporaneous sedimentary facies sequences and regional unconformities (Howitt 1974; Sellwood & Hallam 1974; Ziegler 1975).

TERTIARY OBLIQUE UPLIFTS AND MARGINAL DOWNWARD

In the Early Tertiary renewed rifting — this time followed by the still continuing ocean floor spreading — took place along the north-western margin of Scandinavia. The oblique uplift associated with this rifting, and the later downwarping along the continental margin affected also the mainland remnants of the old domes. In the Møre-Jotunheimen area this may have produced the general profile indicated in Fig. 4, where the 'cuesta' of the original dome now forms the summit hump on the profile, while the more central part of the dome forms a gentle curve sloping down to the coast.

Downwarping of continental margins after the initial upwarps has been ascribed to increased sedimentary load along the margin (e.g. Walcott 1972), to vertical thermal contraction as the initial high heat flow regime moves away from the continental margin together with the mid-oceanic ridge (Sleep 1971, 1973), and to plastic flow of deep crustal material towards the newly created oceanic area (Bott 1973b). These hypotheses are not mutually exclusive. In a

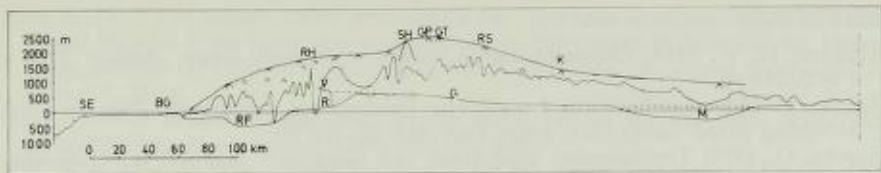


Fig. 4. NW-SE profile section across the Norwegian landmass from lake Mjøsa (M) to the Møre continental shelf (redrawn after Holtedahl 1960, Pl. 15): SE — Storegga; BG — Buagrunden; RF — Romsdalsfjord; RH — Romsdalshorn; V — Vermedal; R — Raumadal; G — Gudbrandsdal; SH — Snohetta; GP — Galdhøpiggen; GT — Glittertind; RS — Rondslottet; K — Kvien.

continental split with an angular course, oceanward flow of deep crustal material as envisaged by Bott (1973b) could possibly cause smaller subsidence on the side of the re-entrant angle than on the opposite protruding side of the rift, because a smaller amount of material would be required to restore isostatic equilibrium in the smaller sector of oceanic lithosphere adjoining the marginal re-entrant. This could explain why no corresponding upland domal remnants are to be seen on the continental shelf of Greenland. In fact, Vann (1974) suggested in his pre-drift reconstruction for the Greenland/Norwegian Sea region that a large gap between the Greenland continental margin and the Lofoten-Troms area of the Norwegian continental margin may be explained by subsidence of that particular part of the Greenland continental margin.

Conclusion

The evidence presented above seems to indicate that the conjunction within the Møre-Jotunheimen and Troms-Norrbotten regions and adjoining offshore areas of continental margin re-entrants, Mesozoic sedimentary troughs of probable rift origin, linear gravity highs and dissected upland areas of deeply eroded continental crust may be explained as a result of Mesozoic mantle plume activity near the present coast in the two regions. These mantle plumes generated domal uplifts and rifts, none of which seems to have evolved beyond the rifting stage. Much later, the early Tertiary rifting and ensuing ocean floor spreading in the Norwegian/Greenland Sea area are thought to have partly followed the older zones of crustal weakness, and thus to have produced the present continental margin with its two re-entrants along the Norwegian coast. The inferred Mesozoic events may be regarded as a northern extension of pre-splitting tectonic activity along the present North American and north-west European Atlantic margins.

Acknowledgements. — I thank Jan Mangerud, Bergen, for helpful discussion about the regional geomorphology of Norway; Knut Åm, Stavanger, for discussions about the interpretations of geophysical data, and George H. Gale and David Roberts, Trondheim, for their critical reading of the manuscript.

REFERENCES

- Ahlmann, H. W. 1919: Geomorphological studies in Norway. *Geogr. Annaler* 1919 - 1 & 2, 210 pp.
- Ångeby, O. 1947: Landformerna i nordvästra Jämtland och angränsande delar av Nord-Trøndelag. *Medd. Lunds Univ. geogr. Inst. Avb.* 12, 202 pp.
- Ångeby, O. 1955: Toppkonstans, erosionsytor och passdaler i Jämtland och Trøndelag. *Medd. Lunds Univ. geogr. Inst.* 30, 1-38.
- Avery, O. E., Burton, G. D. & Heirtzler, J. R. 1968: An aeromagnetic survey of the Norwegian Sea. *J. geophys. Res.* 73, 4583-4600.
- Bacon, M. & Chesher, J. 1975: Results of recent geological and geophysical investigations in the Moray Firth, Scotland. *Norges geol. Unders.* 316, 99-104.
- Barrett, R. L. 1900: The Sundal drainage system in central Norway. *Bull. Am. geogr. Soc.* 32.
- Bott, M. H. P. 1973a: The evolution of the Atlantic north of the Faeroe Islands. In Tarling, D. H. & Runcorn, S. K. (eds.): *Implications of Continental Drift to the Earth Sciences* 1, 175-189. Academic Press, London/New York.
- Bott, M. H. P. 1973b: Shelf subsidence in relation to the evolution of young continental margins. In Tarling, D. H. & Runcorn, S. K. (eds.): *Implications of Continental Drift to the Earth Sciences* 2, 675-683. Academic Press, London/New York.
- Bott, M. H. P. 1975: Structure and evolution of the Atlantic floor between northern Scotland and Iceland. *Norges geol. Unders.* 316, 195-199.
- Bott, M. H. P. & Watts, A. B. 1971: Deep structure of the continental margin adjacent to the British Isles. In Delany, F. M. (ed.): *The geology of the East Atlantic continental margin 2, Europe. Inst. Geol. Sci. Rep. 70/14*, 89-109 (United Kingdom).
- Burke, K. & Dewey, J. F. 1973: Plume-generated triple junctions: key indicators in applying plate tectonics to old rocks. *J. Geol.* 81, 406-433.
- Burke, K. & Whiteman, A. J. 1973: Uplift, rifting and the break-up of Africa. In Tarling, D. H. & Runcorn, S. K. (eds.): *Implications of Continental Drift to the Earth Science* 2, 734-755. Academic Press, London/New York.
- Burke, K. & Wilson, J. T. 1972: Is the African plate stationary? *Nature* 239, 387-390.
- Churkin, M., J. 1969: Paleozoic tectonic history of the Arctic Basin north of Alaska. *Science* 165, 549-555.
- Coney, P. J. 1973: Non-collision tectogenesis in western North America. In Tarling, D. H. & Runcorn, S. K. (eds.): *Implications of Continental Drift to the Earth Sciences* 2, 713-727. Academic Press, London/New York.
- Curry, J. R. 1969: Shore zone sand bodies: barriers, cheniers, and beach ridges. In Stanley, D. J. (ed.): *The New Concepts of Continental Margin Sedimentation: Application to the Geological Record*. 18 pp. American Geological Institute, Washington D.C.
- Dalland, A. 1975: The Mesozoic rocks of Andøy, northern Norway. *Norges geol. Unders.* 316, 271-287.
- Darracott, B. W., Fairhead, J. D., Girdler, R. W. & Hall, S. A. 1973: The East African Rift system. In Tarling, D. H. & Runcorn, S. K. (eds.): *Implications of Continental Drift to the Earth Sciences* 2, 757-766. Academic Press, London/New York.
- Dietz, R. S. & Holden, J. C. 1970: Reconstruction of Pangaea: break-up and dispersion of continents, Permian to Present. *J. geophys. Res.* 75, 4939-4956.
- Dunn, W. W. 1975: North Sea basinal area, Europe — an important oil and gas province. *Norges geol. Unders.* 316, 69-97.
- Eldholm, O. & Windisch, C. C. 1974: Sediment distribution in the Norwegian—Greenland Sea. *Geol. Soc. Am. Bull.* 85, 1661-1676.
- Fox, P. J., Pitman, W. C. III & Shepard, F. 1969: Crustal plates in the Central Atlantic: evidence for at least two poles of rotation. *Science* 165, 487-489.
- Gjelsvik, T. 1970: Volcano on Jan Mayen alive again. *Nature* 228.
- Gjessing, J. 1967: Norway's paleic surface. *Norsk geogr. Tidsskr.* 21, 69-132.
- Hallam, A. 1971: Mesozoic geology and the opening of the North Atlantic. *J. Geol.* 79, 129-157.
- Hamilton, W. 1970: The Uralides and the motion of the Russian and Siberian platforms. *Geol. Soc. Am. Bull.* 81, 3605-3622.
- Heirtzler, J. R., Dickson, G. O., Herron, E. M., Pitman, W. C. III & Le Pichon, X. 1968: Marine magnetic anomalies, geomagnetic field reversals, and motions of the ocean floor and continents. *J. geophys. Res.* 73, 2119-2136.

- Hinz, K. 1972: The seismic crustal structure of the Norwegian continental margin in the Voring Plateau, in the Norwegian deep sea, and on the eastern flank of the Jan Mayen Ridge between 66° and 68°N. *Int. geol. Congr. twenty-fourth Session Canada 1972, Section 8*, 28–36.
- Hinz, K. 1975: Results of geophysical surveys in the area of the Kolbeinsey Ridge and Iceland Plateau. *Norges geol. Unders.* 316, 201–203.
- Hinz, K. & Moe, A. 1971: Crustal structure in the Norwegian Sea. *Nature phys. Sci.* 232 (35), 187–190.
- Hjulström, F. 1936: Einige morphologische Beobachtungen im süd-östlichen Storsjögebiet in Jämtland. *Geogr. Annaler* 18, 348–362.
- Holtedahl, H. & Sellevoll, M. A. 1971: Geology of the continental margin of the eastern Norwegian Sea and of Skagerrak. In Delany, F. M. (ed.): *The geology of the East Atlantic continental margin. Inst. geol. Sci. Rep. 70/14*, 33–52 (United Kingdom).
- Holtedahl, O. 1953: Norges geologi 2. *Norges geol. Unders.* 164 (2), 587–1118.
- Holtedahl, O. (ed.) 1960: Geology of Norway. *Norges geol. Unders.* 208, 540 pp.
- Holtedahl, O. & Dons, J. A. 1960: *Geologisk kart over Norge; berggrunnskart 1: 1 000 000. Geological map of Norway (bedrock)*. Norges geologiske undersøkelse, Oslo.
- Howitt, F. 1974: North Sea oil in a world context. *Nature* 249, 700–703.
- Johnson, G. L. 1968: Marine geology in the environs of Jan Mayen. *Norsk Polarinst. Arb.* 1966, 105–111.
- Johnson, G. L., Ballard, J. A. & Watson, J. A. 1968: Seismic studies of the Norwegian continental margin. *Norsk Polarinst. Arb.* 1966, 112–119.
- Johnson, G. L. & Heezen, B. C. 1967: The morphology and evolution of the Norwegian-Greenland Sea. *Deep Sea Res.* 14, 755–771.
- Johnson, G. L., Southall, J. R., Young, P. W. & Vogt, P. R. 1972: Origin and structure of the Iceland Plateau and Kolbeinsey Ridge. *J. Geophys. Res.* 77, 5688–5696.
- King, Ph. B. 1959: *The Evolution of North America*. 190 pp. The Princeton University Press, New Jersey.
- Laughton, A. S. 1971: South Labrador Sea and the evolution of the North Atlantic. *Nature* 232, 612–617.
- Laughton, A. S. 1975: Tectonic evolution of the northeast Atlantic Ocean: a review. *Norges geol. Unders.* 316, 169–193.
- Le Pichon, X. 1968: Sea-floor spreading and continental drift. *J. geophys. Res.* 73, 3661–3697.
- Linden, W. J. M. van der, 1975: Mesozoic and Cainozoic opening of the Labrador Sea, the North Atlantic and the Bay of Biscay. *Nature* 253, 320–324.
- Lobeck, A. K. 1939: *Geomorphology — an Introduction to the Study of Landscapes*. 731 pp. McGraw-Hill Book Co., Inc., New York/London.
- Machaček, F. 1908: Geomorphologische Studien aus dem norwegischen Hochgebirge. *K.K. geogr. Ges. Wien* 7 (2), 1–61.
- Martinsson, A. 1960: The submarine morphology of the Baltic Cambro-Silurian area. *Bull. geol. Inst. Univ. Uppsala* 38, 11–35.
- Morgan, W. J. 1971: Convection plumes in the lower mantle. *Nature* 230, 42–43.
- Naylor, D., Pegrum, D., Rees, G. & Whiteman, A. 1974: Nordsjøbassengene (The North Sea Trough System). *Noroil* 2, (4), 17–22.
- Nilsen, T. H. 1973: The relation of joint patterns to the formation of fjords in western Norway. *Norsk geol. Tidsskr.* 53, 183–194.
- Nysæther, E., Eldholm, O. & Sundvor, E. 1969: Seismiske undersøkelser av den norske kontinentalsokkel. *Tek. Rapp.* 3, 15 pp. Jordskjelvstasjonen, Universitetet i Bergen, Bergen.
- Oftedahl, Chr. 1972: A sideritic ironstone of Jurassic age in Beitstadfjorden, Trøndelag. *Norsk geol. Tidsskr.* 52, 123–134.
- Ostenso, N. A. 1973: Sea-floor spreading and the origin of the Arctic Ocean Basin. In Tarling, D. H. & Runcorn, S. K. (eds.): *Implications of Continental Drift to the Earth Sciences I*, 165–173. Academic Press, London/New York.
- Ostenso, N. A. 1974: Arctic Ocean margins. In Burk, C. A. & Drake C. L. (eds.): *The Geology of Continental Margins*, 753–763. Springer-Verlag, Berlin/Heidelberg/New York.
- Phillips, J. D. & Luyendyk, B. P. 1970: Central North Atlantic plate motions over the last 40 million years. *Science* 170, 727–729.

- Pitman, W. C. III & Talwani, M. 1972: Sea-floor spreading in the North Atlantic. *Geol. Soc. Am. Bull.* 83, 619-646.
- Rudberg, S. 1954: Västerbottens berggrundsmorfologi. *Geographica* 25, 457 pp.
- Schneider, E. D. 1972: Sedimentary evolution of rifted continental margins. *Geol. Soc. Am. Mem.* 132, 109-118.
- Scrutton, R. A. 1972: The crustal structure of Rockall Plateau microcontinent. *Geophys. J. R. astr. Soc.* 27, 259-275.
- Sellevoll, M. A. 1973: A continuous seismic and magnetic profile across the Norwegian continental shelf and Vøring Plateau. *Norges geol. Unders.* 300, 1-10.
- Sellevoll, M. A. 1975: Seismic refraction measurements and continuous seismic profiling on the continental margin off Norway between 60°N and 69°N. *Norges geol. Unders.* 316, 219-235.
- Sellwood, B. W. & Hallam, A. 1974: Bathonian volcanicity and North Sea rifting. *Nature* 252, 27-28.
- Siggerud, Th. 1972: The volcanic eruption on Jan Mayen 1970. *Norsk Polarinst. Arb.* 1970, 5-18.
- Sleep, N. 1971: Thermal effects of the formation of Atlantic continental margins by continental break-up. *Geophys. J. R. astr. Soc.* 24, 325-350.
- Sleep, N. H. 1973: Crustal thinning on Atlantic continental margin: evidence from older margins. In Tarling, D. H. & Runcorn, S. K. (eds.): *Implications of Continental Drift to the Earth Sciences* 2, 685-692. Academic Press, London/New York.
- Strahler, A. N. 1969: *Physical Geography*. Third edition. 733 pp. John Wiley & Sons, Inc., New York/London.
- Strøm, K. M. 1948: The geomorphology of Norway. *Geogr. J.* 112, (1-3), 19-27.
- Sundvor, E. 1971: Seismic refraction measurements on the Norwegian continental shelf between Andøya and Fugloybanken. *Marine geophys. Res.* 1, 303-313.
- Svela, P. T. 1971: *Gravimetrisk undersøkelse av Lofoten-Vesterålen-området*. Unpublished thesis, University of Bergen, Bergen.
- Talwani, M. & Eldholm, O. 1972: Continental margin off Norway: a geophysical study. *Geol. Soc. Am. Bull.* 83, 3575-3606.
- Talwani, M. & Eldholm, O. 1974: Margins of the Norwegian-Greenland Sea. In Burk, C. A. & Drake, C. L. (eds.): *The Geology of Continental Margins*, 361-374. Springer-Verlag, Berlin/Heidelberg/New York.
- Talwani, M. & Grønlie, G. 1975: A free-air gravity map of the Norwegian-Greenland Sea. *J. geophys. Res.*, in press.
- Torske, T. 1972: Tertiary oblique uplift of western Fennoscandia; crustal warping in connection with rifting and break-up of the Laurasian continent. *Norges geol. Unders.* 272, 43-48.
- Vann, I. R. 1974: A modified predrift fit of Greenland and western Europe. *Nature* 251, 209-211.
- Vogt, P. R. 1973: Early events in the opening of the North Atlantic. In Tarling, D. H. & Runcorn, S. K. (eds.): *Implications of Continental Drift to the Earth Sciences* 2, 693-712. Academic Press, London/New York.
- Vogt, P. R., Johnson, G. L., Holcomb, B., Gilg, J. G. & Avery, O. E. 1971: Episodes of sea-floor spreading recorded by the North Atlantic basement. *Tectonophysics* 12, 211-234.
- Vogt, P. R., Ostenso, N. A. & Johnson, G. L. 1970: Magnetic and bathymetric data bearing on sea-floor spreading north of Iceland. *J. geophys. Res.* 75, 903-920.
- Walcott, R. I. 1972: Gravity, flexure and the growth of sedimentary basins at a continental edge. *Geol. Soc. Am. Bull.* 83, 1845-1848.
- Watts, A. B. 1971: Geophysical investigations on the continental shelf and slope north of Scotland. *Scott. J. Geol.* 7, 189-217.
- Whiteman, A. J., Rees, G., Naylor, D. & Pegrum, R. M. 1975: North Sea troughs and plate tectonics. *Norges geol. Unders.* 316, 137-161.
- Wilson, J. T. 1963: Continental drift. *Scientific American* 208, 86-100.
- Wilson, J. T. 1972: New insights into old shields. *Tectonophysics* 13, 73-94.
- Wilson, J. T. 1973: Mantle plumes and plate motions. *Tectonophysics* 19, 149-164.
- Zernitz, E. R. 1932: Drainage patterns and their significance. *J. Geol.* 40, 498-521.
- Ziegler, P. A. 1975: The geological evolution of the North Sea area in the tectonic framework of North Western Europe. *Norges geol. Unders.* 316, 1-27.

RECENT MAPS PUBLISHED BY NGU

MAPS PRINTED IN COLOUR (On sale from Universitetsforlaget, Nkr. 30,—).

1:250 000	Sauda (in press)	Bedrock geology
	Sulitjelma	Aeromagnetics
	Mo i Rana	—»—
	Bodo	—»—
	Svolvær	—»—
1:100 000	I 19 Bindal	Bedrock geology
	H 19 Helgelandsflesa	—»—
	H 18 Vega	—»—
1: 50 000	2018 III Elvdal	Bedrock geology
	2017 I Jorderi (in press)	—»—
	2017 IV Nordre Osen (in press)	—»—
	1321 I Smøla (in press)	—»—
	1521 II Holonda	Quaternary geology
	1916 III Østre Toten (in press)	—»—
	2018 III Elvdal	—»—
	B30 Aust. Forde	—»—
	1115 I Bergen	Hydrogeology

MAPS IN BLACK AND WHITE (On sale direct from NGU either as paper-copies (Nkr. 12,—) or as transparent-copies (Nkr. 60,—)).

1:100 000	H 17 Flovær	Bedrock geology (Preliminary)
	I 16 Donna	—»— —»—
1: 50 000	1833 III Raisjavrre	Bedrock geology (Preliminary)
	1312 III Orsjødalsvatnet	—»— —»—
	1934 IV Gargia	—»— —»—
	1734 IV Nordreisa	—»— —»—
	1814 II Drøbak	—»— —»—
	1315 I Ullensvang	Aeromagnetics
	1415 I Bjoreio	—»—
	1415 IV Eidfjord	—»—
	1515 I Skurdalen	—»—
	1515 IV Hein	—»—
	1615 I Skjonne	—»—
	1615 IV Uvdal	—»—
	1715 I Strømsåttbygda	—»—
	1715 IV Flå	—»—
	1815 IV Sperillen	—»—
	1314 I Røldal	—»—
	1314 II Suldalsvatnet	—»—
	1314 III Sauda	—»—
	1314 IV Fjæra	—»—
	1414 I Songevatn	—»—
	1414 IV Haukelisæter	—»—
	1315 II Ringedalsvatnet	—»—
	1315 III Odda	—»—
	1415 II Nordmannslågen	—»—
	1415 III Hårteigen	—»—
	1515 II Kalhovd	—»—
	1515 III Lågaros	—»—
	1615 II Nore	—»—
	1615 III Austbygdi	—»—
	1715 II Sigdal	—»—
	1715 III Rollag	—»—
	1815 III Honefoss	—»—
	1113 II Skudeneshavn	—»—
	1113 IV Utsira	—»—

Nr. 322



NGU
Norges geologiske
undersøkelse

CONTENTS:

Pedersen, S.: Intrusive Rocks of the Northern Iveland-Evje Area, Aust-Agder	1
Gustavson, M.: The Low-grade Rocks of the Skälvær Area, S. Helgeland, and Their Relationship to High-grade Rocks of the Helgeland Nappe Complex	13
Faye, G. Chr. & Ødegård, M.: Determination of Major and Trace Elements in Rocks Employing Optical Emission Spectroscopy and X-ray Fluorescence	35
Roberts, D.: Geochemistry of Dolerite and Metadolerite Dykes from Varanger Peninsula, Finnmark, North Norway	55
Torske, T.: Possible Mesozoic Mantle Plume Activity beneath the Continental Margin of Norway	73

ISBN 82-00-31354-9

Printed in Norway by Sentrum Bok- og Aksidenstrykkeri, Trondheim

